THE DAMAGE-ASSOCIATED MOLECULAR PATTERN MOLECULE S100A4 EXERTS ROBUST MUCOSAL ADJUVANT ACTIVITY

ARKA SEN CHAUDHURI

PhD

The Hong Kong Polytechnic University

2020

The Hong Kong Polytechnic University

Department of Health Technology and Informatics

The Damage-associated molecular pattern molecule S100A4 exerts robust mucosal adjuvant activity

Arka Sen Chaudhuri

A thesis submitted in partial fulfilment of the requirements
for the degree of Doctor of Philosophy

June 2020

CERTIFICATE OF ORIGINALITY

I hereby declare that this thesis is my own work and that, to the best of my knowledge and belief, it reproduces no material previously published or written, nor material that has been accepted for the award of any other degree or diploma, except where due acknowledgement has been made in the text.

_____

Arka Sen Chaudhuri
Date- 29th June 2020

Abstract

Lack of a potent and safe mucosal adjuvant has hampered the development of mucosal vaccination largely because of immune tolerance at mucosal sites. Efforts have focused on the exploitation of pathogen-associated molecular pattern (PAMP) molecules (e.g., bacterial toxins). However, a similarly potent class of immune stimulators, the damage-associated molecular pattern (DAMP) molecules, has been largely overlooked. DAMPs are a group of endogenous substances that are released from mammalian cells upon tissue injury. A major advantage of using DAMP molecules as clinically applicable adjuvants lies in its more reliable safety profile because of their human origin. The objective of this study was to identify a potent DAMP molecule that could be exploited for mucosal adjuvanticity using a mouse intranasal immunization model.

A panel of DAMP molecules, including S100A4, cyclophilin A, HMGB1, and uric acid, was initially screened for their mucosal adjuvant activity based on capability to augment antigen specific antibody production after immunization and *in vitro* dendritic cell activation. Uric acid, HMGB1 were unable to deliver any effect, cyclophilin A where promising but S100A4 demonstrated overall superiority, and was chosen for further exploration of its mucosal adjuvant activity. Following intranasal immunization of C57BL/6 mice with OVA, an experimental vaccine antigen, in the presence of S100A4 as an adjuvant, OVA-specific IgG antibody levels in the circulation as well as IgA levels

at various mucosal sites were augmented as analysed by ELISA, which was consistent with the enumeration of the number of antibody-forming cells in the bone marrow by ELISPOT. S100A4 dramatically promoted the formation of the germinal centre as evidenced by the expression of GL-7, a recognized marker for the germinal centre, on spleen B cells using confocal microscopy. Interestingly, increased lipid accumulation in the spleens from mice that received S100A4 was detected using matrix-assisted laser desorption/ionization-time of flight mass spectrometry (MALDI-TOF MS), which also supported S100A4-induced enhancement in germinal centre activity as vigorously proliferating germinal centre B cells require lipid-derived fatty acids for the metabolic energy supply. To my knowledge, this is the first study using this label-free technology to reveal germinal centre responses, which has a broad implication to the study of non-rodent animal models which usually lack commercially available antibodies that recognize germinal centre markers (e.g., GL-7). In addition, S100A4 also facilitated T cell memory responses. Furthermore, my data demonstrated that S100A4 promoted the activation of dendritic cells and mast cells *in vitro*, two cell types critically important for bridging the innate and adaptive immune responses at the mucosal sites. Of note, the potency of S100A4 as a mucosal adjuvant reached impressive levels comparable to cholera toxin which is described as the gold standard mucosal adjuvant. Last but not least, I demonstrated that S100A4 was able to potently promote humoral immune responses against the spike protein of SARS-CoV-2, the virus causing COVID-19, after intranasal immunization using the spike protein as the vaccine antigen.

This study presented compelling data supporting that S100A4 may be exploited as a promising, novel mucosal adjuvant, which has a timely impact on our designing of vaccination strategies especially in the global context of the COVID-19 pandemic. My study has set a solid foundation for further evaluation of the translational significance of S100A4 in boosting mucosal vaccination.

Conference publications describing thesis work

- Arka Sen Chaudhuri and Zou Xiang. The damage-associated molecular pattern molecule cyclophilin A exerts mucosal adjuvanticity following intranasal immunization in mice. Immunology 2019, San Diego, USA
- Arka Sen Chaudhuri and Zou Xiang. Cyclophilin A exerts mucosal adjuvanticity following intranasal immunization in mice. Tsinghua IITU-RIKEN IMS summer program on advanced immunology, 2019, Beijing, China.
- Arka Sen Chaudhuri, Yeh Yu-Wen and Zou Xiang. The Damage-associated Molecular Pattern Molecule S100A4 Exerts Mucosal Adjuvanticity Following Intranasal Immunization in Mice. 17th International Congress of Immunology (IUIS 2019), Beijing, China.
- Arka Sen Chaudhuri, Jia-Bin Sun, Yeh Yu-Wen, Jan Holmgren and Zou Xiang. The damage-associated molecular pattern molecule S100A4 exerts mucosal adjuvanticity following intranasal immunization in mice. Hong Kong Immunology forum 2019, Hong Kong.

Acknowledgements

I would like to express my sincere appreciation to all who have contributed in diverse ways towards the completion of this thesis.

First, I owe a great debt of gratitude to my supervisor and mentor Dr. Zou Xiang. The exceptional support you gave me right from the date I contacted you for my application to the Ph.D. program until I got the offer has nothing to equate with. Your care from the day we first met in Nanjing, then welcoming me at Hong Kong airport, all the way through my entire study period is voluminous to be written. Being coming from a different research background, words are of limit to express my gratefulness for your outstanding academic supervision, meticulous comments, correction, directions, and inspiration that keep me going in my PhD journey and help me grow. Your office was always open for me even at late night at times when I needed for discussion. Thank you very much indeed for all the support during my study. Without your supervision, my PhD study would have been less smooth.

I would also like to extend my special appreciation and heartfelt gratitude to our collaborators Prof Jan Holmgren, and Dr Jia-Bin Sun, Mucosal Immunobiology and Vaccine Centre (MIVAC), University of Gothenburg, for their common interest in S100A4 and fruitful research collaboration. I wish to also acknowledge the immense help from Prof Nils Lycke, also from MIVAC, Gothenburg, for providing perceptive comments, constructive criticisms, helpful advice and the many insights to refine my ideas and shape this research. My thanks also go to Prof Yu Fang, Guizhou Medical University, for helping me with some unique animal techniques.

I am extremely grateful for the suggestions and encouragement from nearly all the faculty members at the Department of Health Technology and Informatics, PolyU. In Particular, I wish to thank Prof Shea-ping Yip, Dr Tony To (co-supervisor), Dr Polly Leung, Dr Helen

Law, Dr Chien-Ling Huang, Dr Kenneth Cheng, Dr Fiona Chen, Dr Chi Ming Wong, Dr Franki TSE, Dr Jung Sun Yoo, Dr Gilman Sium, Dr Liang-Ting Lin, and Dr Jin Cai for listening to my seminars at various occasions and providing constructive comments.

I want to extend my heartfelt indebtedness to Prof. Zhenghong WU and Dr. Xiaole Qi from China Pharmaceutical university, my Master's degree mentor and current collaborator, for teaching me various research techniques which was instrumental also for my PhD project. I would like to express my special appreciation to Dr John Yuen, School of Nursing, PolyU, for his continuous support and encouragement during this thesis work.

I wish to offer my sincere thanks to Dr Raymond Hui, Ms Joey Chiu and Ms Natalie Chen, Health Technology and Informatics; Dr Ryan Chow Ho-yin, Dr Clara Hung Hiu-ling, Dr So Pui-kin, and Dr Rachel Li Wai-sum, University Research Facility in Life Sciences, PolyU, for providing all the technical support and training for different instruments used in this research work. I am deeply thankful to Dr Au Lai Shan, Alice, Mr Tang Wang Him, Vincent, and Mr Ho Hei Man, Centralised Animal Facilities, PolyU, for facilitating all my animal experiment needs and approving my last-minute requests.

I would also like to extend my heartfelt indebtedness to Eden and Olifan for your unreserved support during my study and standing by me as a team. Eden, thank you very much for helping me in all my large-scale experiments from the beginning to the end. Our discussions and your comments have been instrumental to my PhD journey.

I am very grateful to my colleagues for being there in the laboratory and outside when the help was needed. Special thanks to Yao, Arpan, Maruf, In Young, Adenike, Abebe, Limon, Rui, Rashidul, Akbor, Chen Xi, Hasan, Zhirul, Regina, Julie, Chala, Ashley, Marco, Ke Kao, Kelvin, Huige, Nonhlanhla, Mengyao and Chujun, you guys helped me a lot and without your help it would be hard for me to complete this PhD journey. Thank you, Mika, and Jeline for your support and encouragement.

Sumei, thank you for being my ultimate cheerleader and being there for me and supporting me through my ups and downs without your continuous encouragement and motivation it would never be possible. Thank you.

Last but not the least, my inestimable measure of gratitude goes to my parents (Amitava and Anita Sen Chaudhuri), siblings (Ankita and Angira), brother-in-law (Ashim Das) and nieces (Adrija and Aditri) for their kindness, thoughtfulness and unflinching support. I truly appreciate all their sacrifices for me from my undergraduate student days till now.

Table of contents

List of figures

List of tables

List of abbreviations

APC	Antigen-presenting cell
BALF	Bronchoalveolar lavage fluid
DAMP	Damage-associated molecular pattern
ELISA	Enzyme-linked immunosorbent assay
FBS	Fetal bovine serum
HMGB1	High mobility group box 1
LPS	Lipopolysaccharide
MHC	Major histocompatibility complex
M cell	Microfold cell
MALT	Mucosa-associated lymphoid tissue
NALT	Nasopharynx-associated lymphoid tissue
OVA	Ovalbumin
PAMP	Pathogen-associated molecular pattern
PBS	Phosphate-buffered saline
PRR	Pattern recognition receptor
RAGE	Receptor for advanced glycation endproducts
TLR	Toll-like receptor

Chapter 1 — Introduction

1.1 Vaccine

1.1.1 General introduction to vaccination

The immunization history can be traced back to as early as the 10th century in China when inoculation by blowing the smallpox patient-derived powdered scabs into the nostrils of healthy individuals was carried out in a hope to avoid contracting the disease (Gross *et al.*, 1998). It is also recorded that drinking snake venom was practiced as a strategy to strengthen the protective capacity against snake bites by Buddhist monks in India in the 17th century [1]. Of course, these endeavours can only be described as unscientific, primordial ways of "vaccination". The era of disease prevention and even eradication by vaccination started when Edward Jenner demonstrated good protection against smallpox through the inoculation of pus taken from a cowpox pustule in 1796 based on the immune cross-reactivity that can be generated against the human smallpox virus and the cowpox virus (Lombard *et al.*, 2007).

The importance of vaccination in disease control and prevention can be exemplified by three facts. Firstly, the global eradication of smallpox in 1979 was credited to the systematic worldwide implementation of the mass smallpox immunization program (Breman *et al.*, 1980). Secondly, massive polio elimination from most regions of the world has been achieved as a result of world-wide vaccination initiative (Mshelia *et al.*,

[1] A brief history of vaccination, The Immunisation Advisory Centre, 2017; available from: https://www.immune.org.nz/vaccines/vaccine-development/brief-history-vaccination.

2020). Thirdly, only three cases of novel influenza A virus infection were recorded locally in 2017 after 379,500 doses of seasonal influenza vaccine were administered under the Hong Kong government 2017/18 vaccination program[2].

According to the World Health Organization, global vaccination coverage as represented by some of the recommended vaccines for children had reached between 75% and higher than 90% in 2017, albeit with varied coverage for different countries and regions (Piot *et al.*, 2019). Successful implementation of childhood immunization programs in Hong Kong ensures higher than 95% coverage for vaccines against common infectious diseases. The Hong Kong government vaccination programs offer free seasonal influenza and pneumococcal vaccines to eligible high-risk groups and staff members of residential care homes, which has in recent years successfully prevented large-scale outbreaks of influenza as occurred in 1968[3]. A recent comprehensive and systematic review also supports the cost-effectiveness of most of the evaluated vaccination programs in Hong Kong (Wong *et al.*, 2017).

[2] Number of notifiable infectious diseases by month, The Centre for Health Protection, Department of Health for Disease Prevention and Control, The Government of the Hong Kong Special Administrative Region. 2017; available from: https://www.chp.gov.hk/en/statistics/data/10/26/43/6470.html

[3] Vaccination Schemes, The Centre for Health Protection, Department of Health for Disease Prevention and Control, The Government of the Hong Kong Special Administrative Region. 2020; available from: https://www.chp.gov.hk/en/features/17980.html.

1.1.2 Principle of vaccination

According to our modern immunological concepts, vaccination refers to the administration of attenuated antigenic materials to stimulate the development of immune memory toward a specific pathogen, so that the immunized individual can have an augmented capacity to fight against the same pathogen following re-exposure. The major vaccine-induced immune effectors are B cells that are capable of producing antigen-specific antibodies, cytotoxic $CD8^+$ T cells that can recognize and kill pathogens or infected cells, and helper $CD4^+$ T cells that produce cytokines regulating B cell and cytotoxic T cell responses (Aloulou *et al.*, 2019). The highly specific serum IgG and mucosal IgA antibodies produced by plasma cells, which are terminally differentiated B cells, are critical immune effectors that mediate protection (Lightman *et al.*, 2019).

Following the introduction of vaccine antigens which often are proteins into the body, antigen-presenting cells (APCs), especially dendritic cells, phagocytose the antigens. Next, the vaccine antigens are processed into small fragments and displayed on the major histocompatibility complex (MHC) by the APCs. While MHC class I molecules display endogenously produced antigens to the T cell receptor of $CD8^+$ cytotoxic T cells, MHC class II molecules display phagocytosed external antigens which are recognized by the T cell receptor of $CD4^+$ T helper cells. In addition, co-stimulatory molecules, including CD80 and CD86, on APCs need to bind to CD28 on T cells, producing the co-stimulatory signal which is required for the activation and proliferation of naïve T cells (Fig. 1.1) (Bromley *et al.*, 2001). T helper cells can possibly differentiate into three subtypes: Th2

cells that are critical for clearing extracellular pathogens are always induced by dendritic cells under a steady-state or nematode infection; Th1 cells that contribute to the elimination of intracellular pathogens are produced as a result of stimulation by certain intracellular pathogens (Mosmann *et al.*, 2005; Zhu *et al.*, 2010); and the effector T helper cells which primarily work on clearing the pathogens that are not adequately handled by Th1 or Th2 cells are the Th17 cells (Veldhoen *et al.*, 2006). Nonetheless, all the three T helper cell subtypes, i.e., Th1, Th2 and Th17 cells contribute to the development of adequate humoral immune responses and regulate B cell activation and differentiation (Brazolot Millan *et al.*, 1998; Mitsdoerffer *et al.*, 2010; Nakayama *et al.*, 2017). B cell responses begin when free vaccine antigens are taken by specific subcapsular sinus macrophages and translocated into the B cell zone in the secondary lymphoid organs, where the antigens bind to the B cell receptors, which are usually surface anchored IgM molecules (Kuka *et al.*, 2018). B cells are then activated and migrate to the interface between B cell and T cell zones, where T cells are engaged to stimulate the activation and proliferation of B cells, resulting in the formation of the germinal centre (Biram *et al.*, 2020; Suan *et al.*, 2017).

It is in the germinal centre where B cells undergo somatic hypermutation which enhances the antibody affinity. The B cells that produce high-affinity antibodies are selected by follicular dendritic cells to become antibody-forming plasma cells or memory B cells that are central to immunological memory, whereas cells that have lower affinity or no specificity for antigens are eliminated (Papa *et al.*, 2018). Also, in the germinal centre, T

follicular helper cells are capable of promoting massive proliferation and differentiation of antigen-specific B cells to become plasma cells and memory B cells (Qi, 2016). Another major event in the germinal centre is the immunoglobulin class-switch. B cells switch their antibody classes from IgM to IgG, IgE or IgA, depending on the complex cytokine signals which are derived from T helper cells (Chi *et al.*, 2020). In mice, Th1 cells that produce IFN-γ promote class-switch toward IgG2a or IgG2c, while Th2 cells which produce IL-4, IL-13 and IL-5 promote class-switch to IgG1 (Scott-Taylor *et al.*, 2018).

In the germinal centre, vigorously proliferating B cells require a substantial energy supply and it was previously assumed that aerobic glycolysis remained the main source of energy supply for lymphocytes (Jung *et al.*, 2019). An elegant study has recently revealed fatty acid oxidation as a major mechanism for germinal centre B cells to meet their metabolic demand for vigorous proliferation (Weisel *et al.*, 2020).

1.1.3 Application of vaccination

Vaccines are expected to be applied to the general population from infants to old people across the age groups under many circumstances. The Department of Health of the Hong Kong Government continuously updates the immunization schedule for children. In 2020, an additional human papillomavirus vaccine has been added to the list (Table 1.1). Apart from routine immunization programs for high-risk populations, e.g., children, even adults with a lower risk of contracting pandemic diseases are also recommended to receive

vaccination. Travelers are strongly recommended to get immunized before travelling to countries with endemic diseases, such as yellow fever, malaria and cholera (Freedman *et al.*, 2019). Vaccines can also be used for post-exposure prophylaxis. In such cases vaccines are expected to provide complete protection or modify the clinical course of the disease (Bader *et al.*, 2013). For instance, the vaccine that targets measles, mumps and rubella can be protective if administered within 72 hr of initial exposure to measles (Fiebelkorn *et al.*, 2013).

The COVID-19 pandemic, which is caused by the virus SARS-CoV-2, has already hit more than 10 million people with more than 500,000 deaths when this thesis is being compiled. Currently, the viral infection has swept almost all the densely populated areas of the globe. Strategies to conquer or contain this pathogen by developing effective vaccination modalities are desperately needed. A number of vaccine developers and research institutions are currently involved in exploiting various approaches for producing vaccines against SARS-CoV-2 (Conte *et al.*, 2020).

Table 1.1 Hong Kong childhood immunization programme[4]

Age	Vaccines recommended
New-born	Bacilli Calmette-Guerin (BCG) Hepatitis B — first dose
1 month	Hepatitis B — second dose
2 months	DTaP-IPV (diphtheria, tetanus toxoids, acellular pertussis adsorbed and inactivated poliovirus (DTaP-IPV) — first dose Pneumococcal — first dose
4 months	DTaP-IPV — second dose Pneumococcal — second dose
6 months	DTaP-IPV — third dose Hepatitis B — third dose
12 months	Measles, mumps and rubella (MMR) — first dose Pneumococcal — booster dose Varicella — first dose
18 months	DTaP-IPV — booster dose Measles, mumps, rubella and varicella (MMRV) — second dose
Primary 1	Measles, mumps, rubella and varicella (MMRV) — second dose DTaP-IPV — booster dose
Primary 5	Human papillomavirus — first dose
Primary 6	DTaP-IPV — booster dose Human papillomavirus — second dose

[4] Child health – Immunisation, Family Health Service, Department of Health for disease prevention and control, The Government of the Hong Kong Special Administrative Region. 2020; available from: https://www.fhs.gov.hk/english/main_ser/child_health/child_health_recommend.html.

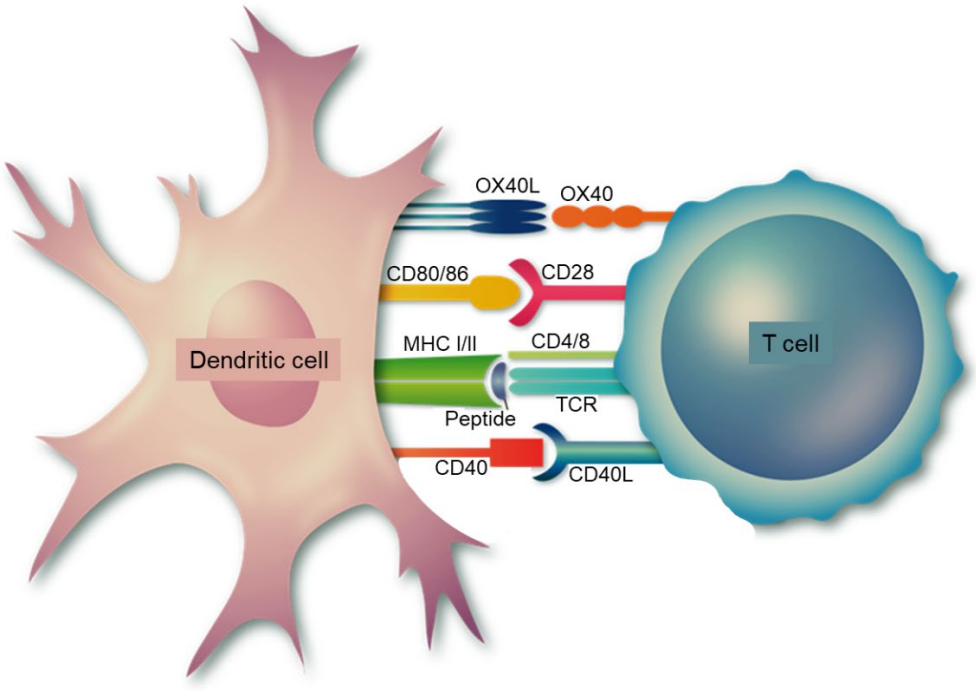

Figure 1.1 Multiple signals are required for T cell activation. The T cell receptor (TCR) engages the antigenic peptide loaded on the MHC complex. Subsequently, co-stimulation occurs through binding of CD80 and CD86 on dendritic cells to CD28 on T cells. Interactions between OX40 and OX40L as well as between CD40 and CD40L also contribute to the co-stimulatory signals that drive T cell activation.

1.1.4 Mucosal vaccination

Parenteral and mucosal vaccines are two major types of vaccines from a vaccine delivery perspective. Parenteral vaccines are delivered through intramuscular or subcutaneous injection while mucosal vaccines are delivered through the mucosal routes without the need for needles (Miquel-Clopés *et al.*, 2019). Mucosal adaptive immune responses are more efficiently induced by the administration of vaccines onto mucosal surfaces and this is why injected vaccines are generally less effective against infection at mucosal surfaces (Su *et al.*, 2016). The mucosal immunological response operates through organized lymphoid tissues known as mucosa-associated lymphoid tissue (MALT). Various types of MALT have been identified, such as gut-associated lymphoid tissue (GALT), bronchus-associated lymphoid tissue (BALT), nasopharynx-associated lymphoid tissue (NALT), and larynx-associated lymphoid tissue (LALT) (Shakya *et al.*, 2016). In addition to MALT, loose lymphoid tissues have been found at mucosal tissues, including ocular tissues, middle ear cavity, genital tracts, and mammary glands (Lycke, 2012). Among all the delivery routes for mucosal vaccination, including nasal, oral, sublingual, rectal and vaginal, nasal immunization is shown to produce the greatest systemic antibody responses in addition to robust mucosal responses. In particular, nasal immunization is particularly potent for mobilizing immune responses at a distant mucosal site such as vaginal mucosa (Lobaina Mato, 2019). Currently, most vaccines are systemically delivered except for a few licensed mucosal vaccines (Table 1.2) which include oral vaccines for polio, cholera, typhoid, and rotavirus diarrhoea, as well as an intranasal vaccine for influenza (Miquel-Clopés *et al.*, 2019; Paul, 2013).

Mucosal vaccination has certain advantages over parenteral vaccination. Firstly, as most pathogens access the body through the mucosal membranes, mucosal immunization delivered at the portal of entry can effectively stimulate local immunity which contributes to blocking infectious agents right at the portal of entry. Although systemic antibodies induced by parenteral vaccines can undoubtedly neutralize pathogens that have entered mucosal tissues by blocking their attachment and invasion to target cells, topical mucosal antibodies generated by mucosal vaccination offer an additional layer of protection by preventing the adherence of pathogens to epithelial cells under the mucosal layer (Mantis *et al.*, 2010). For example, administration of intranasal influenza vaccine induces the production of mucosal antibodies, which perform better than systemic antibodies in the control of upper respiratory tract infection (Calzas *et al.*, 2019; Fan *et al.*, 2019). It has also been discovered that mucosal immunization induces potent B and T cell memory responses (Romeu *et al.*, 2014). Secondly, the production technology of mucosal vaccines is simplified compared with that of parenteral vaccines. For instance, oral vaccines do not require extensive purification for excluding bacterial by-products such as endotoxins because the digestive tract is home to a large number of commensal bacteria and is usually tolerant to such biochemicals. In contrast, injected vaccines must be free from these life-threatening bacteria-derived products e.g., endotoxins (Smith, 2015). Thirdly, mucosal vaccination obviates the use of needles, making it not only practical for mass vaccination during pandemics, but also a safer delivery method free from the risk of blood-borne infections (Otczyk *et al.*, 2010; Schulze *et al.*, 2016).

Mucosal immune reactions are generated at mucosal immune inductive sites, which are concentrated at the portal of entry for pathogens. Major immune inductive sites include various types of MALT as explained in the previous section (Shakya *et al.*, 2016). These inductive sites are covered by follicle-associated epithelium that contains microfold cells (M cells), which are a specialized type of cells for antigen uptake and transport across the mucosal membrane (Nakamura *et al.*, 2018). The importance of the M cells in antigen uptake lies in the fact that they are strategically located on the surface of follicle-associated epithelium, and many APCs are present near or under M cells (Dillon *et al.*, 2019). Similar to systemic immunity, the generation of mucosal immunity starts with antigen uptake by dendritic cells. As antigens are not directly injected into the tissues in mucosal immunization, dendritic cells usually take up antigens transcytosed by M cells, or, less frequently, take up the antigens directly by migrating into the narrow spaces between epithelial cells or even to the outer limit of the epithelium (Dillon *et al.*, 2019). Next, dendritic cells undergo maturation and present the antigens to naïve T cells resulting in the activation of these cells. Activated T cells differentiate into effector T cells and migrate to the B cell follicle in the draining lymph nodes and spleen to initiate the germinal centre reaction.

Being the major immune effector at mucosal surfaces, IgA antibodies exist abundantly in mucosal secretions. In fact, the amount of IgA produced exceeds the sum of all other immunoglobulins produced (Corthésy, 2013). The microenvironment at the mucosa

polarized to the local supply of a panel of cytokines, including IL-4, IL-5, IL-6, IL-10, IL-21 and transforming growth factor β1 (TGF-β1), together contribute to the stimulation of B cells to expand and differentiate into plasma cells that produce secretory IgA (Boyaka, 2017). The released secretory IgA molecules are finally transported to the mucosa through the epithelial cells via polymeric Ig receptor (Turula *et al.*, 2018). Activated circulating B cells and T cells are capable of homing to the original mucosal inductive site or to another mucosal site through the expression of tissue-specific adhesion molecules and chemokine receptors that recognise endothelial counter-receptors in the mucosal vasculature (Silva-Sanchez *et al.*, 2020). For example, IgA-secreting B cells that are activated in mucosal lymphoid tissues express CCR10, while its ligand CCL28 is secreted by epithelial cells throughout the small and large intestines, salivary glands, tonsils, respiratory tract and lactating mammary glands (Gary *et al.*, 2020; Karnezis *et al.*, 2019; Mohan *et al.*, 2017). Therefore, immunization at one mucosal surface can result in protection of other unrelated mucosal regions despite the fact that lymphocytes prefer to home back to the same lymphoid tissue, where the strongest response occurs (Pasetti *et al.*, 2011).

Secretory IgA protects mucosal integrity by three major mechanisms: Firstly, immune exclusion is achieved when secretory IgA blocks the contact between the microorganisms or toxins and their target epithelial cells to prevent the surface damage, colonization, and subsequent massive invasion by the pathogen (Pasetti *et al*., 2011). Secondly, IgA can bind with antigens or microorganisms and form the secretory IgA-antigen complex which is then eliminated from the mucosal lamina propria by antigen excretion (de Sousa-Pereira

et al., 2019). Thirdly, apart from immune exclusion and antigen excretion, secretory IgA can mediate protection against viral infection via intracellular antigen neutralization, which is achieved through direct binding the viral membrane glycoproteins (Bidgood *et al.*, 2014). In addition, it has been reported that secretory IgA present in the interstitial fluids of mucosal tissues prevents pathogens that have penetrated the mucosal barrier from further invading tissues by transporting the infectious agents back into the lumen through polymeric Ig receptor or by mediating antibody-dependent cell-mediated cytotoxicity that leads to the destruction of locally infected cells (Breedveld *et al.*, 2019).

Although mucosal immunization is capable of providing robust immune protection against infectious diseases, the fact that few licensed vaccines are available reflects the difficulty of designing mucosal vaccines. Firstly, substantial amounts of antigens are diluted in mucosal secretions, captured in mucus gels, digested by proteases and nucleases, or excluded by epithelial barriers (Cerutti, 2008). Therefore, the quantity of the vaccine antigen required per dose is hard to be estimated because of antigen instability at mucosal sites and the fact that the dose of mucosal vaccine that actually enters the body cannot be accurately controlled in contrast with parenteral immunization. This problem is particularly significant in oral vaccines as soluble, non-adherent antigens are taken up at low levels in the intestine (Vela Ramirez *et al.*, 2019). Secondly, not all vaccine antigens can penetrate the epithelium and invade mucosal lymphoid tissues effectively owing to inefficient uptake and presentation by M cells (Srivastava *et al.*, 2015). Therefore, mucoadhesives such as chitosan and starch can be used to help to improve the adhesion

of vaccine antigens, especially the non-living ones, to the epithelium (Mehrabi *et al.*, 2018). Lastly, the most challenging barrier that mucosal vaccine developers have to overcome is immunotolerance. This is because the default response to proteins at the mucosal membrane is tolerance instead of productive immunity. There are several proposed mechanisms of mucosal tolerance, including direct inactivation of antigen-sensitized lymphocytes, antagonizing interactions between regulatory and effector T cells, inadequate antigen processing and presentation by mucosal tolerogenic dendritic cells, and generation of "tolerogenic" proteins (Raker *et al.*, 2015). Furthermore, it is also believed that mucosal tolerance is influenced by the commensal bacteria that colonize mucosal surfaces (Belkaid *et al.*, 2014). As a result, mucosal adjuvants with immunostimulatory functions that can potentially overcome the immune barrier effect at mucosal sites are particularly required for successful mucosal vaccination.

Table 1.2 Licensed mucosal vaccines (Miquel-Clopés *et al.*, 2019)

Pathogen	Trade name	Delivery route	Formulation
Vibrio cholerae	Dukoral®	Oral (liquid)	Inactivated
	ShanChol®	Oral (liquid)	Inactivated
	Euvichol®	Oral (liquid)	Inactivated
	Vaxchora®	Oral (liquid)	Live attenuated
Influenza type A and B virus	FluMist™	Intranasal (spray)	Live attenuated
Poliovirus	Biopolio™ B1/3 3	Oral (liquid)	Live attenuated
Rotavirus	Rotarix®	Oral (liquid)	Live attenuated
	RotaTeq®	Oral (liquid)	Live attenuated
Salmonella typhimurium	Typhi Vivotif	Oral (capsules)	Live attenuated
Adenovirus	Approved for military use	Oral (tablets)	Live attenuated

1.2 Adjuvant

1.2.1 General introduction to adjuvant

Adjuvants are molecules or macromolecular structures that can induce more potent and long-lasting protective immune responses to antigens. An ideal mucosal adjuvant is expected to promote uptake of antigens via mucosal surfaces, protect the antigens from being degraded by mucosal proteases, augment dendritic cell activation, and stimulate potent B and T cell responses, apart from being non-carcinogenic, non-pyrogenic, and stable in a wide pH range (Guy, 2007; Newsted *et al.*, 2015; Petrovsky, 2015). Potent stimulation of the production of mucosal IgA is also a feature required of a good mucosal adjuvant (Boyaka, 2017).

However, it is very difficult to develop a perfect adjuvant. Traditionally, researchers try to find a balance between effectiveness and safety (Gupta *et al.*, 1993). Aluminium salt (alum) has been included in the formulations of most injectable vaccines with reliable adjuvanticity and a good safety record. However, alum is not effective in boosting mucosal immunization (Yusuf *et al.*, 2017).

1.2.2 Mechanisms underlying the adjuvanticity

The mechanisms of adjuvants have been ascribed to delivery facilitation and immunostimulation. For mucosal immunization, delivery vehicles can be considered as adjuvants which aid the penetration of vaccine antigens through the mucosa. M cells are

usually the best target for designing delivery molecules to facilitate the uptake of mucosal vaccine antigens. Therefore, M cell-specific antibodies, such as NKM 16-2-4, or M cell-targeting ligands, such as Co1, are possible vehicles for delivering antigens. Apart from these M cell-specific biomolecules, microparticles, liposomes, and immune stimulating complexes are also possible mucosal delivery systems that are under investigation (Kuolee *et al.*, 2008).

For parenteral vaccination, the formation of a depot at the injection site can also facilitate the vaccine delivery, which is perhaps the most widely recognized and oldest mechanism of action for adjuvants. Therefore, some adjuvants can trap the vaccine antigens and thus facilitate slow antigen release at the site of injection, ensuring the constant stimulation of the immune system (Awate *et al.*, 2013). Various adjuvants such as biodegradable micro- and nanoparticles and water-in-oil emulsions [e.g., complete Freund's adjuvant (CFA)] are shown to use the depot effect for exerting adjuvant activity (Herbert, 1968; B. Sun *et al.*, 2016). The cationic adjuvant formulation (CAF) 01, a combination of dimethyldioctadecylammonium/trehalose-6,6-dibehenate (DDA/TDB) that induces long lasting depot effect, is now approved for clinical practice (Sisteré-Oró *et al.*, 2020).

Immunostimulatory molecules under extensive testing include bacterial toxins, cytokines, and toll-like receptor (TLR) agonists which can be recognized by pattern recognition receptors (PRRs). These molecules interact with specific cellular receptors and trigger an immune response. To date, cholera toxin and *Escherichia coli* labile toxin are the most

well-recognized immunostimulators. However, cholera toxin and *Escherichia coli* labile toxin can never be applied in human mucosal immunization owing to their high toxicity (Eriksson *et al.*, 2004). Inflammasome activation, which is critical for the development of adaptive immunity, is also considered as a mechanism of adjuvants (Ivanov *et al.*, 2020). Alum as a clinically applicable adjuvant is capable of inducing the release of IL-1β from macrophages and dendritic cells through activation of the NALP3 inflammasome (Kool *et al.*, 2008).

Non-toxic attenuated forms of cholera toxin and *Escherichia coli* labile toxin have been developed, and their adjuvanticity was initially found to be comparable to the natural form upon nasal administration (Clements *et al.*, 2018; Pizza *et al.*, 2001; Schussek *et al.*, 2020).

Unfortunately, Bell's palsy, a facial paralysis, developed in individuals who had received mucosal vaccines containing LTK63, a mutant form of *Escherichia coli* labile toxin, resulting in a setback in the development of mucosal adjuvants (Lewis *et al.*, 2009). CTA-DD, which is a fusion protein composed of CTA1, the ADP-ribosylating part of cholera toxin, and DD, two Ig-binding domains derived from *Staphylococcus aureus* protein A, has also been under investigation as a promising mucosal adjuvant (Lycke *et al.*, 2010; Schussek *et al*., 2020).

TLR agonists have been extensively investigated as mucosal adjuvants, presumably because they activate key innate signalling pathways and stimulate mucosal dendritic cells

that in turn orchestrate adaptive immune responses following pathogen infection (S. Kumar *et al.*, 2019). The licenced adjuvant IC31 and CpG oligodeoxynucleotide-containing experimental adjuvants target TLR9 and promote Th2 and cytotoxic T cell responses (Sarkar *et al.*, 2019; Schellack *et al.*, 2006). Muramyl dipeptide (MDP), monophosphoryl lipid A (MPL) and flagellin B, which upregulate T cell responses by targeting various types of TLRs, are also being considered as adjuvant candidates (F. Liu *et al.*, 2019; Oh *et al.*, 2019; Pirahmadi *et al.*, 2019). TLR agonists and mutant enterotoxins are the two most attractive types of mucosal adjuvants under experimental investigation. However, stringent safety concerns have hampered the progress of adjuvant development using these approaches (Petrovsky, 2015).

Cytokines such as interferons, interleukins, and granulocyte-macrophage colony-stimulating factor (GM-CSF), have been tested as potential mucosal adjuvants because they can modulate both innate and adaptive immune responses, including differentiation of Th1 and Th2 cells, stimulation of cytotoxic natural killer cells, activation of cytotoxic T cells, and maturation of APCs (Thompson *et al.*, 2011). IL-12 is shown to be an effective mucosal adjuvant for nasal immunization (Wright *et al.*, 2008). IL-2 has been tried as an oral vaccine adjuvant (Hinc *et al.*, 2014). However, these molecules are mostly short-lived and induce dose-dependent toxicity, thus limiting their application in clinical practice.

Some clinically applicable and experimental adjuvants possess both capacities as a delivery facilitator and immune stimulator, such as alum, chitosan, and CFA (Gołoś *et al.*, 2015; Malik *et al.*, 2018; Mohan *et al.*, 2013).

1.2.3 Exploitation of damage-associated molecular pattern (DAMP) molecules as mucosal adjuvants

As discussed above, pathogen derived PAMPs are potent immune stimulators which can be recognized by PRRs such as TLRs (H. Kumar *et al.*, 2011). However, strong immune responses can also be elicited even in sterile conditions such as autoimmune disorders, tumorigenesis, tissue transplantation, ischemia and traumatic responses (Vénéreau *et al.*, 2015). Polly Matzinger proposed the participation of another category of immunostimulators known as DAMPs in immune responses as a "danger theory" (Matzinger, 2002, 2012), which was later confirmed by the recognition of high mobility group box 1 (HMGB1) and uric acid crystals as DAMPs (Eleftheriadis *et al.*, 2013; Kang *et al.*, 2010). DAMPs, also known as alarmins, form a heterogeneous group of endogenous biomolecules that are capable of initiating sterile inflammation and promoting immune responses.

DAMPs are released to the extracellular environment passively during cell necrosis or actively because of cell injury or stress (Kataoka *et al.*, 2014; Murakami *et al.*, 2014). Secreted DAMPs can stimulate an inflammatory response, thus alerting the body of a danger, and finally promote tissue repair through various pathways (Sharma *et al.*, 2016).

In addition to being potent immune stimulators upon release, DAMPs also exert physiological roles intracellularly during the steady state (Sharma *et al.*, 2016).

Different DAMPs reside in different intracellular locations, including nucleus, cytosol and mitochondria, and are differentially released based on the types of trauma (Fig. 1.2) (Anders *et al.*, 2014). Although all DAMPs are capable of inducing proinflammatory responses and share common roles in immune stimulation, each DAMP has its unique functions based on its receptors, as illustrated in Table 1.3 (Roh *et al.*, 2018; Schaefer, 2014). DAMPs contribute significantly to the development of inflammatory responses as they are released immediately after tissue damage at various intensities including life-threatening trauma (Zhang *et al.*, 2010). Being immune stimulators similar to PAMPs, DAMPs are also predicted to have potential mucosal adjuvant activities. DAMPs and PAMPs stimulate immune responses using shared mechanisms, both by binding and activating PRRs, such as TLRs, purinergic receptors and NLRP3, on immune cells (Fig. 1.3) (Anders *et al*., 2014). In addition, several DAMPs, including HMGB1 and S100A12, can also bind to receptor for advanced glycation end products (RAGE) which is a prototypic DAMP receptor (R. Liu *et al.*, 2009). The initial immune responses elicited by RAGE are amplified in the presence of DAMPs as the expression of RAGE is upregulated by the presence of its ligands (Ibrahim *et al.*, 2013). Although DAMPs are structurally heterogeneous, different DAMPs are capable of binding and activating the same PRRs, most often TLR2 and TLR4 (Schaefer, 2014). For example, HMGB1, apart from promoting transcription intracellularly, can bind to TLR2, TLR4 and RAGE upon release

from damaged cells (Lotze *et al.*, 2005). Following stimulation by DAMPs, APCs such as dendritic cells are activated, and differentiation and proliferation of antigen-specific T cells and B cells are promoted, resulting in the expansion of antigen-specific cytotoxic T cells and augmented antibody production (Bianchi, 2007; van Beijnum *et al.*, 2008).

1.2.4 Measurement of adjuvanticity

Adjuvanticity refers to the immunological activity of the adjuvant in terms of its capacity to modify and strengthen the immune response (Guy, 2007). A biomolecule that can only stimulate immune responses to a limited extent can hardly be used as a reliable mucosal adjuvant, because mucosal vaccines require a substantially strong immune potentiator to overcome the mucosal tolerance. Therefore, parameters that can quantify adaptive immune responses are used to assess the adjuvanticity of mucosal adjuvant candidates. The maturation of adaptive immunity involves three crucial components: APCs, lymphocytes and antibodies.

First of all, antigen-specific antibody levels both in systemic circulation and at mucosal sites are fundamentally important for assessing the quality of adjuvants. Serum antigen-specific IgG and mucosal antigen-specific IgA and IgG are thus important readouts.

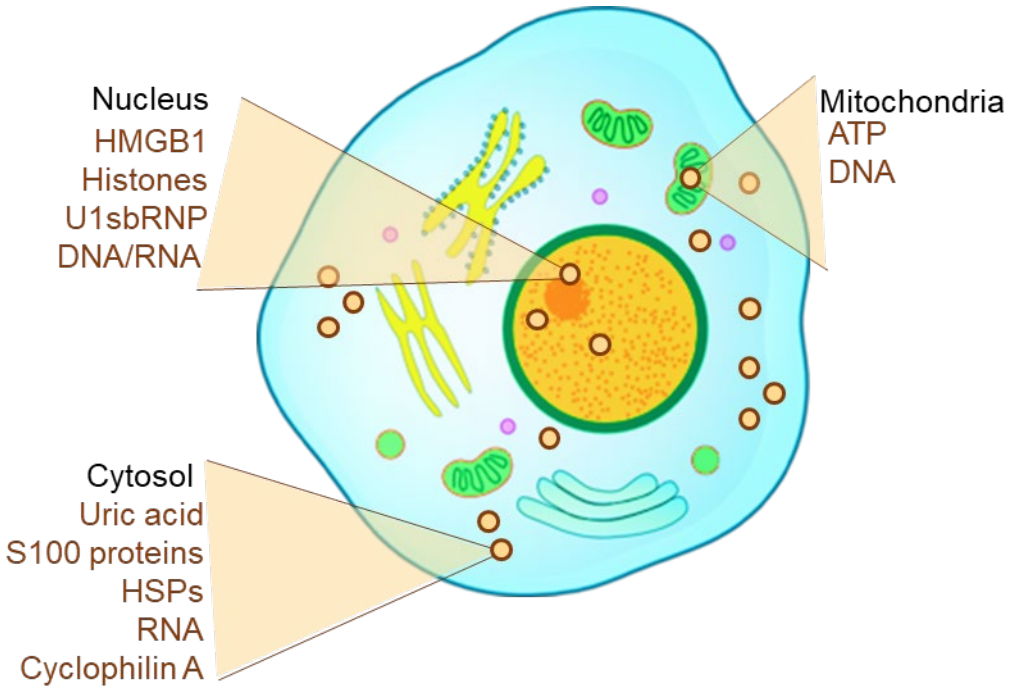

Figure 1.2 Damage-associated molecular pattern (DAMP) molecules have multiple origins. DAMPs are released from various sources during both apoptosis and necrosis. The type of death defines the spectrum of the DAMP molecules released.

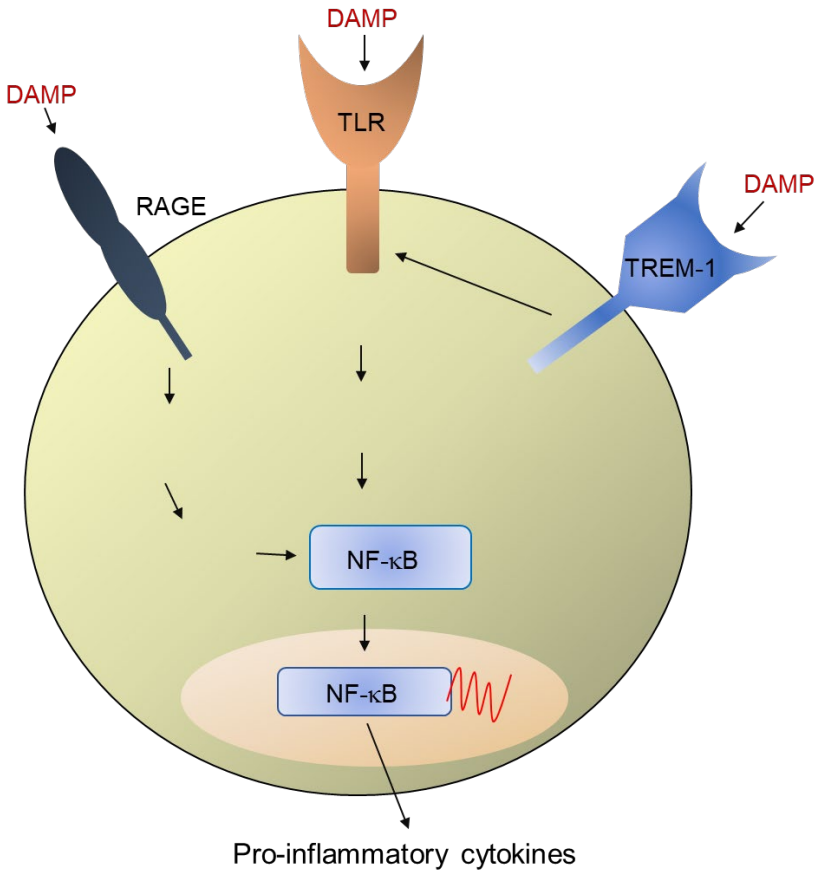

Figure 1.3 Damage-associated molecular pattern (DAMP) molecules can promote inflammation. DAMPs can activate different pattern recognition receptors (PRRs) on dendritic cells, including toll-like receptors (TLR), receptor for advanced glycation end products (RAGE) and triggering receptor expressed on myeloid cells 1 (TREM-1). Despite the different intermediate pathways through which these receptors signal, all the pathways converge finally in the expression and activation of NF-κB, a critical transcription factor for the induction of proinflammatory cytokines.

Table 1.3 Characteristics of damage-associated molecular pattern (DAMP) molecules and their corresponding receptors (Roh et al., 2018; Schaefer, 2014)

DAMP	Mode of release	Receptor	Role in inflammation/ immunity
HMGB1	Passive release Active secretion	TLR2, TLR4 RAGE TIM3	Recruitment/activation of immune cells
IL-1α	Passive release	IL-1R	Strong proinflammatory activity
Histones	Passive release Surface exposure Active secretion	TLR2 TLR4 TLR9	TLR- and inflammasome-dependent inflammatory response
ATP	Passive release Active secretion	P2Y2 P2X7	Macrophage recruitment IL-1β production by dendritic cells Antitumor immunity
Cyclophilin A	Active secretion	CD147	Recruitment of inflammatory cells Release of inflammatory mediators
Uric acid crystals	Passive release	NLRP3	Dendritic cell maturation Neutrophil recruitment
S100s	Passive release	TLR2 TLR4 RAGE	Potent immune-stimulatory activity; monocyte and neutrophil recruitment
Mitochondrial DNA	Passive release	TLR9	Macrophage and neutrophil activation
Mitochondrial transcription factor A	Passive release	RAGE, TLR9	Dendritic cell activation Type I interferon release
Calreticulin	Passive release Surface exposure	CD91	Potent “eat me” signal; mediator of tumour immunogenicity

Moreover, Th1 and Th2 responses in mice will result in preferential class-switch to IgG2c and IgG1, respectively, and therefore, both antibody subclasses can be quantified to indicate the polarization of immune responses by the adjuvant (Tesfaye *et al.*, 2019). Measuring the extent of dendritic cell activation, which represents the potency of the initial immune stimulation, is a simple and direct way to evaluate the effectiveness of adjuvants, as quite some experimental adjuvants do target dendritic cells (Kreutz *et al.*, 2013).

Germinal centres are critical for both class-switch recombination and affinity maturation of B cells, key steps for the generation of high-quality antibody responses. Germinal centre mobilization is a prerequisite condition for the production of high-efficiency neutralizing antibodies that can protect against pathogen infection and bacterial exotoxins. T follicular helper cells are critical for activating germinal centre B cells (Tangye *et al.*, 2020). Both processes involve engagement of CD40 on B cells by CD40L on T cells. Therefore, adjuvant activity can be assessed by measuring germinal centre responses (e.g., T follicular helper cell expansion, germinal centre B cell activation) after immunization.

1.3 Significance of the study

Mucosal vaccines are particularly useful in defence against pathogens that infect by penetrating the mucosal barrier, as mucosal vaccination can more efficiently generate local immune defence mechanisms including both antigen-specific secretory IgA and antigen-specific T cells at mucosal sites. Pathogens that cause gastrointestinal, respiratory

and genital infections are on the top list of targets for mucosal vaccination (Nizard *et al.*, 2014). The lack of satisfactory mucosal adjuvants that effectively mobilize the development of adaptive immunity has always been the hurdle in the implementation of mucosal immunization. For example, most of the SARS-CoV-2 vaccine endeavours currently under development are injection-based except a recombinant protein vaccine modality developed by Vaxart, which is designed to be delivered orally (W. H. Chen *et al.*, 2020).

This pioneering project, which focuses on exploitation of the DAMP molecules as a novel class of mucosal adjuvants, may shed light on the development of potent mucosal adjuvants that also meet the stringent safety standards. In the global context of the fight against the COVID-19 pandemic, this study timely addresses novel mucosal adjuvants for nasal vaccination and is likely to lead to translational and exploitable data with a social impact.

Chapter 2 — Materials and methods

2.1 Immunization

The strain of the mice chosen for this study was C57BL/6, which is one of the most commonly used laboratory rodent strains. All animals studied in this thesis were bred in-house at the Centralized Animal Facilities at the Hong Kong Polytechnic University. Female mice were six to eight weeks old at the start of all experiments. All procedures involving animals were conducted at the Centralized Animal Facilities of the university, and the animal ethics approval was obtained from the Animal Subjects Ethics Sub-Committee of the university.

For most of the immunization assays, mice were intranasally immunized with ovalbumin (OVA) (Sigma-Aldrich; A5503), which is the major protein component in chicken egg white and was used as an experimental vaccine antigen in this study. Given the disturbingly deadly outbreak of COVID-19 at the closing period of my PhD candidature, I also tested the spike protein (the receptor-binding domain; recombinant product from Sino Biological; 40592-V05H) of SARS-CoV-2, which is the causal virus of COVID-19, as an experimental antigen with a timely and translational significance. DAMP molecules, including S100A4 (Gentaur Molecular Products; 01-2081A4M), cyclophilin A (Abcam; Ab202256), uric acid (Sigma-Aldrich; U2625) or HMGB1 (Gentaur Molecular Products; 764006) were tested as an adjuvant. Cholera toxin (List Biological Labs; 100B) and lipopolysaccharide (LPS) from *Escherichia coli* (Sigma-Aldrich; L2654) were used as positive control adjuvants. Cholera toxin, which is an exotoxin produced by *Vibrio cholerae* and responsible for causing cholera diarrhoea,

has been claimed to be a gold standard mucosal adjuvant for experimental use (W. Chen *et al.*, 2010; Sanchez *et al.*, 2011). LPS is a gram-negative bacterial endotoxin that is also a potent immune stimulator.

For immunization, mice were anaesthetized by isoflurane before receiving 20 μl of the vaccine preparation which was pipetted to the mouse's nostrils for being taken up into the nasal cavity along with natural breathing. Each mouse was immunized intranasally 2-4 times with a 10-day interval according to various experimental designs.

2.2 Tissue harvesting and processing

Ten days or three days, depending on the experimental design, after the last immunization, all the mice were killed. Blood, spleen, lymph nodes, vaginal washings, bone marrow, bronchoalveolar lavage fluid (BALF) and the exudates of lungs, nasal tissue, and eyes were collected according to the specific experimental design.

Blood was collected from the jugular vein or facial vein and was allowed to stand for at least 1 hr, preferably 2 hr, to allow clotting. The whole blood was then centrifuged for 5 min at 300 × g followed by aliquoting. Caution was taken during serum collection to avoid red blood cell contamination. Mouse vaginal secretion was collected by rinsing the vaginal mucosal surface with phosphate-buffered saline (PBS) for 5 consecutive days before the mice were killed. The collected vaginal samples from individual mouse were pooled for measurement to avoid the interference of the mouse hormonal circles.

Cervical lymph nodes and spleens were collected three days after the last immunization for investigating the T cell, B cell and germinal centre responses. Single cell preparations were obtained by sieving through a 70-μm cell strainer (Fisher; T_70122363548). The resulting cell suspensions were centrifuged at 400 × g for 5 min. For splenocyte preparation, red blood cells were lysed by the addition of 1 ml of red cell lysis buffer followed by incubation for 1 min. The reaction was stopped by the addition of excess PBS followed by centrifugation. The cell pellet was resuspended in 1 ml of RPMI 1640 cell culture medium (Thermo; 61870127). Next, the cell suspension was transferred into a filter tube to remove cell clusters for flow cytometric analysis.

For bone marrow cell preparation, the bone marrow from mouse tibia and femur was collected by cutting both ends of the bone followed by flushing with cold PBS using a 23-gauge needle and a syringe. Bone marrow cells were filtered through a 70-μm cell strainer followed by centrifugation. Red blood cells were removed using the red cell lysis buffer as described above. For obtaining bone marrow-derived dendritic cells (BMDCs), fresh bone marrow cells were collected from naïve mice and cultured at 37ºC with 5% CO_2 in normal cell culture medium (RPMI 1640) containing HEPES (2.5 mM) and 200 ng/ml FMS-like tyrosine kinase 3 (Flt3) ligand (PeproTech; 250-31L) for 9 days without any disturbance. The purity of BMDCs were confirmed by the surface expression of CD11c and MHC class II using flow cytometry (Fig. 2.1). Similarly for obtaining bone marrow-derived mast cells (BMMCs), fresh bone marrow cells were cultured at 37ºC with 5%

CO_2 in cell culture medium (RPMI1640) containing HEPES (2.5 mM), L-glutamine (4 mmol/l), 2-mercaptoethanol (50 μmol/l), sodium pyruvate (1 mmol/l), non-essential amino acids (0.1 mmol/l), penicillin/streptomycin (100 μg/ml) (all from Sigma-Aldrich), 10% fetal bovine serum (FBS) (Life Technologies; 10270106) and 10 ng/ml IL-3 (PeproTech; 213-13) for 3 weeks. The medium was changed every 3-4 days and adherent cells were removed. Mast cell differentiation was confirmed by the surface expression of c-Kit and FcεRI using flow cytometry (Fig. 2.2).

For harvesting the lungs, nose and eyes, blood was removed by cardiac puncture prior to excising the tissues. Lung, eye and nasal tissues were removed and homogenized using the Precellys Evolution Homogenizer (Bertin Technologies) in the presence of the radioimmunoprecipitation assay (RIPA) buffer and the protease inhibitor (Life Technologies; 89900) for 45 sec at 2ºC. Homogenized tissue samples were then centrifuged at 10,000 × g for 20 min at 4ºC before collecting the supernatant.

BALF was collected by lavaging the mouse lungs 3 times with 1 ml PBS and the retained fluid was centrifuged at 400 × g for 5 min and 4ºC before collecting the supernatant.

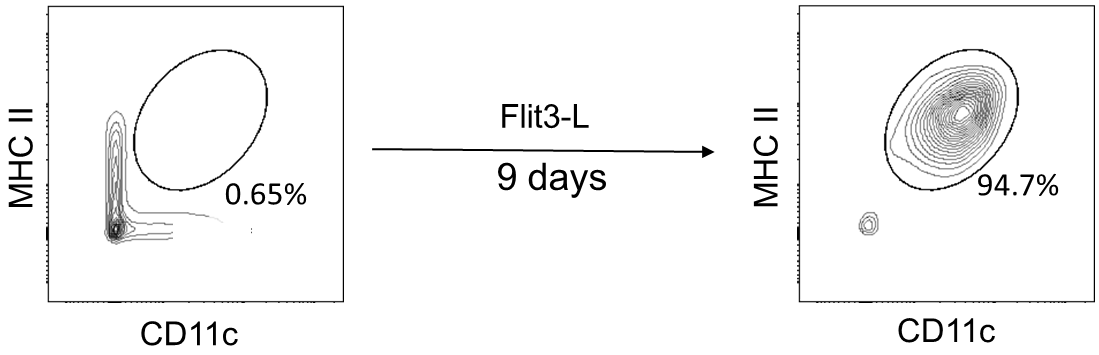

Figure 2.1 Differentiation of dendritic cells from bone marrow. Bone marrow cells were incubated in the presence of 200 ng/ml Flt3 ligand for 9 days. The purity of dendritic cells was confirmed using flow cytometry. Numbers adjacent to outlined areas indicate percentages of $CD11c^{+}$MHC class II^{+} cells in the respective circled gates.

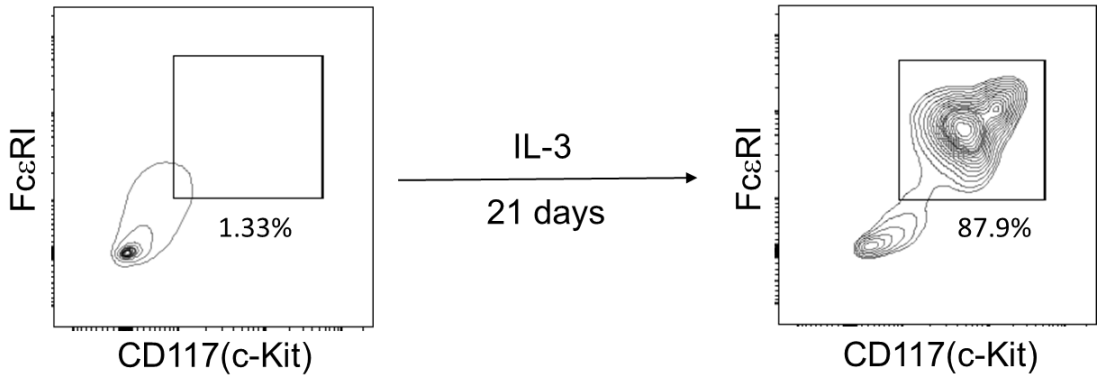

Figure 2.2 Differentiation of mast cells from bone marrow. Bone marrow cells were incubated in the presence of 10 ng/ml IL-3 for 21 days. The purity of mast cells was confirmed using flow cytometry. Numbers adjacent to outlined areas indicate $FcεRI^{+}$ and c-Kit^{+} cells in the gated population.

2.3 Tissue analysis

2.3.1 ELISA

Enzyme-linked immunosorbent assay (ELISA) was employed to measure the titres of serum OVA-specific antibodies after mucosal immunization. The antibody classes measured included total IgG and IgA as well as IgG subclasses including IgG1 and IgG2c. A 96-well flat-bottom ELISA plate (Thermo Fisher Scientific; 467320) was coated with 100 µl OVA (200 µg/ml in PBS), followed by an overnight incubation at 4ºC. Next, the ELISA plate was washed for 2 times using a washing buffer containing 0.01% Tween-20 dissolved in PBS. The wells were then incubated with 100 µl blocking buffer – PBS containing 1% FBS, followed by incubation at 37ºC for 1 hr. After washing, mouse serum was added at 10 µl/well after a two-fold serial dilution with PBS followed by incubation at 37ºC for 2 hr. Next, the plate was washed 5 times to maximally reduce unspecific binding. Goat anti-mouse secondary antibodies for IgG (Southern Biotech; 1030-05), IgG1 (Southern Biotech; 1070-05), IgG2c (Southern Biotech; 1079-05) or IgA (Southern Biotech; 1040-05) conjugated with horseradish peroxidase were added at a dilution of 1:3000, followed by incubation at 37ºC for 1 hr. After washing 5 times, 100 µl of O-phenylenediamine dihydrochloride (OPD) solution (Thermo Scientific; 34006 and 34062) was added to each well for colour development at room temperature. To stop the reaction, 100 µl of 2.5 M H_2SO_4 was added to each well when the colour strength development in wells containing positive control samples discontinued, which usually took about 10 to

30 min. The optical density (OD) or absorbance was measured at 490 nm using a spectrophotometer (BMG SPECTROStar Nano microplate reader).

2.3.2 ELISpot

The enzyme-linked immunospot (ELISpot) was used to measure frequency of OVA-specific IgG secreting plasma cells at the single-cell level in bone marrow after immunization. A 96-well MultiScreen$_{HTS}$ HA filter ELISpot plate (Merck; MSHAS4510) was coated with 100 µl OVA (200 µg/ml in PBS), followed by an overnight incubation at 4ºC. Next, the plate was washed 3 times using PBS and incubated with 100 µl blocking buffer – PBS containing 10% FBS, followed by incubation at room temperature for 1 hr. After washing with PBS, 100 µl complete culture medium were added into each well and the plate was incubated at 37ºC for 2 hr. Next, 100 µl complete media containing 1×10^6 bone marrow cells from each mouse were added into each well followed by incubation at 37ºC overnight. The plate was washed 3 times and a goat anti-mouse secondary antibody conjugated with horseradish peroxidase for IgG was added at a 1:2000 dilution, followed by incubation at room temperature for 4 hr. After washing 3 times, 3-amino-9-ethylcarbazole (AEC) substrate (BD; 551951) was used for developing the colour (Davis *et al.*, 2020). When the desired intensity of the immunospots was reached, the plate was rinsed with running water. The number of spots was recorded.

2.3.3 Flow cytometry

For cell surface marker staining, cells in 5-ml FACS tubes were incubated with relevant fluorescent antibodies for 15 min on ice in darkness. After the incubation, cells were washed by PBS, resuspended in 200 µl PBS containing 1% FBS and stored on ice protected from light until analysis with a flow cytometer (BD FACSAria III). For intracellular molecule staining, where necessary, the protein transport inhibitor brefeldin (eBioscience; 00−4506−51) was used at a concentration recommended by the manufacturer. Cells were fixed using a fixation buffer (Thermo; 88−8824−00) followed by incubation with relevant fluorescent antibodies diluted in the permeabilization buffer (Thermo; 88−8824−00) for 15 min on ice in darkness before analysis.

For measuring dendritic cell activation, expression of co-stimulatory molecules CD80 and CD86 in $CD11c^{+}$MHC class II^{+} cells was analysed. B cell activation was examined by measuring the frequency of $CD69^{+}CD38^{+}$ cells in $B220^{+}CD3^{-}$ cells. Frequencies of $GL\text{-}7^{+}FAS^{+}CD38^{-}$ in $B220^{+}CD3^{-}$ cells were recorded for measuring germinal centre expansion. Follicular helper T cell expansion was determined by the percentage of $PD\text{-}1^{+}CXCR5^{+}Foxp3^{-}$ cells in $CD4^{+}$ cells.

For assessing T cell memory responses, spleens were harvested from mice 3 days after the boost immunization. Single splenocytes were re-stimulated *in vitro* with 200 µg/ml OVA followed by incubation for 72 hr. CD4 T cell activation was confirmed by

measuring the intracellular expression of the nuclear proliferation marker Ki-67 using flow cytometry. All the antibodies used in flow cytometry are listed in Table 2.1.

2.3.4 Immunohistochemistry

For the germinal centre response analysis, spleen tissue samples were sectioned using CryoStar™ NX70 Cryostat (Thermo Fisher Scientific) followed by immunohistochemistry staining. Slides were first incubated in 0.2% Triton X-100 in PBS for 10 min followed by washing with PBS. Next, slides were incubated in paraformaldehyde (4%) for 30 min followed by an overnight incubation with a blocking solution (10-20% FBS and 5% bovine serum albumin) (Lee *et al.*, 2018). After washing with PBS, slides were incubated overnight at 4ºC with primary antibodies including GL-7-Alexa Fluor 488 (1:50 dilution), Ki-67-Horizon V450 (1:30 dilution) and CD45R/B220-biotin (1:500 dilution) followed by a 4 hr incubation at room temperature with streptavidin-Alexa Fluor 594 at a 1:150 dilution. Next, the slides were washed in PBS and mounted with an anti-fade mounting medium and a coverslip. Dried slides were examined under a Leica TCS SPE Confocal microscope with 60 × zoom. The details of the antibodies used are explained in Table 2.1. Data was analysed using LAS X Leica software.

Table 2.1 List of antibodies used in this project

Antibody	Source
CD11c-PE	Life Technologies-eBioscience™; 12-0114-83
MHC class II-APC	Life Technologies-eBioscience™; 17-5320-82
CD80-PerCP-Cy™5.5	BD; 560526
CD86-FITC	Life Technologies-eBioscience™; 11-0862-85
CD45 (B220)-FITC	Life Technologies-eBioscience™; 11-0452-85
CD3-Brilliant Violet 421™	Bio-gene; 564008
CD69-PerCP-Cy™5.5	BD; 551113
CD38-PE	Biolegend; 102708
GL-7-Alexa Fluor® 647	BD; 561529
CD95 (FAS)-PE-Cy™7	BD; 557653
CD279 (PD-1)-PE-Cyanine 7	Life Technologies-eBioscience™; 25-9985-82
CXCR5 -PE-CF594	BD; 562856
Foxp3-Brilliant Violet 421™	Biolegend; 126419
CD4-APC-H7	BD; 560181
Ki-67-FITC	BD; 556026
GL-7-Alexa Fluor 488	Life Technologies-eBioscience™; 53-5902-82
Ki-67-Horizon V450	BD; 561281
CD45R/B220-biotin	BD; 553086
Streptavidin-Alexa Fluor 594	Life Technologies-eBioscience™; S32356
CD117 (c-Kit)-APC	Biolegend; 105812
FcεR1-PE	Life Technologies-eBioscience™; 12-5898-83
TNF-α–PE-Cyanine7	Life Technologies-eBioscience™; 25-7423-82
IL-13-PE	Life Technologies-eBioscience™; 12-7133-41

2.3.5 Matrix-assisted laser desorption/ionization (MALDI) time-of-flight (TOF) mass spectrometry (MS)

Spleens were sectioned using CryoStar™ NX70 Cryostat in the absence of the optimal cutting temperature compound (OCT). The sections were embedded onto an indium tin oxide (ITO)-coated conductive glass slide and left to dry in a vacuum desiccator overnight.

Next, a layer of MALDI matrix [2,5-dihydroxybenzoic acid (30 mg/ml) dissolved in a mixture of 70% acetonitrile and 30% water containing 0.1% trifluoroacetic acid] is applied by aerosol spraying onto the dried slides. Matrix-coated slides were then mounted on the MALDI target adapter after wiping off the matrix from the outer regions of the slide using tissue wetted with ethanol to ensure optimum electric contact with the adapter. Slides were then analysed for lipids and fatty acids using a Bruker UltrafleXtreme MALDI-TOF mass spectrometer. Results were processed using SCiLS Lab 2020 Pro software.

2.3.6 RNA extraction, cDNA synthesis and RT-qPCR

Total RNA was isolated using the RNeasy Mini Kit (Qiagen; 74106). cDNA was synthesized using the RevertAid First Strand cDNA Synthesis Kit (Thermo Fisher Scientific; K1622). The generated cDNA was used as a template for RT-qPCR, which was performed with the ViiA 7 Real-Time PCR System (Applied Biosystems) using the Power SYBR™ Green PCR Master Mix (Thermo Fisher Scientific; A25776). PCR was carried out with an initial incubation at 50°C for 2 min, 95°C for 2 min, and then 40 cycles

of 95°C for 15 sec followed by a last incubation at 60°C for 1 min. The specificity of the reaction was verified by melt curve analysis. For comparison between the transcript levels between different samples, the 2-ΔΔCt method was used. GAPDH was amplified as an internal control. The forward and reverse primers used are described in Table 2.2.

2.4 Data presentation and statistical analysis

Where appropriate, data were plotted as mean ± standard error of the mean (SEM). Comparisons of the means between independent groups were analysed by Mann-Whitney *U* test using GraphPad Prism 7.00. $P < 0.05$ was considered as statically significant.

Table 2.2 Target genes and primers

Target Gene	Forward primer sequence (5'-3')	Reverse primer sequence (5'-3')
GAPDH	GGTGAAGGTCGGTGTGAACGGA	TGTTAGTGGGGTCTCGCTCCTG
IL-33	GATGGGAAGAAGCTGATGGTG	TTGTGAAGGACGAAGAAGGC
NLRP3	TGCTCTTCACTGCTATCAAGCCCT	ACAAGCCTTTGCTCCAGACCCTAT
IFN-γ	TAGCCAAGACTGTGATTGCGG	AGACATCTCCTCCCATCAGCAG
TNF-α	AAGCCTGTAGCCCACGTCGTA	AGGTACAACCCATCGGCTGG
IL-1β	GGAGAACCAAGCAACGACAAAATA	TGGGGAACTCTGCAGACTCAAAC
IL-2	CCTGAGCAGGATGGAGAATTACA	TCCAGAACATGCCGCAGAG
IL-6	CCACTTCACAAGTCGGAGGCTTA	CCAGTTTGGTAGCATCCATCATTTC
IL-10	GCCAGAGCCACATGCTCCTA	GATAAGGCTTGGCAACCCAAGTAA
CD40	GTTTAAAGTCCCGGATGCGA	CTCAAGGCTATGCTGTCTGT
CD80	GGTATTGCTGCCTTGCCGTT	TCCTCTGACACGTGAGCATC
CD86	TCCTGTAGACGTGTTCCAGA	TGCTTAGACGTGCAGGTCAA

Chapter 3 ─ Results

3.1 Screening of DAMP molecules as a potential candidate for mucosal adjuvant

3.1.1 S100A4 and cyclophilin A potently promote antigen-specific antibody production after mucosal immunization

Four DAMP molecules, including S100A4, cyclophilin A, uric acid and HMGB1, were initially selected to test for their mucosal adjuvant activities based on the fact that none of them had been formally described as mucosal adjuvants. S100A4 had been implicated as important for mucosal immunization (J. B. Sun *et al.*, 2017); cyclophilin A (Hou *et al.*, 2016), uric acid (Mortellaro *et al.*, 2012) and HMGB1 (Fagone *et al.*, 2011) had been used as adjuvants for parenteral immunization. To this end, mice were divided into six groups; each group was immunized with the experimental vaccine antigen OVA in the presence or absence of a candidate DAMP molecule as an adjuvant (Fig 3.1A) according to the formulations illustrated in Table 3.1.

Nasal immunization adjuvanted with any of the four chosen DAMP molecules except uric acid induced antigen-specific humoral immune responses. Substantially increased OVA-specific total IgG, IgG1 and IgG2c levels were observed after immunization adjuvanted with S100A4 or cyclophilin A (Fig 3.1B and C). HMGB1 also demonstrated a trend of adjuvant activity with enhanced OVA-specific antibody levels, albeit not reaching statistical significance (Fig 3.1D). In contrast, uric acid failed to facilitate the production of antigen-specific antibodies (Fig 3.1E). Among the three DAMP molecules that demonstrated positive responses, S100A4 most consistently enhanced the antibody levels

(Fig 3.1B). Mice immunized with OVA and LPS as a positive control adjuvant produced the highest levels of OVA-specific antibodies (Fig 3.1F).

3.1.2 S100A4 and cyclophilin A activate dendritic cells

As one of the mechanisms of the adjuvant effects is mediated through directly activating dendritic cells, I next assessed the responses of dendritic cells to the stimulation of the four candidate DAMP molecules *in vitro*.

To this end, BMDCs were cultured from bone marrow cells in the presence of Flt3-L and the purity of BMDCs ($CD11c^+$MHC class II^+) reached about 92% (Fig 3.2A). Next, BMDCs were incubated overnight with cyclophilin A (1 μg/ml), S100A4 (1 μg/ml), uric acid (50 μg/ml), or HMGB1(10 μg/ml), followed by the measurement of the expression of the co-stimulatory molecules CD80 and CD86. S100A4 and cyclophilin A substantially enhanced the expression of both CD80 and CD86, but neither uric acid nor HMGB1 upregulated the expression of the two co-stimulatory molecules (Fig 3.2).

Table 3.1 Animal grouping and vaccination regimen

Group	Group size	Immunization regimen	Dosing
1	5	OVA (10 μg)	2 times with a 10-day interval
2	5	OVA (10 μg) + S100A4 (5 μg)	
3	5	OVA (10 μg) + cyclophilin A (5 μg)	
4	5	OVA (10 μg) + HMGB1 (10 μg)	
5	5	OVA (10 μg) + uric acid (50 μg)	
6	5	OVA (10 μg) + LPS (5 μg)	

Next, I tried to confirm the findings using tissue resident dendritic cells from the spleen. Spleen contains multiple subsets of myeloid and lymphoid cells. About 1-2% of spleen cells are dendritic cells. Total spleen cells from naïve mice were incubated with S100A4 (1 μg/ml), cyclophilin A (1 μg/ml), HMGB1 (10 μg/ml), or uric acid (50 μg/ml) for 24 hr and expression of the co-stimulatory molecules CD86 and CD80 by $CD11c^{+}$MHC class II^{+} dendritic cells was measured. S100A4 substantially enhanced the expression of both CD80 and CD86 in these spleen dendritic cells. However, cyclophilin A, uric acid and HMGB1 failed to upregulate the expression of the two molecules (Fig 3.3).

3.2 S100A4 exerts the most consistent adjuvant effects

Among the four DAMP molecules examined, S100A4 demonstrated robust adjuvant activities most consistently in terms of antigen-specific antibody augmentation and dendritic cell activation in both spleen and BMDCs. It has previous been reported that S100A4 knockout mice have compromised adaptive immune responses after immunization even in the presence of cholera toxin, the most potent experimental mucosal adjuvant (J. B. Sun *et al.*, 2017). Based on this finding and my data, S100A4 was chosen for further in-depth investigation.

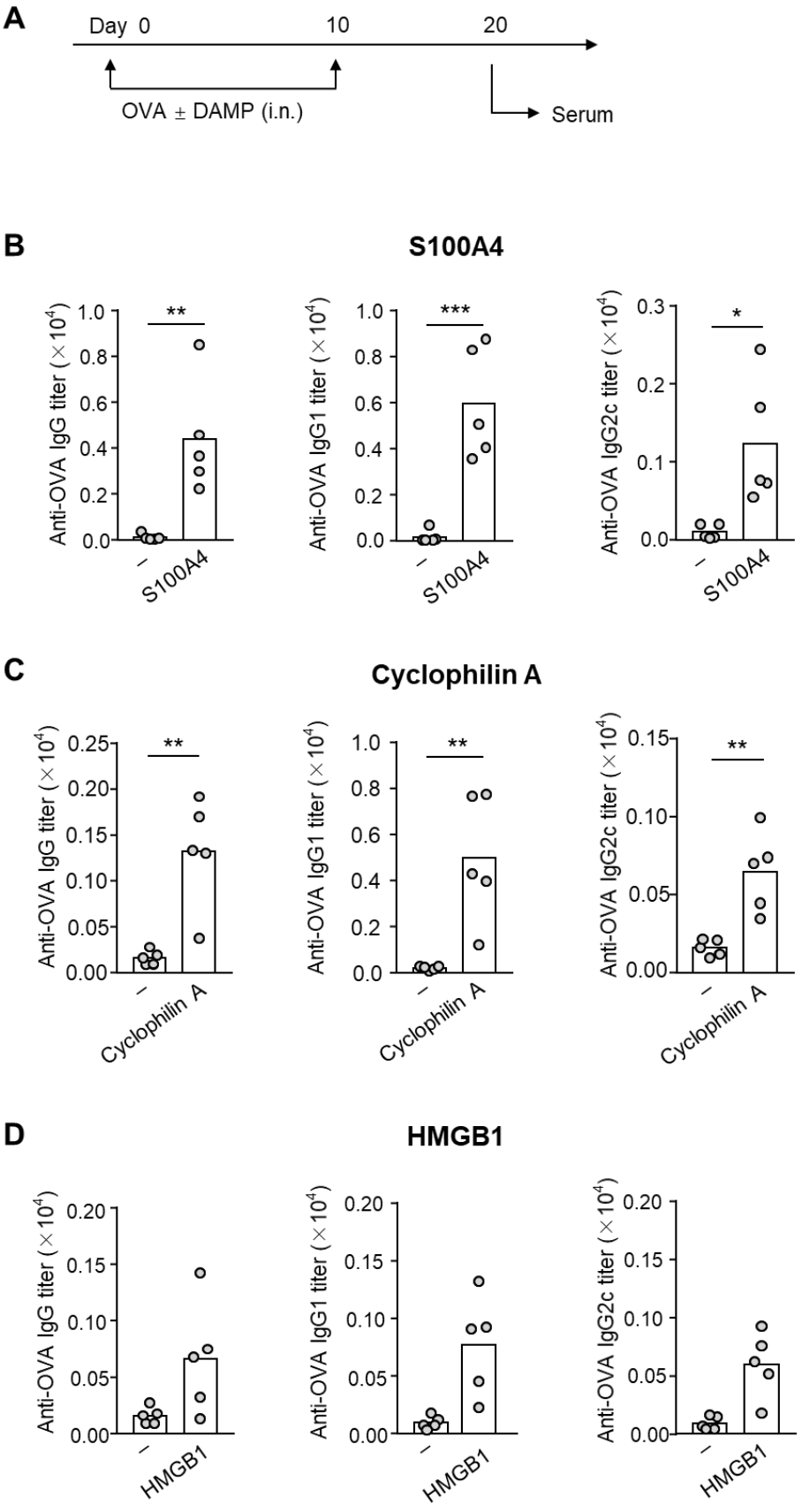
A
Day 0
10
20
OVA ± DAMP (i.n.)
Serum
B
S100A4
Anti-OVA IgG titer (×10^4)
Anti-OVA IgG1 titer (×10^4)
Anti-OVA IgG2c titer (×10^4)
**
***
*
–
S100A4
C
Cyclophilin A
Cyclophilin A
D
HMGB1
HMGB1

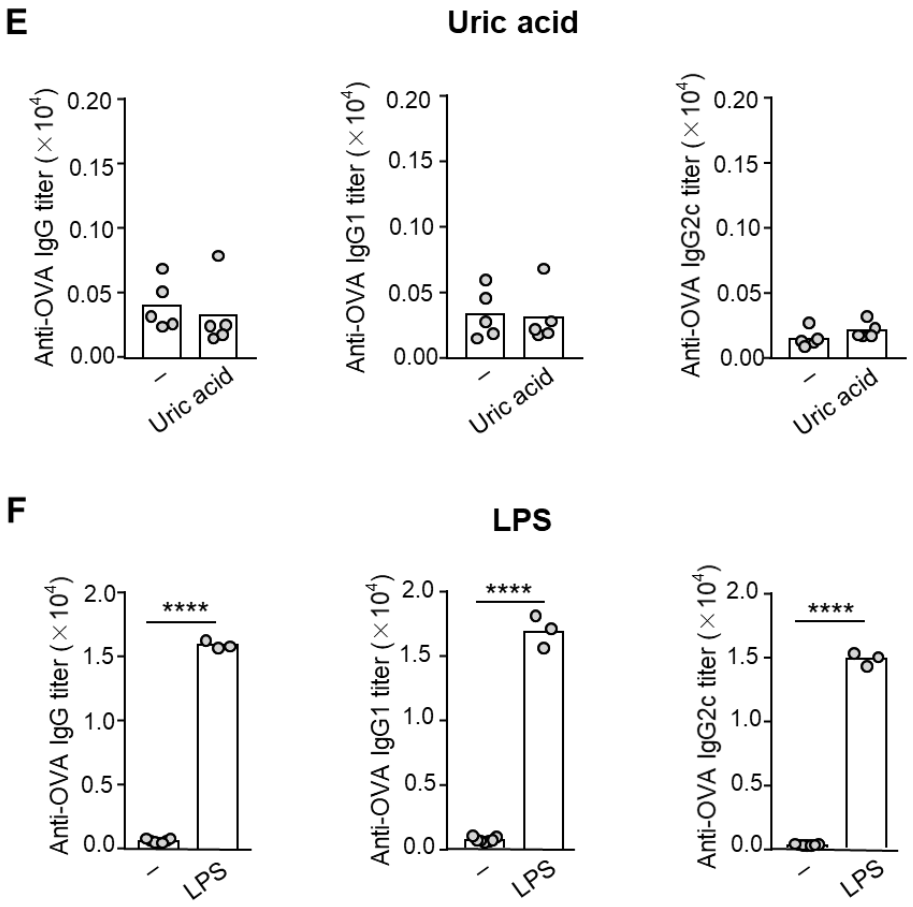

Figure 3.1 S100A4 and cyclophilin A promote antigen-specific antibody production after mucosal immunization. Mice were immunized intranasally with 10 μg OVA alone or with OVA mixed with various types of adjuvant candidates (5 μg per dose except uric acid which was 50 μg) twice at an interval of 10 days. Serum was collected 10 days after the last intranasal immunization (A). Serum anti-OVA IgG, IgG1 and IgG2c antibody levels for the adjuvant candidates S100A4 (B), cyclophilin A (C), HMGB1 (D), uric acid (E) and LPS (F) were examined by ELISA. Each dot represents data from one individual mouse and columns indicate the average values. *P < 0.05, **P < 0.01, ***P < 0.001 and ****P < 0.0001 by Mann-Whitney U test.

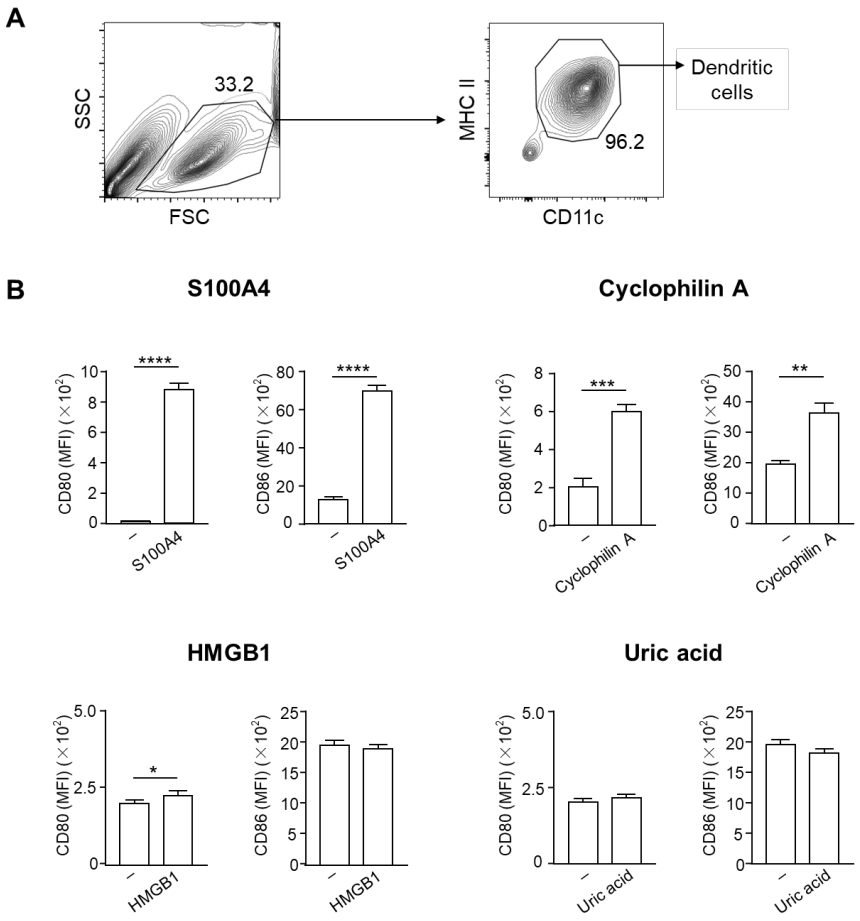

Figure 3.2 S100A4 and cyclophilin A activate bone marrow-derived dendritic cells. Bone marrow-derived dendritic cells (BMDCs) were obtained by culturing bone marrow cells in the presence of Flt3-L and the dendritic cell identity was confirmed by the expression of CD11c and MHC class II using flow cytometry (A). BMDCs ware incubated overnight with S100A4 (1 µg/ml), cyclophilin A (1 µg/ml), HMGB1 (10 µg/ml) or uric acid (50 µg/ml). Activation of dendritic cells as gated in (A) was analysed by measuring the expression of CD80 and CD86 using flow cytometry (B). Bars represent the mean fluorescent intensity (MFI) of CD80 and CD86. Numbers in or adjacent to outlined areas indicate percent cells in each gate. Data are expressed as mean+SEM of 3 biological replicates. $*P < 0.05$ $**P < 0.01$, $***P < 0.001$ and $****P < 0.0001$ by unpaired *t*-test.

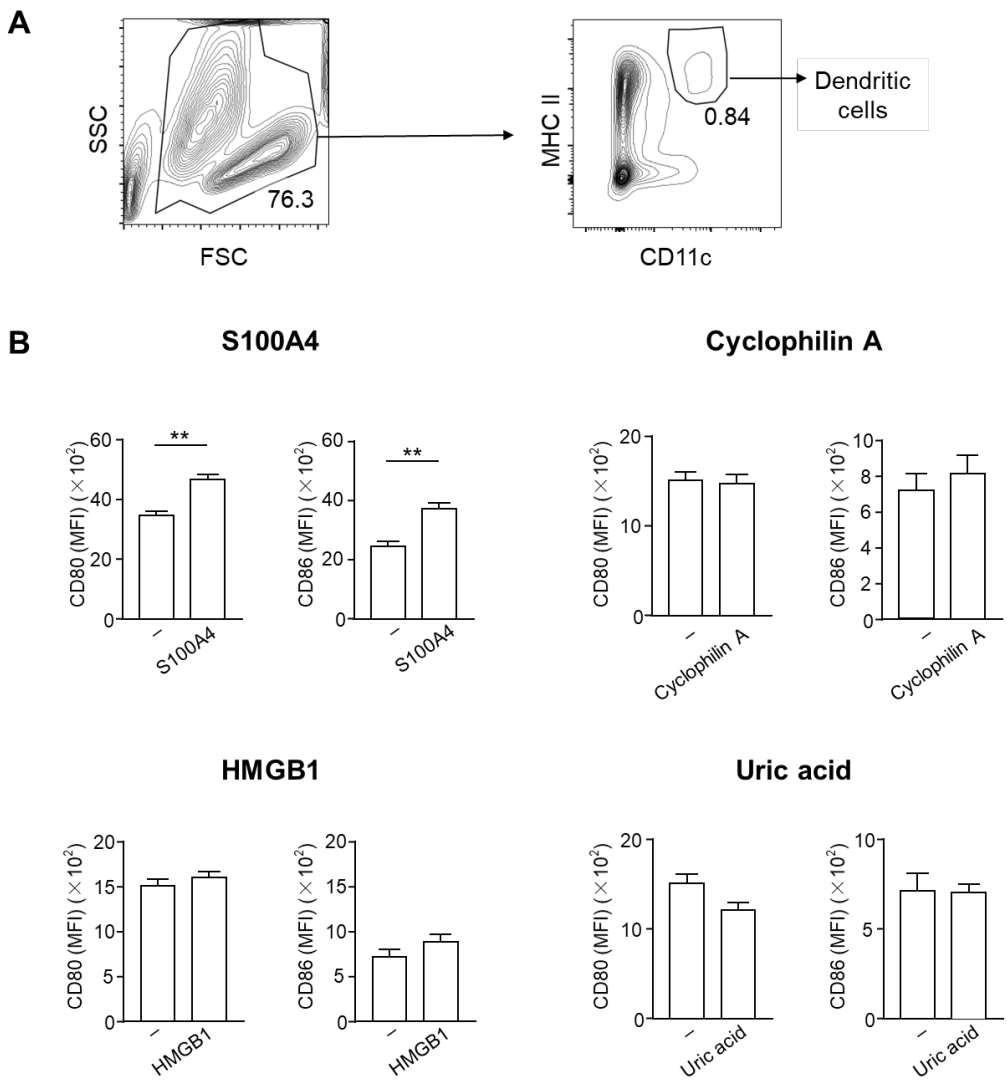

Figure 3.3 S100A4 activates spleen dendritic cells. Spleens were harvested from naïve C57BL/6 mice and dendritic cells were gated by the expression of CD11c and MHC class II using flow cytometry (A). Spleen cells ware incubated overnight with S100A4 (1 μg/ml), cyclophilin A (1 μg/ml), HMGB1 (10 μg/ml) or uric acid (50 μg/ml). Activation of dendritic cells as gated in (A) was analysed by measuring the expression of CD80 and CD86 using flow cytometry (B). Bars represent the mean fluorescent intensity (MFI) of CD80 and CD86. Numbers in or adjacent to outlined areas indicate percent cells in each gate. Data are expressed as mean+SEM of 3 biological replicates. $^{**}P < 0.01$ by unpaired *t*-test.

3.3 S100A4 dose-dependently promotes antibody production

In my initial screening experiments, 2 immunization doses with S100A4 at 5 μg/dose demonstrated potential adjuvant activity. Next, the dose effect of S100A4 was further investigated.

Mice were immunized twice with OVA at an interval of 10 days in the absence or presence of S100A4 at three different amounts of S100A4 per dose, i.e., 5 μg, 10 μg, and 20 μg. OVA-specific total IgG and IgG1 levels were gradually increased with the increasing dose of S100A4. Furthermore, the responses of individual mice were also more consistent at a higher dose (Fig 3.4). As 20 μg S100A4 per dose demonstrated further augmented antibody responses, 20 μg per dose was selected for the future experiments.

3.4 Antigen-specific antibody production is correlated with the number of immunizations

To investigate the effect of the number of immunizations on the quality of antigen-specific antibody production, I immunized mice intranasally with OVA in the presence or absence of S100A4 (20 μg) three times at an interval of 10 days. Blood was collected 5 days prior to the start of the first immunization and 5 days after each immunization (Fig 3.5A). There was a progressive enhancement of the OVA-specific antibody responses with the increasing numbers of immunization (Fig 3.5B). Thus, it was decided to use 3 doses of immunization and 20 μg S100A4 per dose for future experiments.

3.5 S100A4 augments the production of antigen-specific antibodies both in the circulation and at mucosal sites after intranasal immunization

Next, I would systematically investigate the humoral immune responses of mice after 3 doses of nasal immunization using a formulation of 10 μg OVA and 20 μg S100A4 per dose (Fig 3.6A). Serum anti-OVA total IgG, IgG1 and IgG2c levels were robustly augmented after immunization adjuvanted with S100A4 (Fig 3.6B). Furthermore, S100A4 potentiated mucosal antibody production in mucosal tissues evidenced by enhanced OVA-specific IgA, total IgG and IgG1 antibody levels in lung exudates (Fig 3.6C). Importantly, not only were substantial antibody levels potentiated in the lungs, a mucosal site that was close to the immunization site, but also similarly increased levels of antigen-specific IgA and IgG at a remote site, vaginal mucosal surface, were observed (Fig 3.6D).

Of note, immunization adjuvanted with S100A4 promoted antigen-specific antibody production to levels comparable to those achieved by using cholera toxin, the gold standard mucosal adjuvant (Fig 3.6).

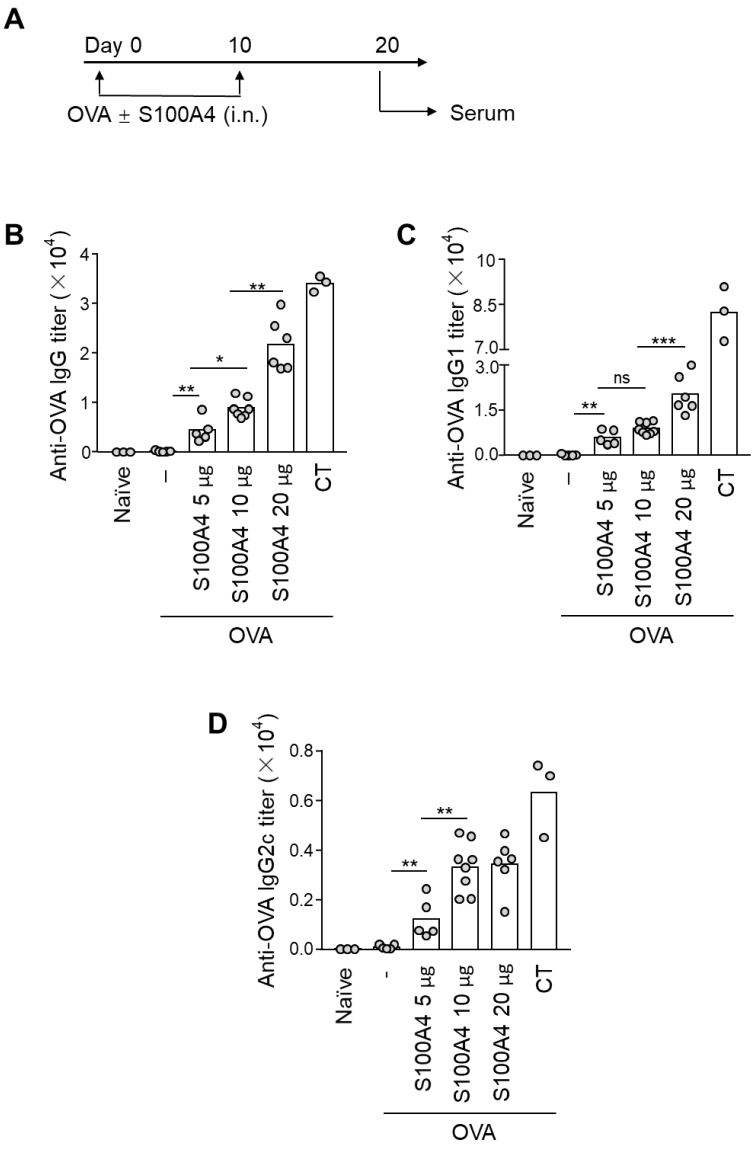

Figure 3.4 S100A4 dose-dependently promotes antigen-specific antibody production in mice. Mice were treated intranasally with 10 μg OVA alone or with OVA mixed with S100A4 at 5 μg, 10 μg, or 20 μg, or with cholera toxin (CT; 1 μg) twice at an interval of 10 days. Naïve mice were included as background controls. Serum was collected 10 days after the last intranasal immunization (A). Serum levels of anti-OVA total IgG (B), IgG1 (C) and IgG2c (D) were measured by ELISA. Each dot represents data from one individual mouse and columns indicate the average values. *$P < 0.05$ **$P < 0.01$ and ***$P < 0.001$ by Mann-Whitney U test.

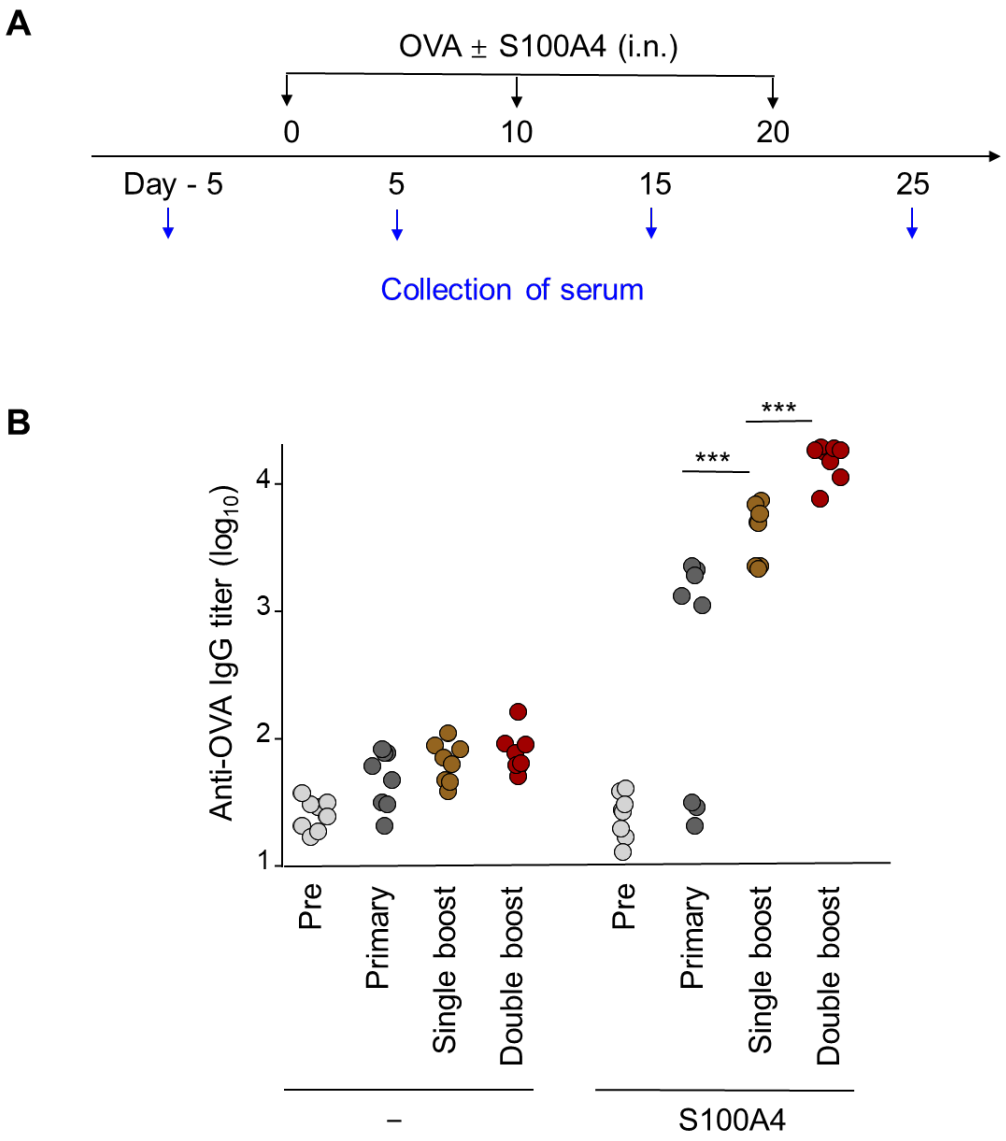

Figure 3.5 Higher levels of antigen-specific antibody production are correlated with the number of immunizations adjuvanted with S100A4. (A) Mice were treated intranasally with 10 μg OVA alone or OVA mixed with 20 μg of S100A4 as adjuvant three times at an interval of 10 days. Serum was collected 5 days after each intranasal immunization. Pre-immunization serum was collected (5 days before the first immunization) as background control. (B) Serum levels of anti-OVA IgG were measured by ELISA. Each dot represents data from one individual mouse. ***$P < 0.001$ by Mann-Whitney *U* test.

3.6 S100A4 promotes the expansion of bone marrow plasma cells that secrete antigen-specific antibodies

Long-lived plasma cells migrate to and reside in the survival niches in the bone marrow where these cells continue to produce antibodies (Chu *et al.*, 2013). Therefore, I next investigated the accumulation of plasma cells that secrete antigen-specific antibodies after immunization. Mice were immunized similarly as previously described, and 10 days after the last immunization bone marrow cells were collected (Fig 3.7A) and analysed using an ELISpot assay for OVA-specific IgG antibody-producing cells. S100A4 significantly increased the number of OVA-specific IgG-producing cells in the bone marrow (Fig 3.7B and C). These results were consistent with the antibody regulation after immunization with S100A4 as an adjuvant (Fig 3.6).

3.7 S100A4 activates immune cells in the spleen and lymph nodes after intranasal immunization

Spleen and lymph nodes are important secondary lymphoid organs where productive immune responses are inducted. I therefore undertook to investigate major immune reactions involved in these two organs after an immunization schedule as described previously for antibody analysis (Fig 3.6A). Spleens and lymph nodes were harvested 3 days after the final immunization.

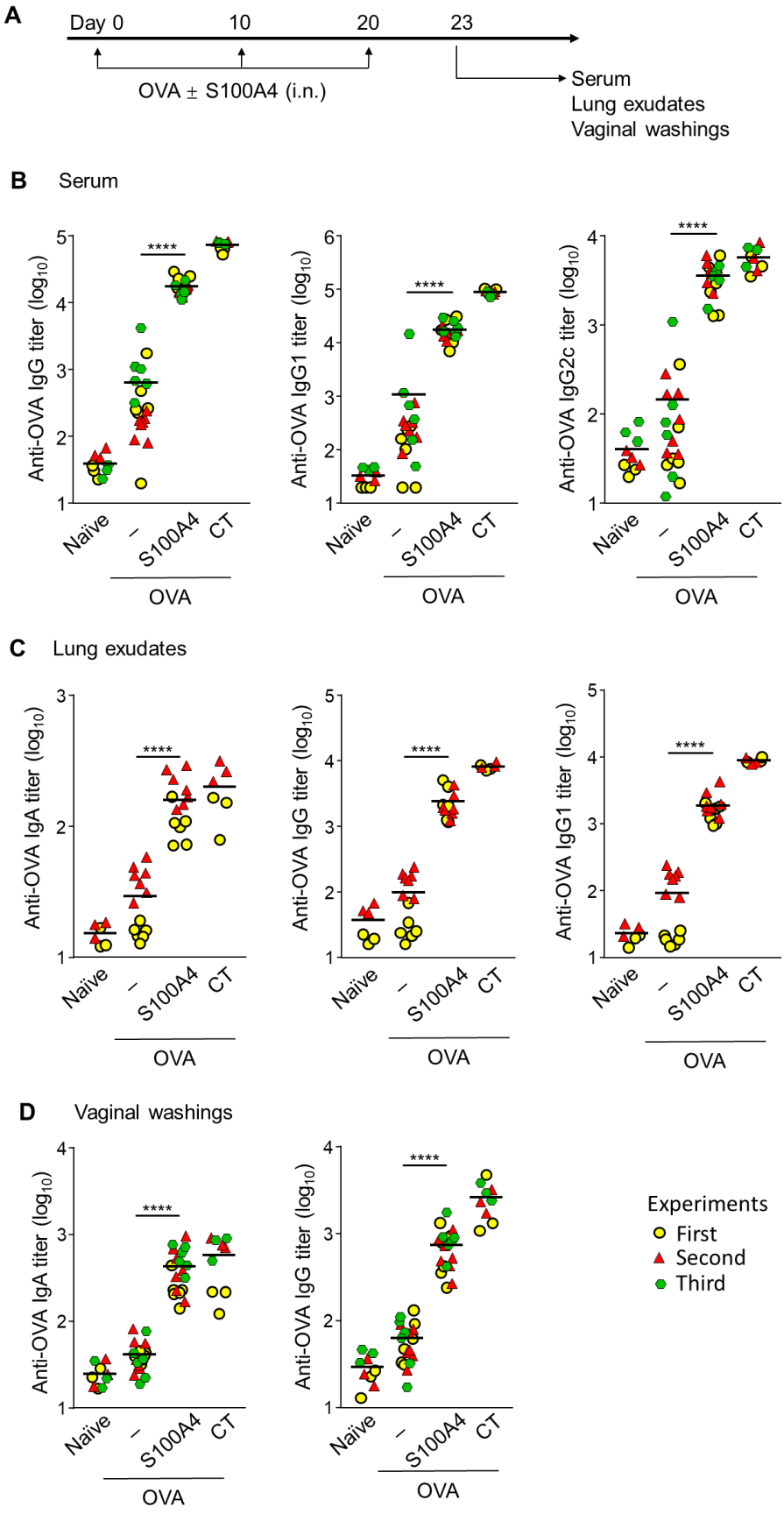
A
Day 0
10
20
23
OVA ± S100A4 (i.n.)
Serum
Lung exudates
Vaginal washings
B
Serum
Anti-OVA IgG titer (log10)
Anti-OVA IgG1 titer (log10)
Anti-OVA IgG2c titer (log10)
****
Naïve
–
S100A4
CT
OVA
C
Lung exudates
Anti-OVA IgA titer (log10)
Anti-OVA IgG titer (log10)
Anti-OVA IgG1 titer (log10)
D
Vaginal washings
Anti-OVA IgA titer (log10)
Anti-OVA IgG titer (log10)
Experiments
First
Second
Third

Figure 3.6 S100A4 augments the production of antigen-specific antibodies both in the circulation and at mucosal sites after intranasal immunization. Mice were immunized intranasally with 10 μg OVA alone or mixed with 20 μg of S100A4 or 1 μg cholera toxin (CT) three times at an interval of 10 days. Naïve mice were included as background control (A). Serum, lung exudates, and vaginal washings were collected three days after the last immunization. Levels of anti-OVA total IgG, IgG1 and IgG2c in serum (B); IgA, total IgG and IgG1 in lung exudates (C); and IgA and total IgG in vaginal washings (D) were measured by ELISA. Each coloured symbol represents data from one individual mouse and columns indicate the average values. Symbols of the same colour represent data from one experiment. Data from 2 (C) or 3 (B and D) experiments were pooled. ****$P < 0.0001$ by Mann-Whitney *U* test.

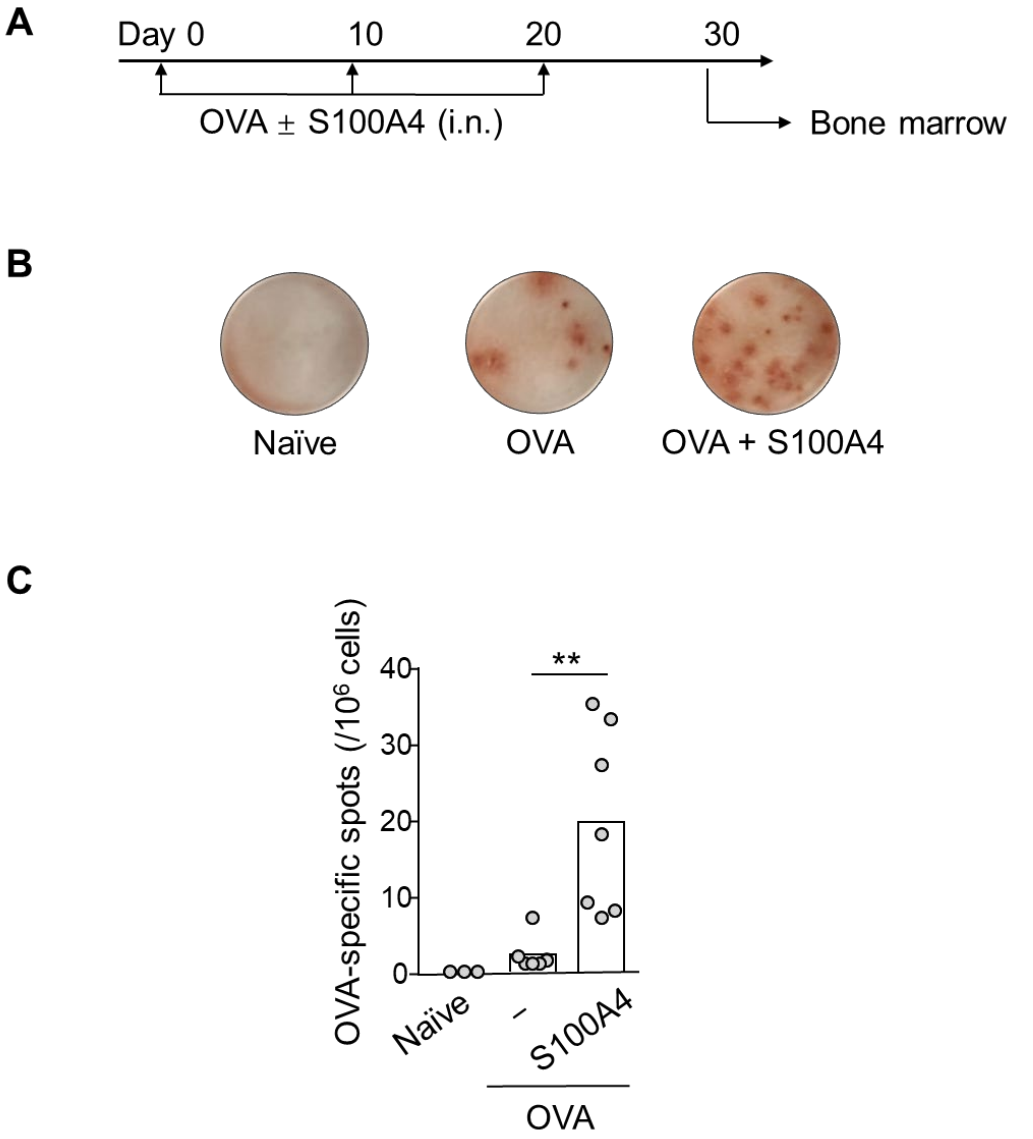

Figure 3.7 S100A4 promotes the expansion of bone marrow plasma cells that secrete antigen-specific antibodies. Mice were treated intranasally with 10 µg OVA alone or mixed with 20 µg of S100A4 as adjuvant three times at an interval of 10 days. Bone marrow was harvested 10 days after the last immunization (A). Plasma cells that secrete OVA-specific antibodies were enumerated by an ELISpot assay. Bone marrow from naïve mice was used as background controls. Representative images of spots are shown (B). Spots were enumerated and plotted (C). Each dot represents data from one individual mouse and columns indicate the average values. $^{**}P < 0.01$ by Mann-Whitney *U* test.

3.7.1 S100A4 promotes B cell activation

Intranasal delivery of S100A4 stimulated the generation of activated B cells ($CD69^+CD38^+$) in both the spleens and lymph nodes. The capacity of S100A4 in activating B cells was comparable to cholera toxin (Fig 3.8).

3.7.2 S100A4 promotes the expansion of T follicular helper cells

T follicular helper cells are critical for activating B cells in the secondary lymphoid organs. T follicular helper cells were identified by surface expression of CXCR5 and PD-1 (CD279) (Fig 3.9A and Fig 3.10A). Frequencies of $PD\text{-}1^+CXCR5^+Foxp3^-$ in $CD4^+$ cells were analysed and the results demonstrate a significant expansion of T follicular helper cells in both the spleen (Fig 3.9B and C) and cervical lymph nodes (Fig 3.10B and C) after intranasal immunization with S100A4. Again, the effect of S100A4 in promoting the expansion of T follicular helper cells was comparable to that of cholera toxin.

3.7.3 S100A4 promotes germinal centre formation

Initiating a strong germinal centre response is a quality demanded from a strong adjuvant (Lycke, 2010). It has been previously reported that mice deficient in S100A4 have compromised germinal centre formation even after immunization with the strong adjuvant cholera toxin (J. B. Sun *et al.*, 2017), which predicts that exogenously added S100A4 might be able to promote germinal centre activity. Therefore, I next tried to confirm a strong induction of germinal centre responses after S100A4-adjuvanted immunization

using various technical approaches including flow cytometry, confocal microscopy, and MALDI-TOF mass spectrometry.

3.7.3.1 S100A4 promotes germinal centre B cell expansion

Germinal centre B cells (GL-7^{+}FAS^{+}B220^{+}CD3^{-}CD38^{-}) in the spleens and lymph nodes were analysed using flow cytometry (Fig 3.11A and Fig 3.12A) as reported previously (Y. Wang *et al.*, 2017). Frequencies of these germinal centre B cells were increased in both spleens (Fig 3.11B and C) and lymph nodes (Fig 3.12B and C) after immunization with S100A4 as an adjuvant.

3.7.3.2 S100A4 promotes germinal centre morphology

The above described data demonstrating an expansion of germinal centre B cells using flow cytometry was next confirmed using immunohistochemistry and confocal microscopy to demonstrate the appearance of the typical germinal centre morphology. Mouse spleens were cryosectioned followed by immunofluorescent staining for the expression of Ki-67, GL-7 and B220, representing the proliferating germinal centre B cells as previously reported (J. B. Sun *et al*., 2017). Immunization with S100A4 overwhelmingly promoted the morphological changes associated with germinal centre formation, as evidenced by the expansion of GL-7^{+} and Ki-67^{+} cells (Fig 3.13).

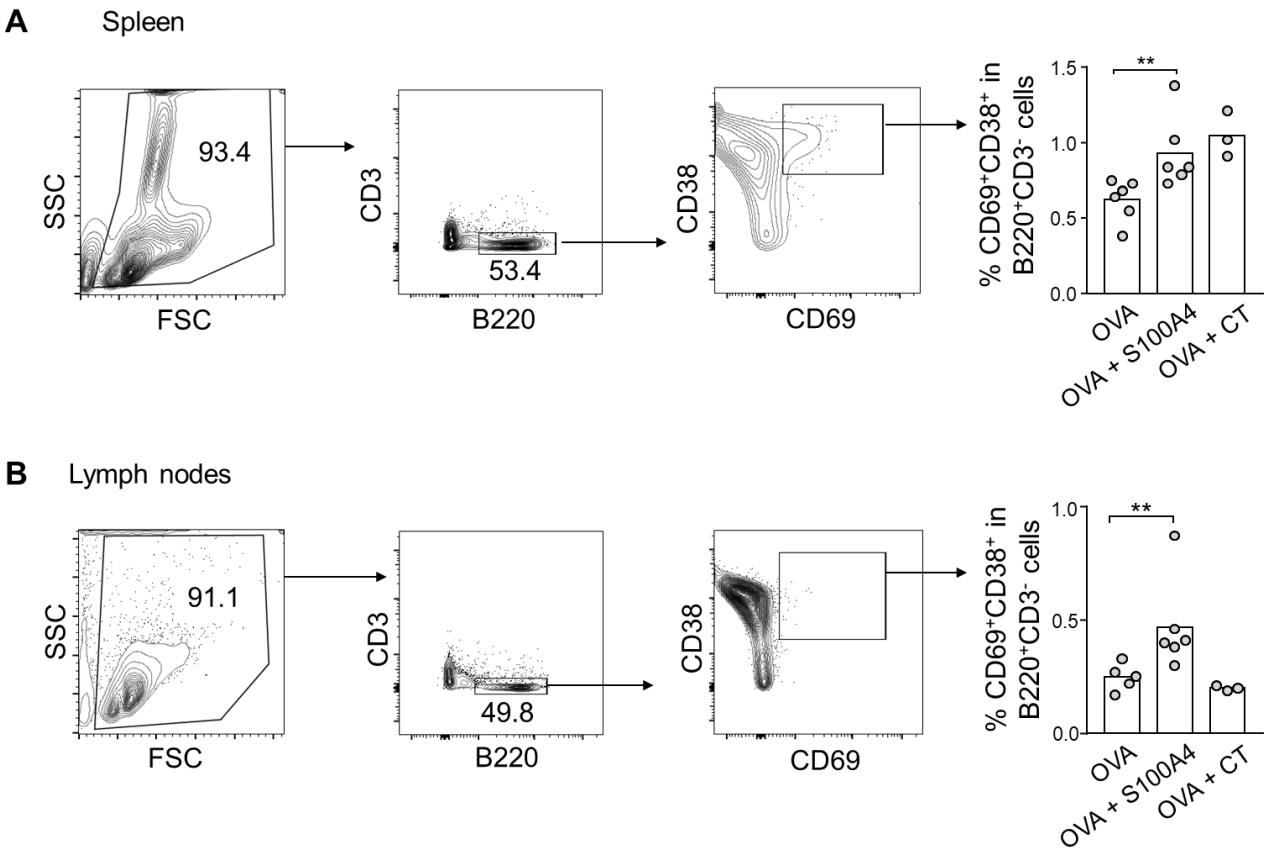

Figure 3.8 Splenic and lymph node B cells are activated after immunization with S100A4 as an adjuvant. Mice were treated intranasally with 10 μg OVA alone or mixed with 20 μg of S100A4 or 1 μg cholera toxin (CT) 3 times at an interval of 10 days. Spleens and cervical lymph nodes were harvested 3 days after the last immunization. Activated B cells ($CD69^+CD38^+B220^+CD3^-$) in spleens (A) and cervical lymph nodes (B) were analysed using flow cytometry. Arrows indicate gating strategies. Numbers in or adjacent to outlined areas indicate percent cells in each gate. Each dot represents data from one individual mouse and columns indicate the average values. $^{**}P < 0.01$ by Mann-Whitney *U* test.

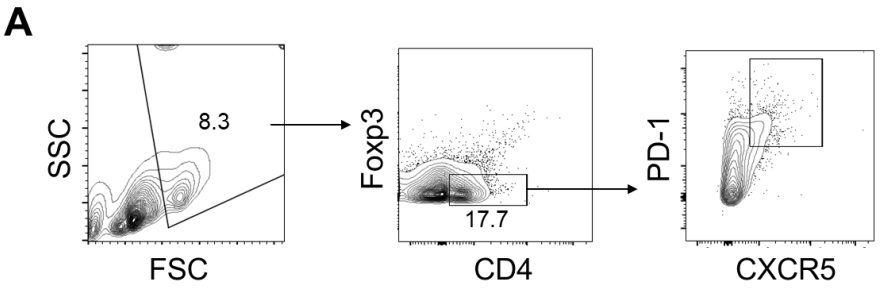
A
SSC
FSC
8.3
Foxp3
CD4
17.7
PD-1
CXCR5

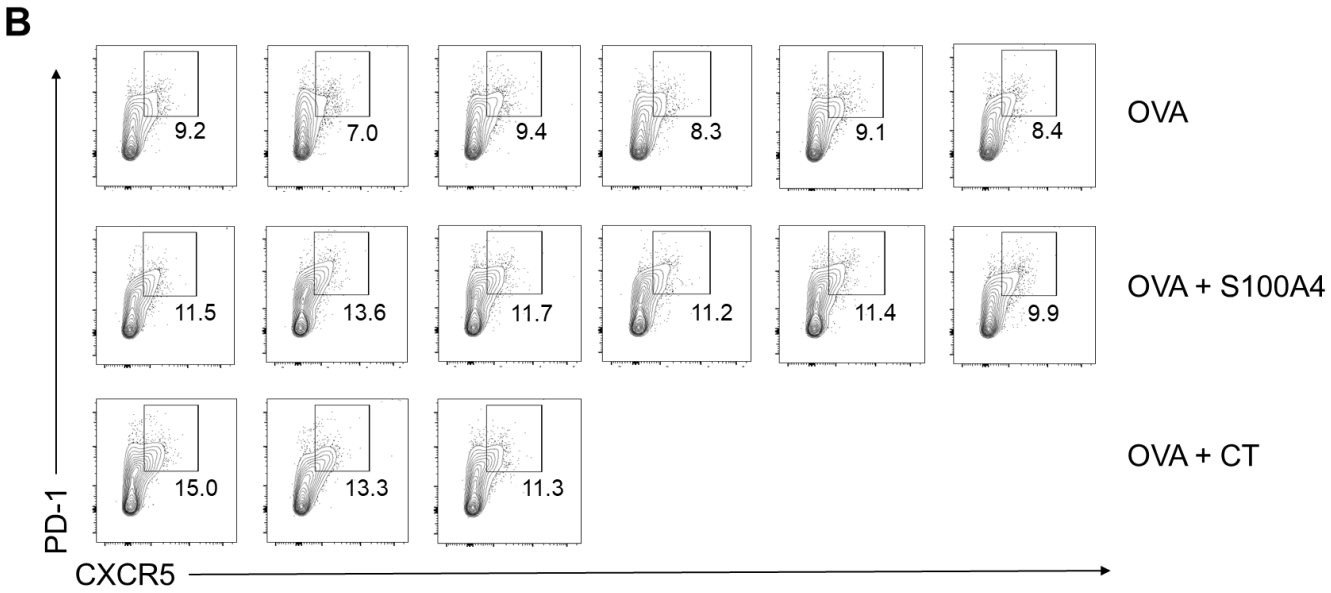
B
9.2
7.0
9.4
8.3
9.1
8.4
OVA
11.5
13.6
11.7
11.2
11.4
9.9
OVA + S100A4
15.0
13.3
11.3
OVA + CT
PD-1
CXCR5

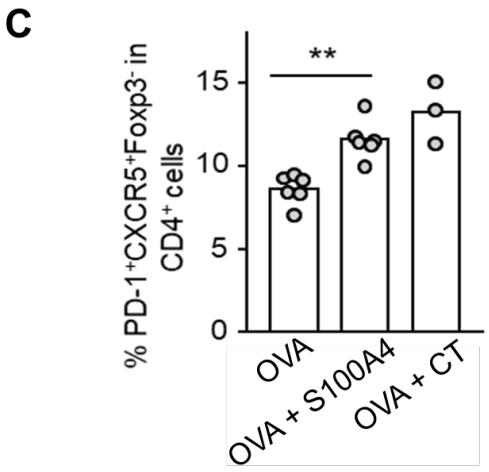
C
**
% PD-1+CXCR5+Foxp3- in CD4+ cells
15
10
5
0
OVA
OVA + S100A4
OVA + CT

Figure 3.9 S100A4 supports the expansion of T follicular helper cells in the spleen. Mice were immunized intranasally with 10 μg OVA alone or mixed with 20 μg of S100A4 or 1 μg cholera toxin (CT) as adjuvant for 3 times at an interval of 10 days. Spleens were harvested 3 days after the last immunization. (A) T follicular helper cells were identified as PD-1^{+}CXCR5^{+}Foxp3^{-}CD4^{+} cells using flow cytometry. Arrows indicate gating strategies. (B) Each panel represents an individual mouse and the number denotes the percentage of T follicular helper cells. (C) Data for individual mice in (B) were plotted. Numbers in or adjacent to outlined areas indicate percent cells in each gate. Each dot represents data from one individual mouse and columns indicate the average values. $^{**}P < 0.01$ by Mann-Whitney *U* test.

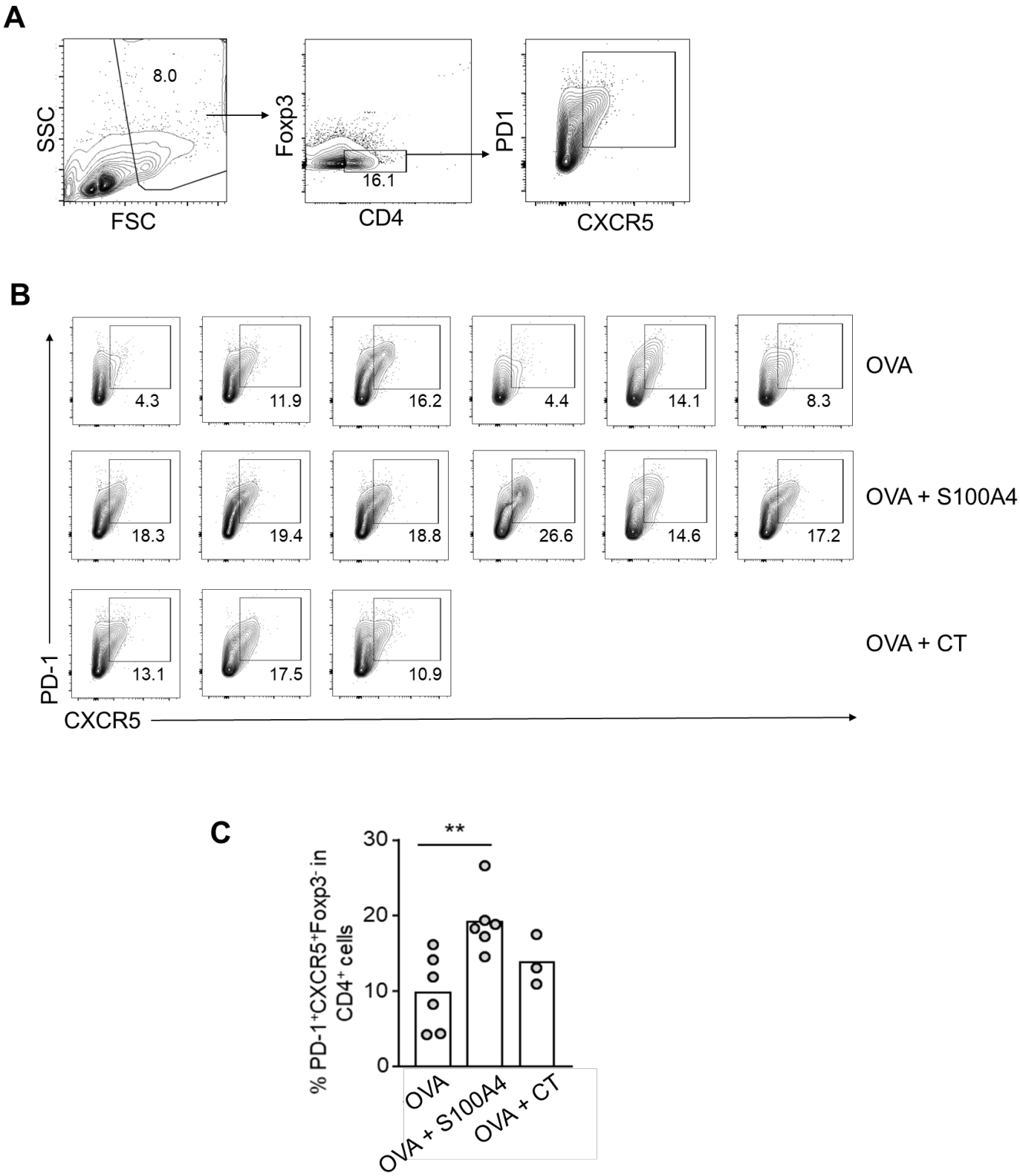
A
8.0
SSC
FSC
Foxp3
16.1
CD4
PD1
CXCR5
B
4.3
11.9
16.2
4.4
14.1
8.3
OVA
18.3
19.4
18.8
26.6
14.6
17.2
OVA + S100A4
13.1
17.5
10.9
OVA + CT
PD-1
CXCR5
C
**
% PD-1+CXCR5+Foxp3- in CD4+ cells
30
20
10
0
OVA
OVA + S100A4
OVA + CT

Figure 3.10 S100A4 supports the expansion of T follicular helper cells in lymph nodes. Mice were immunized intranasally with 10 μg OVA alone or mixed with 20 μg of S100A4 or 1 μg cholera toxin (CT) as adjuvant for 3 times at an interval of 10 days. Cervical lymph nodes were harvested 3 days after the last immunization. (A) T follicular helper cells were identified as PD-1^{+}CXCR5^{+}Foxp3^{-}CD4^{+} T cells using flow cytometry. Arrows indicate gating strategies. (B) Each panel represents an individual mouse and the number denotes the percentage of T follicular helper cells. (C) Data for individual mice in (B) were plotted. Numbers in or adjacent to outlined areas indicate percent cells in each gate. Each dot represents data from one individual mouse and columns indicate the average values. $^{**}P < 0.01$ by Mann-Whitney *U* test.

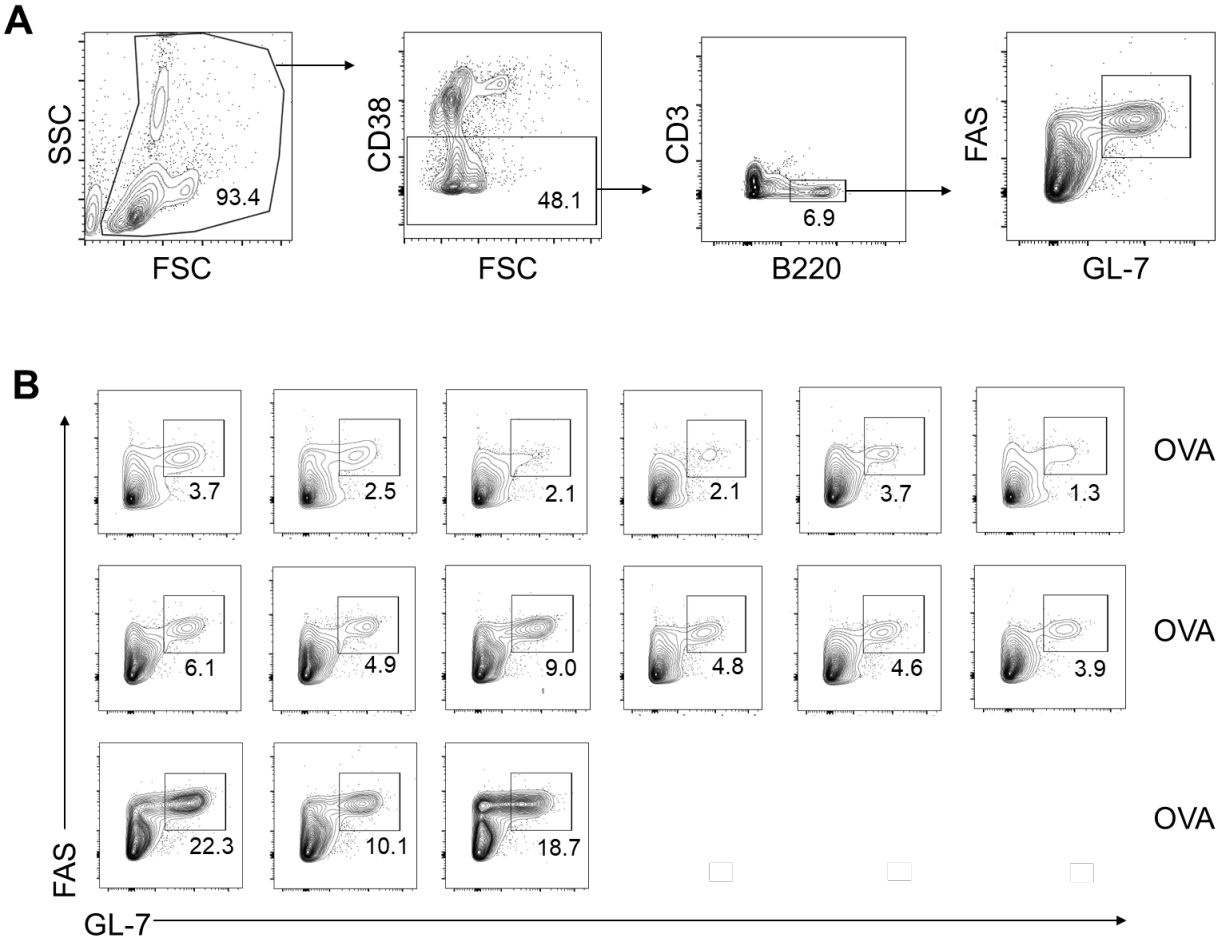
A
SSC
FSC
93.4
CD38
FSC
48.1
CD3
B220
6.9
FAS
GL-7
B
OVA
OVA + S100A4
OVA + CT
3.7
2.5
2.1
2.1
3.7
1.3
6.1
4.9
9.0
4.8
4.6
3.9
22.3
10.1
18.7
FAS
GL-7
C
% GL-7+FAS+ in B220+CD3- CD38- cells (log10)
2
1
0
**
OVA
OVA + S100A4
OVA + CT

Figure 3.11 S100A4 promotes the expansion of germinal centre B cells in the spleen. Mice were immunized intranasally with 10 μg OVA alone or mixed with 20 μg of S100A4 or 1 μg cholera toxin (CT) as adjuvant for 3 times at an interval of 10 days. Spleens were harvested 3 days after the last immunization. (A) Germinal centre B cells were identified as GL-7^{+}FAS^{+}B220^{+}CD3^{-}CD38^{-} cells using flow cytometry. Arrows indicate gating strategies. (B) Each panel represents an individual mouse and the number denotes the percentage of germinal centre B cells. (C) Data for individual mice in (B) were plotted. Numbers in or adjacent to outlined areas indicate percent cells in each gate. Each dot represents data from one individual mouse and columns indicate the average values. $^{**}P < 0.01$ by Mann-Whitney *U* test.

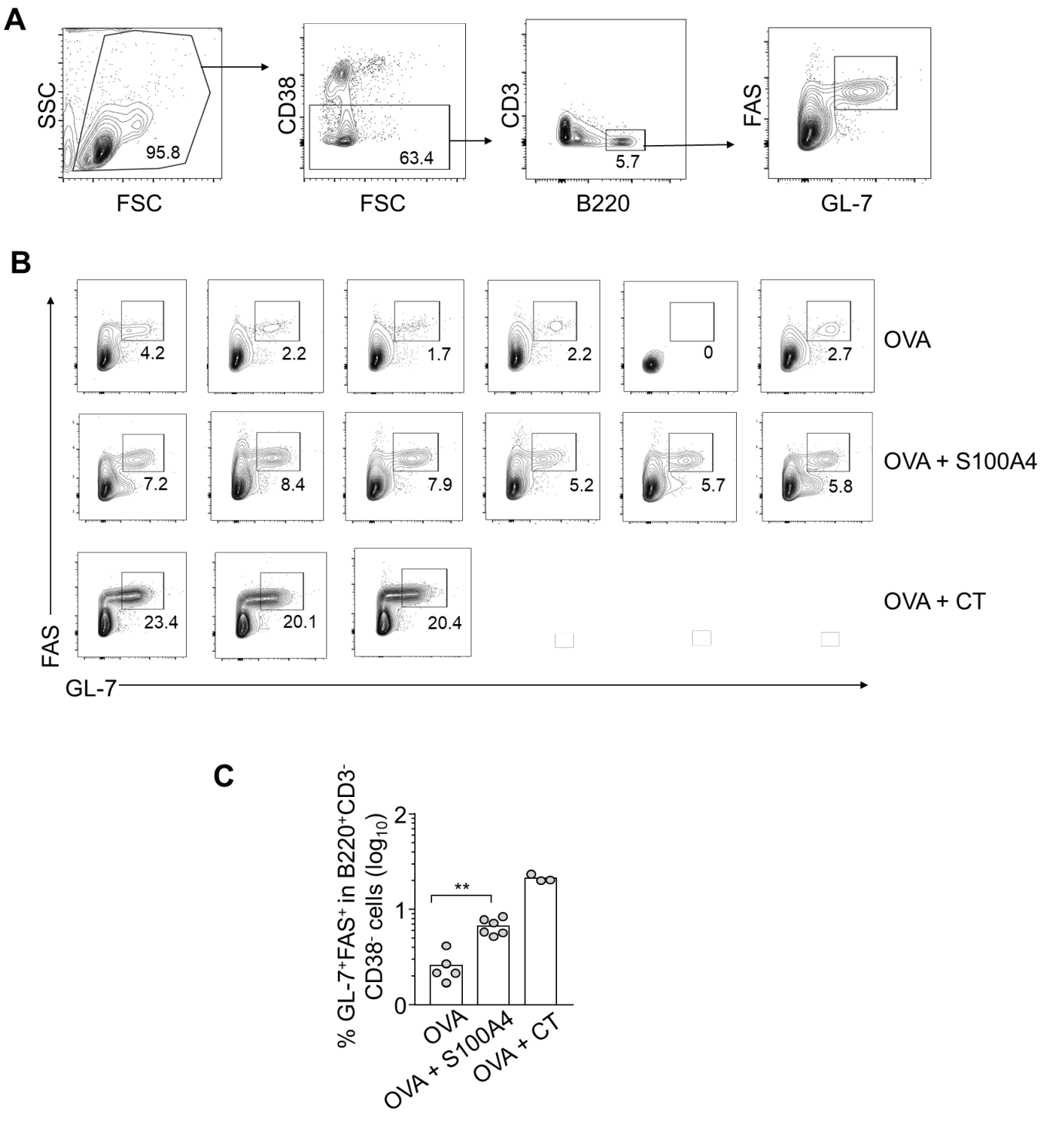
A
SSC
95.8
FSC
CD38
63.4
FSC
CD3
5.7
B220
FAS
GL-7
B
4.2
2.2
1.7
2.2
0
2.7
OVA
7.2
8.4
7.9
5.2
5.7
5.8
OVA + S100A4
23.4
20.1
20.4
OVA + CT
FAS
GL-7
C
% GL-7+FAS+ in B220+CD3- CD38- cells (log10)
2
1
0
**
OVA
OVA + S100A4
OVA + CT

Figure 3.12 S100A4 promotes the expansion of germinal centre B cells in the lymph node. Mice were immunized intranasally with 10 μg OVA alone or mixed with 20 μg of S100A4 or 1 μg cholera toxin (CT) as adjuvant for 3 times at an interval of 10 days. Cervical lymph nodes were harvested 3 days after the last immunization. (A) Germinal centre B cells were identified as GL-7^{+}FAS^{+}B220^{+}CD3^{-}CD38^{-} using flow cytometry. Arrows indicate gating strategies. (B) Each panel represents an individual mouse and the number denotes the percentage of germinal centre B cells. (C) Data for individual mice in (B) were plotted. Numbers in or adjacent to outlined areas indicate percent cells in each gate. Each dot represents data from one individual mouse and columns indicate the average values. $^{**}P < 0.01$ by Mann-Whitney *U* test.

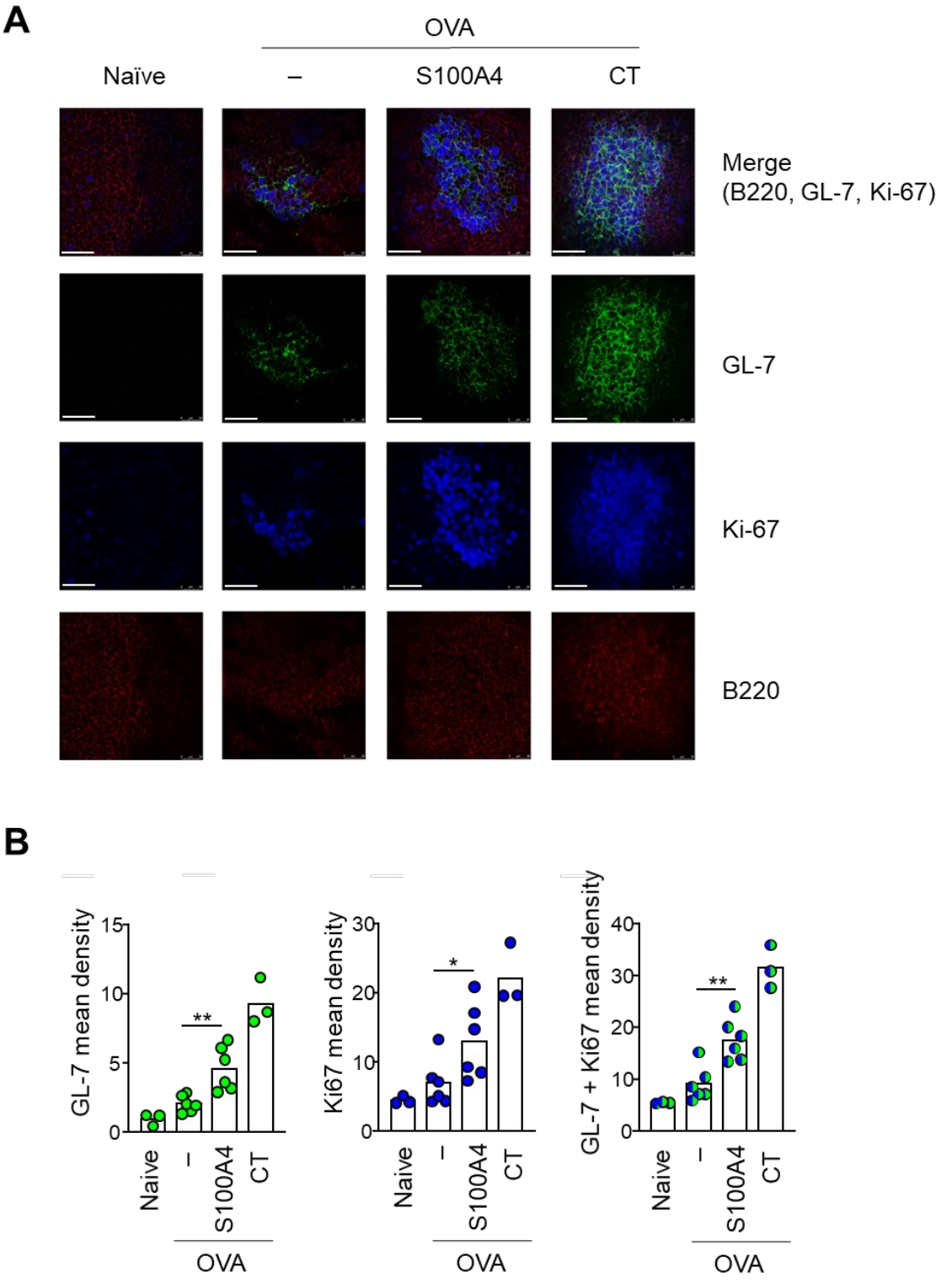
A
OVA
Naïve
–
S100A4
CT
Merge
(B220, GL-7, Ki-67)
GL-7
Ki-67
B220
B
GL-7 mean density
Ki67 mean density
GL-7 + Ki67 mean density
Naive
–
S100A4
CT
OVA
**
*
**

Figure 3.13 S100A4 promotes the germinal centre morphology in the spleen. Mice were immunized intranasally with 10 μg OVA alone or mixed with 20 μg of S100A4 or 1 μg cholera toxin (CT) as adjuvant for 3 times at an interval of 10 days. Spleens ware harvested 3 days after the last immunization. (A) Spleen sections were analysed by immunohistochemistry to visualize germinal centre B cells. Red, B220; green, GL-7; blue, Ki-67. Upper panels, merged images. Scale bar, 25 μm. Each column represents data of one individual mouse from one of the treatment groups. (B) The fluorescence intensities were quantified. Each dot represents data from one individual mouse and columns indicate the average values. *$P < 0.05$, **$P < 0.01$ by Mann-Whitney *U* test.

3.7.3.3 Intranasal immunization adjuvanted with S100A4 promotes lipid accumulation in the spleen

It has recently been reported that germinal centre B cells require active oxidation of fatty acids instead of glycolysis to meet the energetic challenge of rapid cell proliferation (Weisel *et al*., 2020). In order for efficient germinal centre development to take place, animals need to mobilize lipid transport to the germinal centres. Therefore, I attempted to measure the accumulation of lipids using MALDI-TOF mass spectrometry after S100A4-adjuvanted immunization. As a cutting-edge technology, MALDI-TOF uses pulses of laser light to vaporize the sample matrix, during which process some molecules become ionized through protonation. The laser pulse can also fragment a molecule into a variety of charged and neutral particles. The pattern of ionized oligo molecules can be recorded to reflect the original matrix property, e.g., lipid concentration.

A total of 348 lipids, including fatty acyls, glycolipids, glycerophospholipids, polyketides, prenol lipids, and sterol lipids, were identified in the spleens. Around 83% of the total lipids were glycerolipids and glycerophospholipids which were the dominant fatty acids (Fig 3.14A). A shotgun lipidomics approach was used to analyse all lipid classes together. Abundance of total lipids was increased in the spleen after immunization with S100A4 (Fig 3.14B). The lipid intensities were quantified and expressed using intensity box plot, clearly demonstrating a remarkable increase for the S100A4-adjuvanted group (Fig 3.14C). Principal component analysis revealed complete separation of S100A4-adjuvanted immunization and the OVA only control as well as the naïve mouse control

(Fig 3.14D). Overall, administration of cholera toxin seemed to have mobilised more lipids than S100A4 (Fig 3.14).

As MALDI-TOF is a label-free technology, it will demonstrate its superiority in investigating animal models based on non-rodent species which do not have a dynamic panel of commercial antibodies.

3.7.4 S100A4 promotes T cell memory response upon antigen re-stimulation

Successful vaccination results in the generation of memory cells including memory T cells which can be activated upon re-encounter with the antigen. To confirm whether S100A4 as an effective adjuvant could induce memory T cell responses, we immunized mice with OVA in the presence or absence of S100A4 and mouse spleens were harvested three days after the last immunization (Fig 3.15A). Splenocytes were stimulated with OVA for 72 hr. Splenic CD4 T cell proliferation was increased if the mice had previously received S100A4 as evidenced by enhanced expression of the proliferation marker Ki-67 (Fig 3.15B and C).

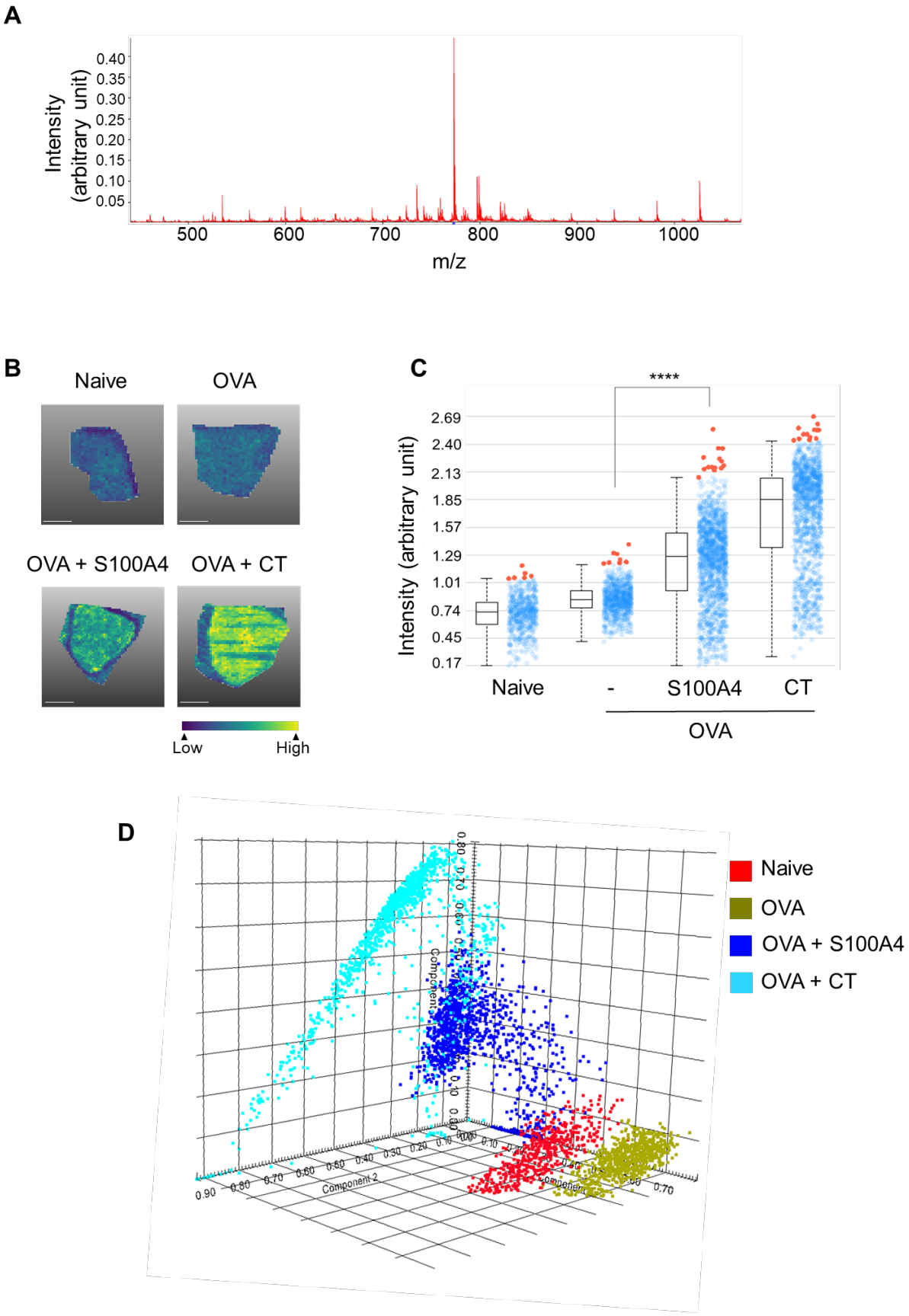
A
Intensity (arbitrary unit)
0.40
0.35
0.30
0.25
0.20
0.15
0.10
0.05
500
600
700
800
900
1000
m/z
B
Naive
OVA
OVA + S100A4
OVA + CT
Low
High
C
****
Intensity (arbitrary unit)
2.69
2.40
2.13
1.85
1.57
1.29
1.01
0.74
0.45
0.17
Naive
-
S100A4
CT
OVA
D
Component 1
Component 2
Component 3
Naive
OVA
OVA + S100A4
OVA + CT

Figure 3.14 Intranasal immunization adjuvanted with S100A4 promotes lipid accumulation in the spleen. Mice received three intranasal immunizations at an interval of 10 days. For each immunization, mice were intranasally administered with 10 μg OVA alone or OVA admixed with 20 μg S100A4 or 1 μg cholera toxin (CT). Spleens were collected 3 days after the last immunization. (A) Average MALDI mass spectra of lipids are shown based on the samples in all the treatment groups. (B) The intensity and distribution of lipids within a range of mass-to-charge (m/z) ratio (754.8 ± 314.3 Da) are shown as MALDI MSI ion pseudo-colour images. (C) Expression of overall levels of the identified lipids was quantified by intensity box plots. (D) Principal component analysis of MALDI MSI data using the score plot of the three first principal components (PC1–PC3) displays various lipid mass spectra highlighting different lipid signatures between various treatment groups. Results show one representative mouse (B) or represent 3-6 mice (C and D) in each treatment group. ****$P < 0.0001$ by Kruskal-Wallis test (C).

3.8 Antigen-specific antibody production is correlated with immune cell activation in the secondary lymphoid organs after immunization adjuvanted with S100A4

Some of my immunization assays and cellular response analyses in the spleen and lymph nodes were based on the same mouse experiment. It would be interesting to see whether there were correlations between the antigen-specific antibody production levels and various cellular responses in individual mice. Indeed, good correlations were observed (Fig 3.16). Specifically, following immunization with OVA and S100A4, serum anti-OVA antibody levels were correlated to T follicular helper cell expansion, B cell activation, germinal centre formation, T cell memory response (Fig 3.16). Of note, the correlations between the germinal centre activity based on GL-7 measurement and lipid abundance further confirm the reliability of using the lipid abundance determined by the label-free MALDI-TOF technique as a surrogate marker for germinal centre response. Taken together, my data support strong internal consistency of some of the assays adopted in this study.

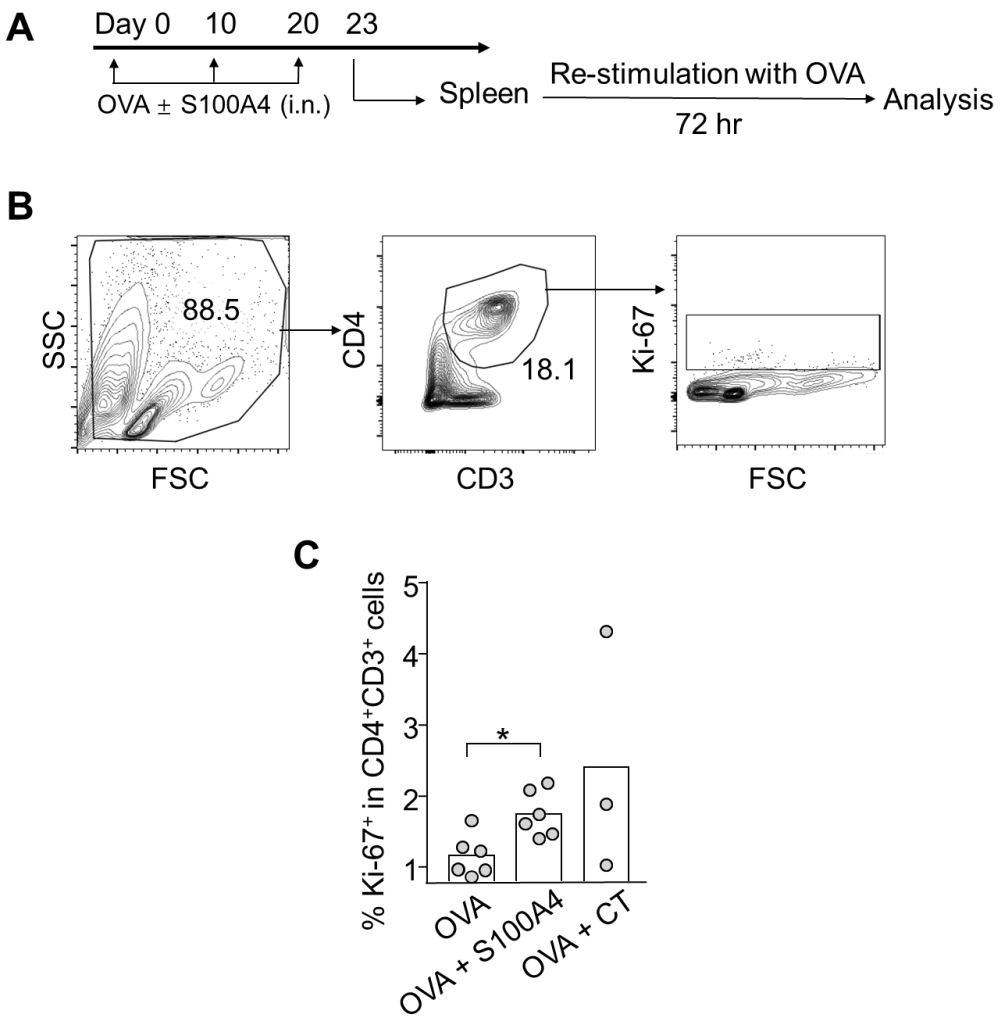

Figure 3.15 S100A4 promotes T cell memory response upon antigen re-stimulation. Mice received three intranasal immunizations at an interval of 10 days. For each immunization, mice were intranasally administered with 10 µg OVA alone or OVA admixed with 20 µg S100A4 or 1 µg cholera toxin (CT). Spleens were collected 3 days after the last immunization and re-stimulated *in vitro* with 200 µg OVA for 72 hr (A). The frequency of Ki-67$^+$ cells in CD4$^+$CD3$^+$ cells were analysed using flow cytometry (B). Frequencies of proliferating T cells were plotted (C). Arrows indicate the gating strategies (B). Numbers in or adjacent to outlined areas indicate percent cells in each gate. Each dot represents data from one individual mouse and columns indicate the average values (C). *$P < 0.05$ by Mann-Whitney U test.

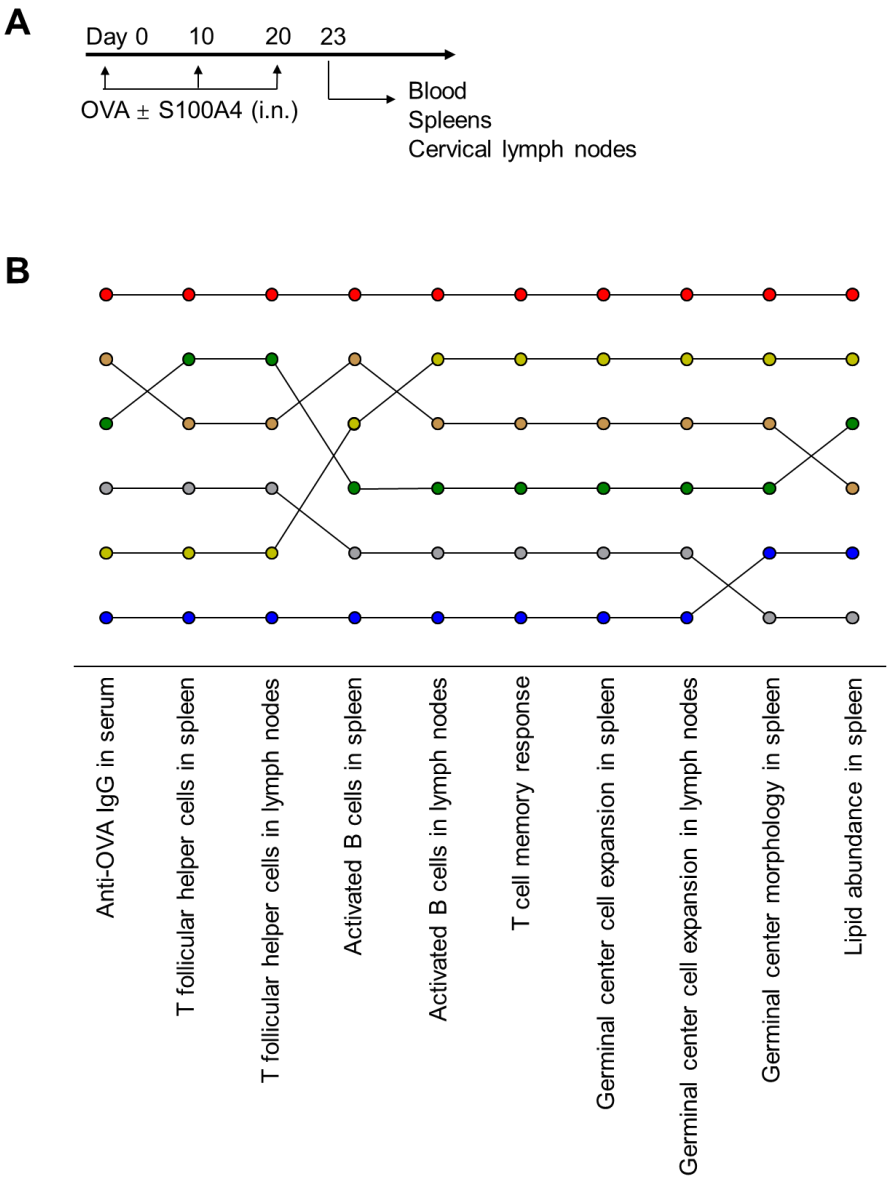

Figure 3.16 Antigen-specific antibody production is correlated with immune cell activation in the secondary lymphoid organs after immunization adjuvanted with S100A4. In this figure, the previously displayed data regarding the group that received S100A4 (Fig 3.6B, 3.8, 3.9C, 3.10C, 3.11C, 3.12C, 3.13B, 3.14C, and 3.15C) based on a common mouse immunization model (A) were processed and the expression levels of each (coloured dot) of the readouts were ranked at the single mouse level (B). Each line represents an individual mouse.

3.9 Dendritic cells express RAGE and TLR4, the two receptors for S100A4

It is reported that S100A4 triggers intracellular signalling pathways through RAGE and TLR4 in $CD11b^+$ cells (Björk *et al.*, 2013). I have already demonstrated robust activation of dendritic cells, the most important antigen-presenting cells, by S100A4 (Fig 3.2 and 3.3). Therefore, it was interesting to demonstrate whether dendritic cells express these two types of receptors. BMDCs clearly expressed both RAGE and TLR4 as analysed using flow cytometry (Fig 3.17A).

In order to demonstrate whether the two receptors were functionally needed for BMDC activation by S100A4, these cells were further incubated for 1 day with S100A4 or S100A4 pre-mixed with FPS-ZM1 or TAK-242, inhibitors of RAGE and TLR4, respectively. Cell surface expression of CD86 and intracellular production of IL-1β was measured by flow cytometry for the stimulatory effect of S100A4 (Fig 3.17B). S100A4 failed to stimulate BMDCs when either RAGE or TLR4 was blocked, suggesting that both receptors might be required for S100A4 activation in dendritic cells.

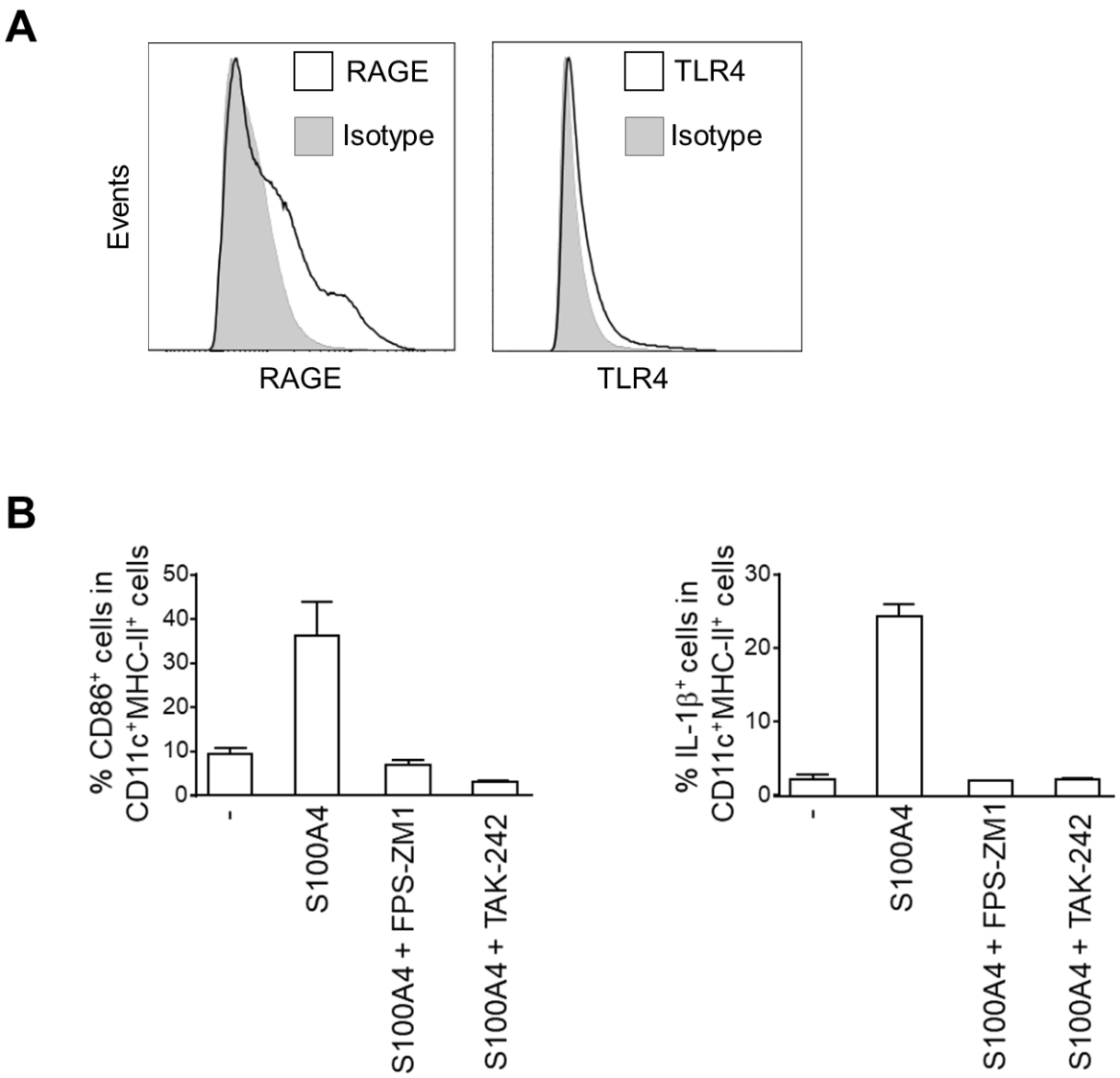

Figure 3.17 Dendritic cells express RAGE and TLR4, two receptors known for S100A4. (A) Bone marrow-derived dendritic cells (BMDC) were stained with anti-RAGE and anti-TLR4 antibodies or with their respective isotype control antibodies followed by flow cytometric analysis. (B) BMDCs were incubated for 1 day with S100A4 or S100A4 pre-mixed with FPS-ZM1 or TAK-242, inhibitors of RAGE and TLR4, respectively. Cell surface expression of CD86 and intracellular production of IL-1β were measured by flow cytometry. Data are expressed as histograms representing one out of three separate experiments (A) or as mean+SEM of 3 individual cell cultures.

3.10 S100A4 enhances cytokine expression in dendritic cells

mRNA expression of a group of cytokines and molecules that have crucial immune regulatory activities was upregulated in BMDCs following incubation with S100A4 (Fig 3.18). Specifically, the transcript levels of a number of cytokines that are critical to adaptive immunity, including IL-1β, IL-2, IL-6 and IL-10, were augmented after treatment with S100A4. IL-1β is of paramount importance for the inflammasome response that is essential for the development of adaptive immunity (Ciraci *et al.*, 2012). IL-2 plays a key role in the survival and growth of T cells (Boyman *et al.*, 2012). As a B cell growth factor, IL-6 promotes the production of IgG (Maeda *et al.*, 2010). IL-10 also contributes to the development of humoral adaptive immune responses (Couper *et al.*, 2008). Furthermore, S100A4 upregulated the co-stimulatory molecules, including CD80, CD86 and CD40. Modestly augmented expression of NLRP3 and TGF-β1 was observed after treatment with S100A4. IFN-γ failed to be upregulated at least at the mRNA level (Fig 3.18).

3.11 Mast cells express receptors for S100A4 and respond to stimulation by S100A4

The contribution to mucosal immune responses by mast cells has been firmly established (Reber *et al.*, 2015). In particular, mast cell activators have been described as potential adjuvants (McLachlan *et al.*, 2008). First of all, I demonstrated that, similar as BMDCs, BMMCs expressed both RAGE and TLR4, the two known receptors for S100A4 (Fig 3.19A). Next, BMMCs were incubated with S100A4 followed by measurement of the intracellular cytokine production. S100A4 was capable of promoting TNF-α production

at the protein level analysed by flow cytometry (Fig 3.19B). Furthermore, S100A4 substancially upregulated the mRNA expression of IL-1β, IL-9, IL-10 and TNF-α (Fig 3.19C). Mast cell-associated TNF-α, which can be potently released during activation, is a critical cytokine for mobilizing dendritic cells (Shelburne *et al.*, 2009). IL-9 facilitates humoral immune recall responses (Takatsuka *et al.*, 2018).

3.12 The adjuvanticity of S100A4 is not affected by the residual amount of contaminating LPS

As the S100A4 protein used in this project was a recombinant protein produced from *Escherichia coli*, there was a risk that residual LPS contamination might have confounded our observation. To exercise the maximum scientific stringency, I next investigated whether the previous findings were based on a real and true effect of S100A4 itself but not the effect of residual LPS contamination.

In order to determine the exact amount of residual LPS present in the recombinant S100A4, a Limulus amebocyte lysate assay was carried out. It turned out that the residual amount of LPS was equivalent to 0.099 EU in 1 μg of S100A4, and this LPS contamination level translates roughly to 10 pg of LPS in every 1 μg of S100A4 (Dawson *et al.*, 1988).

To investigate the effect of residual LPS in the recombinant S100A4 on its adjuvant activity, I performed both *in vivo* immunization and *in vitro* dendritic cell assays. First of

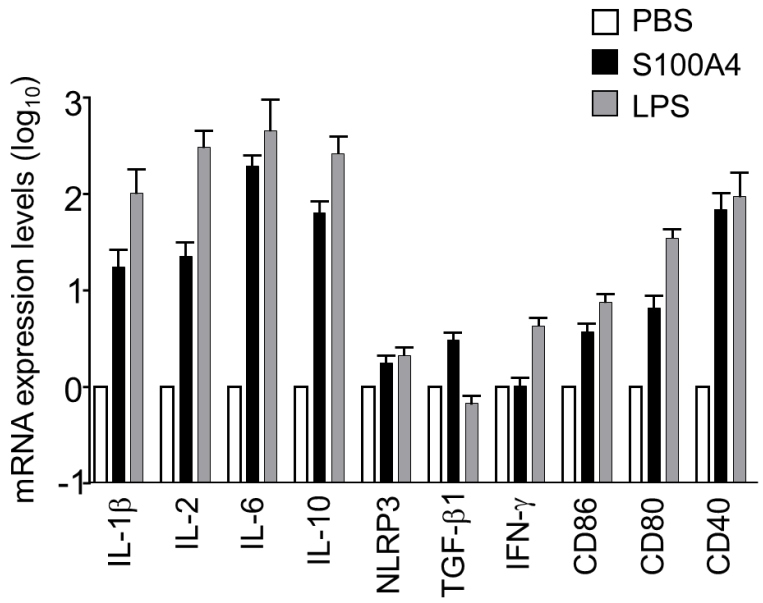

Figure 3.18 S100A4 enhances cytokine expression in dendritic cells. Bone marrow-derived dendritic cells were incubated with or without 1 μg/ml S100A4 for 3 hr followed by mRNA purification and real-time reverse transcription PCR analysis for the transcript expression of a number of cytokine genes. Cells were stimulated with 1 μg/ml LPS as a positive control. Gene expression was normalized using GAPDH as the calibrator gene. Data are express as mean+SEM of 3 biological replicates.

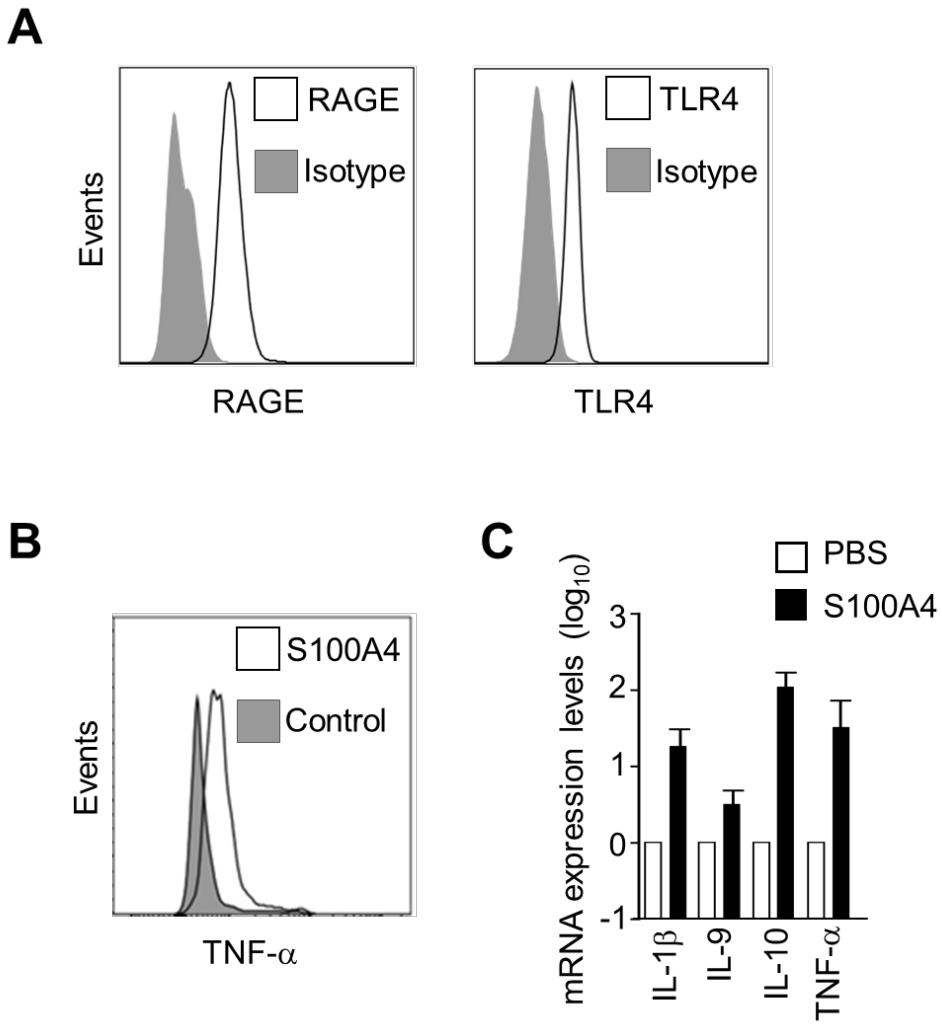

Figure 3.19 Mast cells express receptors for S100A4 and respond to stimulation by S100A4. (A) Bone marrow-derived mast cells (BMMCs) were stained with anti-RAGE and anti-TLR4 antibodies or with their respective isotype control antibodies followed by flow cytometric analysis. (B and C) BMMCs were incubated for 4 hr (B) or 3 hr (C) in the presence or absence of S100A4 at 1 μg/ml. The intracellular production of TNF-α was measured using flow cytometry (B). Levels of mRNA expression of a panel of cytokines were assessed using real-time reverse transcription PCR analysis; gene expression was normalized using GAPDH as the calibrator gene (C). Representative data out of three separate experiments are shown (A and B), or data are expressed as mean+SEM of 3 biological replicates (C).

all, mice were similarly immunized as previously described, i.e., three intranasal immunizations at an interval of 10 days with OVA in the presence of various doses of S100A4 or various amounts of LPS corresponding to the residual LPS present in a given S100A4 dose. Ten days after the last immunization, blood was collected and OVA specific total IgG antibody production in serum was measured.Residual LPS amounts present in various doses of S100A4 failed to promote OVA-specific IgG production, supporting the true adjuvant effect of S100A4 (Fig 3.20A).

To further rule out a possible confounding effect of LPS contamination on dendritic cell activation, I next incubated BMDC with LPS at 10 pg/ml (identical to the residual level of LPS in 1 μg/ml S100A4), and observed no enhancement in the expression of the genes under study. In contrast, both S100A4 (1 μg/ml) and LPS at a higher concentration (1 μg/ml) demonstrated potent stimulatory effects (Fig 3.20B).

Further support of the true effect of S100A4, but not the residual endotoxin contamination, that is responsible for dendritic cell activation, comes from the fact that the effect of the recombinant S100A4 on promoting CD80, CD86 and IL-1β was substantially suppressed by a neutralizing antibody against S100A4 (Fig 3.20C).

In my mRNA regulation study (Fig 3.18), S100A4, but not LPS, stimulated the expression of TGF-β1. This also supports that it is S100A4, but not the residual LPS contamination, stimulated dendritic cells.

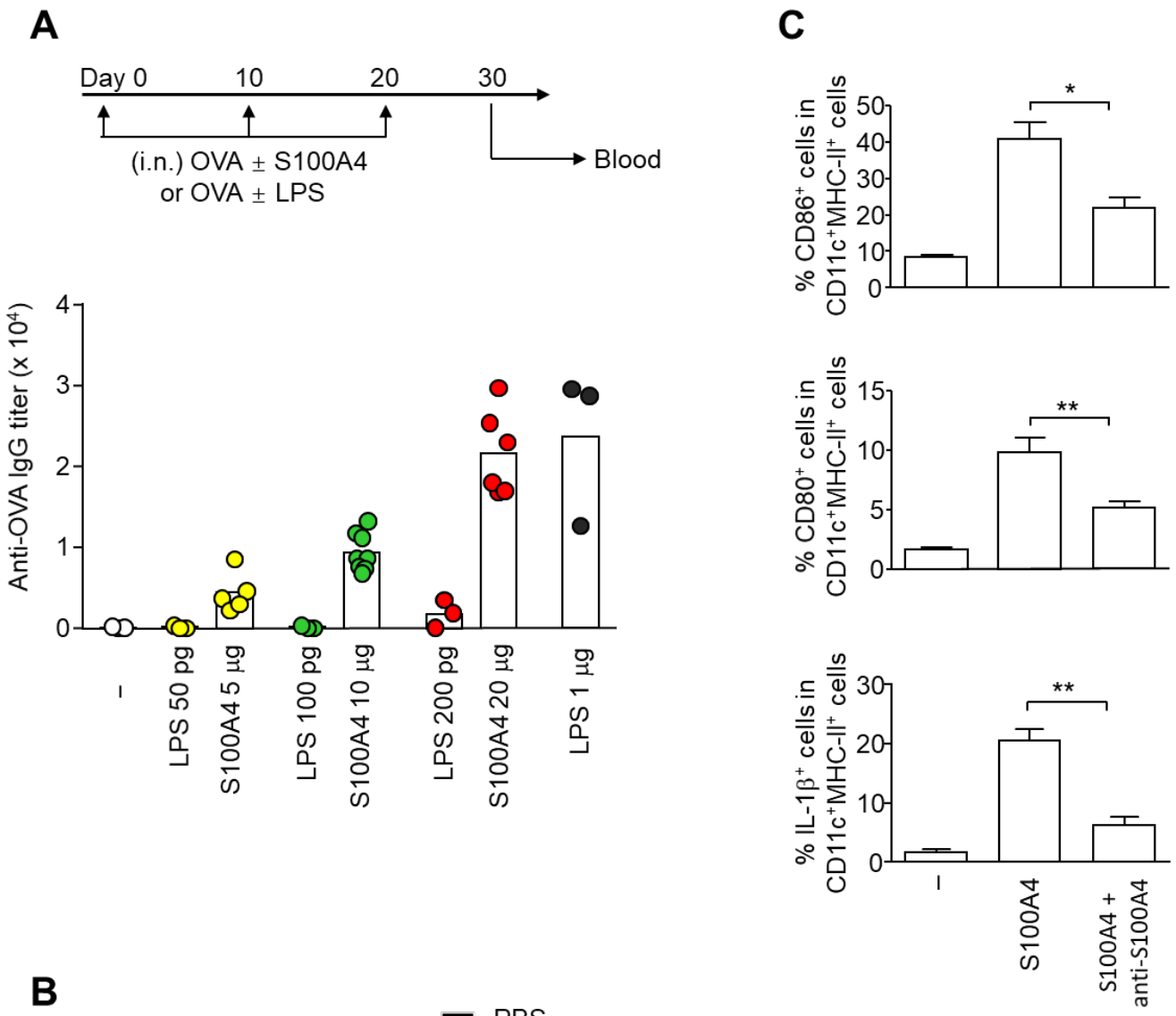
A
Day 0
10
20
30
Blood
(i.n.) OVA ± S100A4
or OVA ± LPS
Anti-OVA IgG titer (x 10⁴)
–
LPS 50 pg
S100A4 5 µg
LPS 100 pg
S100A4 10 µg
LPS 200 pg
S100A4 20 µg
LPS 1 µg
C
% CD86⁺ cells in CD11c⁺MHC-II⁺ cells
% CD80⁺ cells in CD11c⁺MHC-II⁺ cells
% IL-1β⁺ cells in CD11c⁺MHC-II⁺ cells
S100A4
S100A4 + anti-S100A4
B
PBS
S100A4 1 µg/ml
LPS 10 pg/ml
LPS 1 µg/ml
mRNA expression levels (log10)
IL-1β
IL-2
IL-6
IL-10
CD86
CD80
CD40

Figure 3.20 The adjuvant activity of S100A4 is not dependent on the residual amount of contaminating LPS. (A) Mice were immunized intranasally three times at a 10-day interval with OVA alone, OVA together with various amounts of S100A4 or with the corresponding residual LPS present in each S100A4 dose. Serum was collected 10 days after the last immunization. OVA-specific total IgG levels were analysed by ELISA. Columns close to each other represent the pair that received identical amounts of LPS (exogenously added versus residual contamination in S100A4). (B) BMDCs were incubated with S100A4 or corresponding residual LPS present as indicated for 3 hr and levels of mRNA expression of a panel of cytokines that could be augmented by both LPS and S100A4 were assessed using real-time reverse transcription PCR analysis. Gene expression was normalized using GAPDH as the calibrator gene. (C) Bone marrow-derived dendritic cells (BMDCs) were incubated for 1 day in the absence or presence of S100A4, or S100A4 pre-mixed with anti-S100A4 antibody. The frequencies of activated BMDC with enhanced expression of CD86, CD80 or IL-1β were measured using flow cytometry. Each dot represents data from an individual mouse and dots of the same colour indicate an identical amount of LPS the mouse received; columns indicate the average values (A), or representative data out of three separate experiments are shown (B), or data are expressed as mean+SEM of 3 biological replicates (C). $*P < 0.05$; $**P < 0.01$ by Mann-Whitney *U* test.

3.13 S100A4 promotes spike-specific antibody responses after intranasal immunization with the SARS-CoV-2 spike protein

In all the previous immunization assays, OVA was used as an experimental antigen. At the last stage of my thesis work, the world has been devastated by the COVID-19 pandemic, which is caused by the virus SARS-CoV-2. Therefore, I tested the adjuvant effect of S100A4 in boosting vaccination against COVID-19. As the spike protein of SARS-CoV-2 is a viral antigen that has been predicted to exert protective immune responses (W. H. Chen *et al.*, 2020), recombinant spike protein has been chosen to be the vaccine antigen. Thus, mice were intranasally immunized with spike protein in the presence or absence of S100A4 (Fig 3.21A). As shown in Fig 3.21B, spike protein-specific total IgG and IgG1 antibody levels were substantially increased in S100A4-adjuvanted immunization. In addition to serum antibody levels, S100A4-induced dramatic enhancement of mucosal spike protein-specific IgA responses at various mucosal sites was observed. These included the airways as reflected from the antibody accumulation in BALF (Fig 3.21C), lung parenchyma (Fig 3.21D), nasal mucosa (Fig 3.21E), eye mucosa (Fig 3.21F) and vaginal secretion (Fig 3.21G). The confirmation of the presence of spike protein-specific IgA in the eye mucosa is unique and has not been widely reported in vaccination studies. I believe that this is a very important finding as direct contact with the conjunctiva is also described as a possible route for coronavirus transmission (Hui *et al.*, 2020). Therefore, immune defence built up at the eye mucosa can possibly contribute to the vaccine efficacy. These data support a strong spike protein-specific antibody production in various compartments including circulation and mucosal

surfaces. In this immunization experiment, I lowered the amount of S100A4 to 10 μg per dose with 3 doses of immunization, compared with 20 μg in the major immunization experiments using OVA as an experimental vaccine antigen (Fig 3.6). Overall, S100A4 at this dose was still comparable to the efficacy of cholera toxin at 1 μg (Fig 3.21).

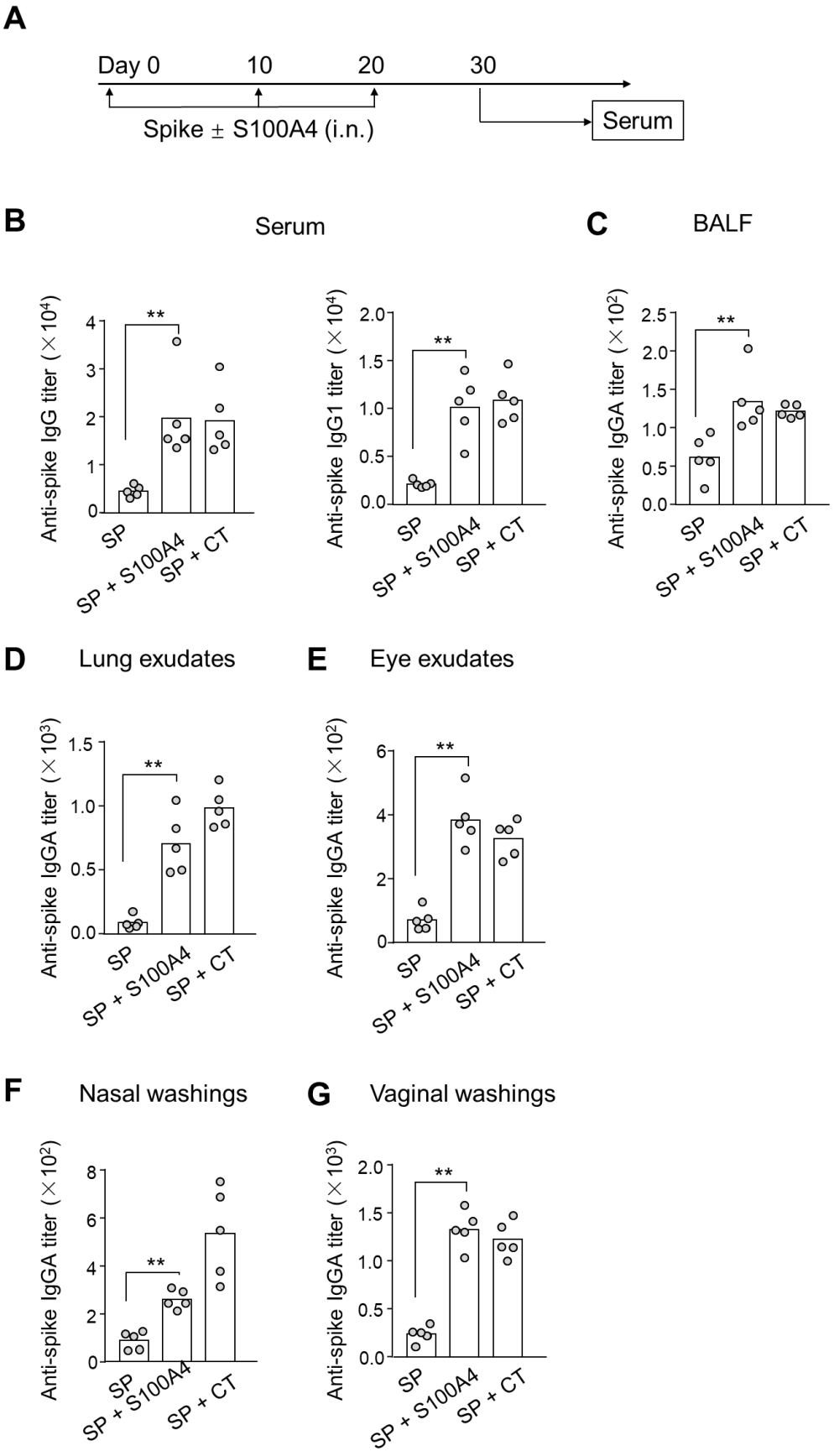
A
Day 0
10
20
30
Spike ± S100A4 (i.n.)
Serum
B
Serum
C
BALF
Anti-spike IgG titer (×10⁴)
Anti-spike IgG1 titer (×10⁴)
Anti-spike IgGA titer (×10²)
D
Lung exudates
E
Eye exudates
Anti-spike IgGA titer (×10³)
Anti-spike IgGA titer (×10²)
F
Nasal washings
G
Vaginal washings
Anti-spike IgGA titer (×10²)
Anti-spike IgGA titer (×10³)
**
SP
SP + S100A4
SP + CT

Figure 3.21 S100A4 promotes spike-specific antibody responses after intranasal immunization with the SARS-CoV-2 spike protein (SP). Mice received three intranasal immunizations at an interval of 10 days. For each immunization, mice were intranasally administered with 5 μg SP in PBS or admixed with 10 μg S100A4. Serum, BALF, lung exudate, eye exudate, nasal washing and vaginal washing samples were collected 10 days after the last immunization (A). Levels of anti-SP IgG and IgG1 in serum (B) as well as anti-SP IgA in BALF (C), lung exudates (D), eye washings (D), nasal washings (E) and vaginal washings (F) were measured by ELISA. Each dot represents measurement from one individual mouse. $^{**}P < 0.01$ by Mann-Whitney *U* test.

Chapter 4 — Discussion

4.1 DAMP molecules can be a game changer for mucosal vaccination

It has been previously demonstrated that mice deficient in the calcium-binding protein S100A4 have compromised adaptive immune responses even after mucosal immunization with the strong experimental adjuvant cholera toxin (J. B. Sun *et al.*, 2017). This finding suggests that it is likely that S100A4 might exert immune stimulatory adjuvant activity when supplied exogenously. It has also previously been suggested that IL-1 family cytokines exert potent mucosal adjuvant effects (Kayamuro *et al.*, 2010; Muñoz-Wolf *et al.*, 2018). Both S100A4 and IL-1 family cytokines are described as the DAMP family molecules (Bertheloot *et al.*, 2017). Therefore, it is very likely that other DAMP molecules in addition to the IL-1 family cytokines can also be candidate mucosal adjuvants. In fact, in this project I have screened four DAMP molecules, including S100A4, cyclophilin A, HMGB1, and uric acid, for the measurement of their mucosal adjuvant activity. The rationale behind the selection of these four candidates is that none of them have been formally described as a mucosal adjuvant, despite the reported adjuvant activities of cyclophilin A (Hou *et al*., 2016) and HMGB1 (Grover *et al.*, 2014) in parental immunization. The screening process was carried out in two steps. Firstly, after immunization using one of these four DAMP molecules as an adjuvant, the total antigen-specific antibody production in serum was measured using ELISA. Secondly, the DAMP molecules were examined for their capacity to activate dendritic cells *in vitro.* S100A4 consistently demonstrated robust effects in both *in vivo* and *in vitro* examinations. Therefore, I focused on S100A4 for its adjuvant effects in greater detail in the rest of my study.

I have generated compelling data demonstrating the strong adjuvant activity of S100A4 following intranasal immunization. S100A4 not only consistently augmented the production of antigen-specific serum IgG but also greatly enhanced the mucosal secretion of antigen-specific IgA, which is critical for mucosal immune defence in all the important mucosal sites, i.e., nose, airways, lungs and genital tract. Of note, antigen-specific antibody production driven by S100A4 was overall comparable to cholera toxin, the gold standard experimental mucosal adjuvant. Furthermore, my data have unequivocally supported the remarkable capacity of S100A4 in augmenting germinal centre responses and promoting dendritic cell activation, qualities required of potent adjuvants.

4.2 S100A4 exhibits dynamic immune regulatory functions

Th1 and Th2 responses in mice will result in preferential class-switch to IgG2c and IgG1, respectively (Tesfaye *et al.*, 2019), and therefore, both antibody subclasses can be quantified to indicate the polarization of immune responses by the adjuvant. S100A4 as an adjuvant promoted both serum IgG1 and IgG2c, two subclasses of IgG, demonstrating an activating role of S100A4 in driving both Th1 and Th2 differentiation of helper T cells.

One of the main criteria for a good adjuvant is to activate inflammasomes (Ivanov *et al.*, 2020), which was previously indicated as one of the functions of DAMP molecules (Lage *et al.*, 2014). It has been shown that dendritic cells from S100A4 knockout mice failed to promote inflammasome-associated caspase-1 and IL-1β production upon treatment with cholera toxin (J. B. Sun *et al*., 2017). My work demonstrated that extracellular S100A4

treatment on BMDC not only upregulated the three critical costimulatory molecules, CD40, CD80 and CD86, but also enhanced the production of IL-1β, IL-2, IL-6, and IL-10, which are important for the activation, development and proliferation of T and B lymphocytes (Mellman, 2013).

The germinal centre is formed when the activated antigen-specific T helper cells attract antigen-specific B cells to migrate toward follicular dendritic cells, and these B cells which can secrete high affinity antibodies are selected by follicular dendritic cells for further activation (Haberman *et al.*, 2019). Germinal centre T follicular helper cells found in lymphoid tissues are extremely crucial for the generation and maintenance of a strong antibody response (Crotty, 2014). My data strongly suggest that after immunization with S100A4 as an adjuvant the frequencies of germinal centre B cells and T follicular helper cells in both the spleen and cervical lymph nodes were expanded, which suggests that S100A4 plays a crucial role in promoting the germinal centre activation.

T call memory response is a critical component of the adaptive immune responses. Following the antigen-driven expansion and the death of effector T cells after antigen clearance, some of the remaining T cells differentiate into memory T cells of two different types: central memory and effector memory T cells (Soon *et al.*, 2019). The former are located in lymphoid organs and bone marrow and have a high proliferative potential whereas the latter stay in peripheral tissues in a preactivated form that enables them with

immediate action upon pathogen recognition. My data demonstrated enhanced T cell memory response after immunization adjuvanted with S100A4.

Classically, the mast cell is defined as an important innate immune cell type and critical regulator and effector in the development and exacerbation of allergic pathology. Mast cells are typically activated by IgE, which triggers the rapid release of allergic mediators such as histamine in allergic responses (Galli *et al.*, 2012). Mast cells are also master producers of a huge spectrum of proinflammatory cytokines and chemokines. In recent decades increased attention has been given to the role of mast cells in regulating both innate and adaptive immune responses in defence against pathogen invasion (Abraham *et al.*, 2010). More specifically, mast cell-associated TNF-α and other mediators can directly impact adaptive immune responses through promoting the maturation of dendritic cells and the migration of these cells to draining lymph nodes in part through the release of TNF-α (Heib *et al.*, 2007; Jawdat *et al.*, 2006; Shelburne et al., 2009; Suto *et al.*, 2006). At the mucosal membrane mast cells and dendritic cells form the first line of defence by sharing an overlapping territorial space strategically important for resisting invasion of the infectious agents (Galli *et al.*, 2005). Mast cells reside at sites of pathogen entry such as the skin and mucosal surfaces, including the gastrointestinal and respiratory tracts (Vliagoftis *et al.*, 2005). Mast cells have also been found to be present in nasal mucosal tissues (Fang *et al.*, 2013). Interestingly, mast cells have been particularly implicated from a vaccine development point of view (Fang *et al.*, 2016). McLachlan and colleagues reported that mast cell activators such as compound 48/80 can be used as highly effective

vaccine adjuvants for boosting both intradermal and intranasal immunization (McLachlan *et al.*, 2008). This finding has been supported by various studies which reveal the roles of mast cell activation in providing mucosal adjuvanticity (Bento *et al.*, 2019; Fang *et al.*, 2010; Fang et al., 2013). In my work, I have demonstrated that S100A4 could promote TNF-α production by mouse bone marrow-derived mast cells. This finding supports the possible contribution of mast cells in intranasal immunization adjuvanted by S100A4.

4.3 MALDI-TOF mass spectrometry is a potential label-free technique for germinal centre investigation

It is in the germinal centre that high affinity B cells and long-lived plasma cells are formed (Shlomchik *et al.*, 2019; Suan *et al.*, 2017) and clonal expansion requires vigorous cell proliferation, which demands adequate energy supply through activation of relevant metabolic pathways (Jung *et al*., 2019; Waters *et al.*, 2018). A recent study has elegantly demonstrated that germinal centre B cells use fatty acids instead of aerobic glycolysis for energy supply required for vigorous cell proliferation and survival (Weisel *et al*., 2020). This finding indicates that a successful germinal centre reaction requires a substantial amount of fatty acids which can be generated by lipid metabolism. I therefore undertook to employ the cutting-edge technology MALDI-TOF to quantitatively assess the lipid accumulation in the spleen, with an attempt to correlate the lipid dynamics to the germinal centre activity after immunization. To my knowledge, this is the first study that revealed germinal centre response using MALDI-TOF.

MALDI-TOF has become increasingly popular in biomedical research including microbial identification (Jang *et al.*, 2018), drug development (Beeman *et al.*, 2017; Guitot *et al.*, 2017), and tumour biology (Rodrigo *et al.*, 2014). MALDI-TOF has also become an important tool for immunological research. Whole-cell MALDI-TOF can be used to monitor the functional status of peripheral blood mononuclear cells which reveals signatures associated with sepsis progression (Daumas *et al.*, 2018). This method is also described as a reliable method to identify various immune cell types and their activity (Ouedraogo *et al.*, 2012; Ouedraogo *et al.*, 2013). In addition to analysis of proteins, MALDI-TOF has also been successfully used for the analysis of lipids in biological samples (Schiller *et al.*, 2007). MALDI-TOF offers a unique set of qualities including high sensitivity, minute sample consumption, and label-free detection, all of which are highly desirable in biomedical research. MALDI-TOF may have the potential to be exploited as a high-throughput screening and detection technique (Haslam *et al.*, 2016).

Interestingly, the combined intensity of various lipid species in the immunized mice adjuvanted with either S100A4 or cholera toxin was dramatically increased. Importantly, lipid accumulation in the spleen based on analysis using MALDI-TOF correlated very well with the measurement of the established germinal centre marker GL-7 using conventional techniques, such as flow cytometry and immunohistochemistry. Taken together, this finding strongly suggests that lipid measurement by MALDI-TOF can provide a surrogate marker for predicting germinal centre activity.

The availability of a full spectrum of antibodies recognizing various mouse antigens makes research on mouse models relatively easier. However, it is challenging for the investigation of animal models using species other than mice (e.g., rabbits, pigs, and chickens) owing to the lack of commercial antibodies including the germinal centre-specific antibody GL-7. My work suggests that MALDI-TOF can be used as a label-free tool for assessing the germinal centre reaction, which may provide a solution for investigating those animal models for which very limited commercial antibodies are available. For example, no GL-7 antibodies recognizing the rabbit or guinea pig germinal centre cells are commercially available.

4.4 S100A4 presents a promising adjuvant formulation for 2019-nCoV and other infectious diseases

The COVID-19 pandemic, caused by SARS-CoV-2, has devastated the world and its people since the end of 2019. SARS-CoV-2 is a novel virus of the Coronaviridae family, and the virus enters airways and lung epithelia through attaching to the angiotensin converting enzyme-2 (ACE2) and TMPRSS2 receptors by their spike protein (Perrotta *et al.*, 2020). Up to date, the virus has infected more than 10 million people and caused over half a million fatalities worldwide. No specific, reliable antiviral treatment is currently available. In addition to the development of therapeutic strategies, research with an orientation to the development of efficient vaccination approaches is desperately demanded for conquering the pandemic.

To test the effect of S100A4 in boosting the nasal vaccination against COVID-19, I chose 10 μg S100A4 for each dose of the 3 immunizations, which was half of the dose used in the previous major immunization studies using OVA as an experimental antigen. My data demonstrated that, at this dose, S100A4 still achieved an overall adjuvant activity comparable to cholera toxin at 1 μg per dose, with remarkably augmented anti-spike protein IgG antibody levels in serum as well as both IgG and IgA spike protein-specific antibody production in various mucosal compartments. As SARS-CoV-2 mainly infects humans through the airways, the mucosal accumulation of virus-specific antibodies at both upper and lower airways constitutes a critical defence mechanism against viral entry. After immunization of mice with spike protein mixed with S100A4, spike protein-specific IgA levels at nasal mucosa, airways and the lungs were consistently augmented. Eye exudates also contained substantially augmented spike protein-specific IgA, which suggests the build-up of possible mucosal defence at the eye mucosa. A recent study by our Hong Kong local colleagues suggested that direct contact with conjunctiva is a possible route for SARS-CoV-2 transmission (Hui *et al*., 2020).

In addition to COVID-19, other infectious diseases are still around. In the 2015 declaration “Transforming our world: the 2030 Agenda for Sustainable Development”, World Health Organization called on member states to end the epidemics of AIDS, tuberculosis, malaria and neglected tropical diseases by 2030, and to conquer hepatitis

and other transmissible diseases[5]. HIV/AIDS, malaria, and tuberculosis, the so-called "big three", desperately warrant effective vaccines (Hotez *et al.*, 2016). Novel mucosal vaccination modalities may provide a workable technical solution. Given the potent stimulatory role of S100A4 on the production of mucosal antigen-specific antibody, the exploitation of S100A4 as a mucosal adjuvant in the design of vaccine formulations against HIV/AIDS, malaria, and tuberculosis could be an interesting topic. It is worth noting that intranasal immunization adjuvanted with S100A4 potently stimulated the production of antigen-specific IgG and IgA at the genital tract, which highlights the potential of S100A4 being exploited as an effective adjuvant to be formulated in vaccines against sexually transmitted diseases.

4.5 S100A4 is predicted to be a safe adjuvant

S100A4 is expressed in many normal cells, including fibroblasts, endothelial cells, smooth muscle cells, lymphocytes, neutrophils, and macrophages (Chaabane *et al.*, 2015; Li *et al.*, 2010; Mishra *et al.*, 2012). S100A4 has been found to regulate a diverse range of normal physiological processes such as the growth, survival, differentiation, and motility of various types of cells (Donato, 2001). However, I should point out here that clinically oriented research on S100A4 has largely focused on its cancer metastasis-promoting properties (Boye *et al.*, 2010; Lukanidin *et al.*, 2012; Mishra et al., 2012).

[5] Transforming our world: implementing the 2030 agenda through sustainable development goal indicators, Special Sponsored Issue of the Journal of Public Health Policy, Violence and Health: Merging Evidence and Implementation, 2016; available from: https://www.who.int/violenceprevention/project_groups/2_JPHP_VPA_Special_Issue_Lee_et_al.pdf?ua=1

Although S100A4 has been demonstrated to be a cancer metastasis-promoting factor, this does not preclude its applicability as an adjuvant in vaccination. First of all, no documented evidence has shown that this protein is critical for the initiation of oncogenesis. Tumours develop as a result of multiple factors. Interestingly, overexpression of S100A4 (endogenous expression) in mouse models that are prone to the development of cancers only enhances the metastasis of established tumours but not the rates of tumour development (Ambartsumian *et al.*, 1996). Second, no evidence has shown that exogenous S100A4 (but not the endogenous protein) has the potential to induce cancer metastasis. The third point can be derived from examples wherein successful therapeutic strategies have focused on the exploitation of a number of cytokines (e.g., IL-6, TGF-β, and TNF-α) as a treatment modality for certain diseases [e.g., IL-6 for promoting neural regeneration in the treatment of brain diseases (Leibinger *et al.*, 2013)], despite the fact that these cytokines have been shown to contribute to the initiation and metastasis of cancer (Landskron *et al.*, 2014). Therefore, I believe that S100A4, as a human endogenous protein expressed in many normal cells, will have a better safety profile compared with microbial PAMP molecules. Of course, rigorous safety evaluations have to be undertaken before S100A4 can be used clinically.

4.6 Future perspectives

This research project has exclusively relied on the use of mice, both *in vitro* and *in vivo*, as an experimental model. Therefore, confirmation of my findings on other commonly used experimental animals for vaccine research, such as rabbits or guinea pigs, can be

considered. Compared with rodents which lack nasopharyngeal tonsils, rabbits and guinea pigs have a nasal cavity and a nasal-associated lymphoid tissue structure, i.e., NALT, more closely related to humans (Casteleyn *et al.*, 2010; L. Wang *et al.*, 2005). In particular, it is reported that rabbit NALT can impact immune responses at ear and eye mucosa as the lymphoid tissue is present in both the lacrimal duct and the nasopharynx where the entrances of the eustachian tubes are located (Casteleyn *et al.*, 2010). Furthermore, rabbits have much bigger eyes than mice which makes it more convenient to collect eye washings for antigen-specific IgA measurement for addressing infectious agents, e.g., SARS-CoV-2, that can transmit through conjunctiva. Similar nasal immunization protocols as used for mice developed in this project can be adapted to the rabbit or guinea pig immunization models. There is no linear correlation between the amounts of vaccine antigens and adjuvants and body weights. Usually the optimal doses of vaccine antigens and adjuvants in rabbits are 5-10-fold those in mice. The optimal doses for nasal immunization can be titrated. Apart from measuring antigen-specific antibody levels both in the circulation and mucosal secretions, germinal centre responses in the spleen and cervical lymph nodes can be analysed by the label-free MALDI-TOF technology which was developed and optimized during this project. As I commented above, MALDI-TOF provides an advantage because the antibody panels for rabbits or guinea pigs are much narrower than mice. Neither rabbit nor guinea pig antibodies against the germinal centre marker GL-7 are available.

The majority of my *in vivo* study has been based on the OVA-immunization model. To fundamentally demonstrate the applicability of S100A4 as a mucosal adjuvant, one needs to combine S100A4 with a pathogen-associated vaccine antigen (e.g., spike protein from coronavirus or components of other pathogens) for immunization followed by measurement of neutralizing antibody production and pathogen challenge assays. Furthermore, certain infectious diseases, especially those caused by viruses, relied on the generation of cytotoxic CD8 T cells for pathogen clearance and protection. Therefore, the efficiency of S100A4 in boosting CD8 T cell responses warrants further investigation.

In this project, I initially screened only four DAMP molecules based on the fact that none of these four had been reported to exert mucosal adjuvanticity. The screening can be further expanded. In addition to S100A4, other DAMP molecules, e.g., cyclophilin A, are also worth being further assessed for their mucosal adjuvant effects. Furthermore, the synergistic effects between various types of DAMP molecules, as well as that between DAMPs and other adjuvant candidates are worth exploring.

4.7 Concluding remarks

Most of the human vaccines that have been developed rely on the use of syringes and needles for delivery. The lack of safe, potent mucosal adjuvants that effectively mobilize the development of adaptive immunity has deferred the overall realization of mucosal immunization which obviates the need for needle injection. For example, most of the SARS-CoV-2 vaccine endeavours currently under development are still needle- and

injection-based. Mucosal vaccination, which offers better compliance and stronger mucosal immune defence, is the pursuit of many enthusiastic researchers. I certainly feel privileged to be one of them.

In this pioneering project, I focused on the evaluation of the DAMP molecules, in particular S100A4, as a novel class of mucosal adjuvants. I have presented compelling evidence supporting that S100A4 may be exploited as a promising, novel mucosal adjuvant, which provides one more technological pathway to the many strategies that form the global efforts in designing COVID-19 vaccines. I do envisage that my work will spur further dedicated research focusing on S100A4 by global colleagues in the mucosal vaccinology community, which may pave the way to the final successful licencing of S100A4 in clinical use.

References

Abraham, S. N., & St John, A. L. 2010. Mast cell-orchestrated immunity to pathogens. *Nat Rev Immunol.* 10: 440-452.

Aloulou, M., & Fazilleau, N. 2019. Regulation of B cell responses by distinct populations of CD4 T cells. *Biomed J.* 42: 243-251.

Ambartsumian, N. S., Grigorian, M. S., Larsen, I. F., Karlstrøm, O., Sidenius, N., Rygaard, J., Georgiev, G., & Lukanidin, E. 1996. Metastasis of mammary carcinomas in GRS/A hybrid mice transgenic for the mts1 gene. *Oncogene.* 13: 1621-1630.

Anders, H. J., & Schaefer, L. 2014. Beyond tissue injury-damage-associated molecular patterns, toll-like receptors, and inflammasomes also drive regeneration and fibrosis. *J Am Soc Nephrol.* 25: 1387-1400.

Awate, S., Babiuk, L. A., & Mutwiri, G. 2013. Mechanisms of action of adjuvants. *Front Immunol.* 4: 114.

Bader, M. S., & McKinsey, D. S. 2013. Postexposure prophylaxis for common infectious diseases. *Am Fam Physician.* 88: 25-32.

Beeman, K., Baumgärtner, J., Laubenheimer, M., Hergesell, K., Hoffmann, M., Pehl, U., Fischer, F., & Pieck, J. C. 2017. Integration of an In Situ MALDI-Based High-Throughput Screening Process: A Case Study with Receptor Tyrosine Kinase c-MET. *SLAS Discov.* 22: 1203-1210.

Belkaid, Y., & Hand, T. W. 2014. Role of the microbiota in immunity and inflammation. *Cell.* 157: 121-141.

Bento, D., Jesus, S., Lebre, F., Gonçalves, T., & Borges, O. 2019. Chitosan Plus Compound 48/80: Formulation and Preliminary Evaluation as a Hepatitis B Vaccine Adjuvant. *Pharmaceutics.* 11: 72.

Bertheloot, D., & Latz, E. 2017. HMGB1, IL-1α, IL-33 and S100 proteins: dual-function alarmins. *Cell Mol Immunol.* 14: 43-64.

Bianchi, M. E. 2007. DAMPs, PAMPs and alarmins: all we need to know about danger. *J Leukoc Biol.* 81: 1-5.

Bidgood, S. R., Tam, J. C., McEwan, W. A., Mallery, D. L., & James, L. C. 2014. Translocalized IgA mediates neutralization and stimulates innate immunity inside infected cells. *Proc Natl Acad Sci U S A.* 111: 13463-13468.

Biram, A., & Shulman, Z. 2020. T cell help to B cells: Cognate and atypical interactions in peripheral and intestinal lymphoid tissues. *Immunol Rev.* 10.1111/imr.12890.

Björk, P., Källberg, E., Wellmar, U., Riva, M., Olsson, A., He, Z., Törngren, M., Liberg, D., Ivars, F., & Leanderson, T. 2013. Common interactions between S100A4 and S100A9 defined by a novel chemical probe. *PLoS One.* 8: e63012.

Boyaka, P. N. 2017. Inducing Mucosal IgA: A Challenge for Vaccine Adjuvants and Delivery Systems. *J Immunol.* 199: 9-16.

Boye, K., & Maelandsmo, G. M. 2010. S100A4 and metastasis: a small actor playing many roles. *Am J Pathol.* 176: 528-535.

Boyman, O., & Sprent, J. 2012. The role of interleukin-2 during homeostasis and activation of the immune system. *Nat Rev Immunol.* 12: 180-190.

Brazolot Millan, C. L., Weeratna, R., Krieg, A. M., Siegrist, C. A., & Davis, H. L. 1998. CpG DNA can induce strong Th1 humoral and cell-mediated immune responses against hepatitis B surface antigen in young mice. *Proc Natl Acad Sci U S A.* 95: 15553-15558.

Breedveld, A., & van Egmond, M. 2019. IgA and FcαRI: Pathological Roles and Therapeutic Opportunities. *Front Immunol.* 10: 553.

Breman, J. G., & Arita, I. 1980. The confirmation and maintenance of smallpox eradication. *N Engl J Med.* 303: 1263-1273.

Bromley, S. K., Iaboni, A., Davis, S. J., Whitty, A., Green, J. M., Shaw, A. S., Weiss, A., & Dustin, M. L. 2001. The immunological synapse and CD28-CD80 interactions. *Nat Immunol.* 2: 1159-1166.

Calzas, C., & Chevalier, C. 2019. Innovative Mucosal Vaccine Formulations Against Influenza A Virus Infections. *Front Immunol.* 10: 1605.

Casteleyn, C., Broos, A. M., Simoens, P., & Van den Broeck, W. 2010. NALT (nasal cavity-associated lymphoid tissue) in the rabbit. *Vet Immunol Immunopathol.* 133: 212-218.

Cerutti, A. 2008. The regulation of IgA class switching. *Nat Rev Immunol.* 8: 421-434.

Chaabane, C., Heizmann, C. W., & Bochaton-Piallat, M. L. 2015. Extracellular S100A4 induces smooth muscle cell phenotypic transition mediated by RAGE. *Biochim Biophys Acta.* 1853: 2144-2157.

Chen, W., Patel, G. B., Yan, H., & Zhang, J. 2010. Recent advances in the development of novel mucosal adjuvants and antigen delivery systems. *Hum Vaccin.* 6: 11561.

Chen, W. H., Strych, U., Hotez, P. J., & Bottazzi, M. E. 2020. The SARS-CoV-2 Vaccine Pipeline: an Overview. *Curr Trop Med Rep*: 1-4.

Chi, X., Li, Y., & Qiu, X. 2020. V(D)J recombination, somatic hypermutation and class switch recombination of immunoglobulins: mechanism and regulation. *Immunology*.

Chu, V. T., & Berek, C. 2013. The establishment of the plasma cell survival niche in the bone marrow. *Immunol Rev.* 251: 177-188.

Ciraci, C., Janczy, J. R., Sutterwala, F. S., & Cassel, S. L. 2012. Control of innate and adaptive immunity by the inflammasome. *Microbes Infect.* 14: 1263-1270.

Clements, J. D., & Norton, E. B. 2018. The Mucosal Vaccine Adjuvant LT(R192G/L211A) or dmLT. *mSphere.* 3: e00215-18.

Conte, C., Sogni, F., Affanni, P., Veronesi, L., Argentiero, A., & Esposito, S. 2020. Vaccines against Coronaviruses: The State of the Art. *Vaccines (Basel).* 8.

Corthésy, B. 2013. Multi-faceted functions of secretory IgA at mucosal surfaces. *Front Immunol.* 4: 185.

Couper, K. N., Blount, D. G., & Riley, E. M. 2008. IL-10: the master regulator of immunity to infection. *J Immunol.* 180: 5771-5777.

Crotty, S. 2014. T follicular helper cell differentiation, function, and roles in disease. *Immunity.* 41: 529-542.

Daumas, A., Alingrin, J., Ouedraogo, R., Villani, P., Leone, M., & Mege, J. L. 2018. MALDI-TOF MS monitoring of PBMC activation status in sepsis. *BMC Infect Dis.* 18: 355.

Davis, C. W., Jackson, K. J. L., McCausland, M. M., Darce, J., Chang, C., Linderman, S. L., Chennareddy, C., Gerkin, R., Brown, S. J., Wrammert, J., Mehta, A. K., Cheung, W. C., Boyd, S. D., Waller, E. K., & Ahmed, R. 2020. Influenza vaccine-induced human bone marrow plasma cells decline within a year after vaccination. *Science*.

Dawson, M., Novitsky, T., & Gould, M. 1988. Microbes, endotoxins and water. *Pharm. Engineering.* 8: 145-148.

de Sousa-Pereira, P., & Woof, J. M. 2019. IgA: Structure, Function, and Developability. *Antibodies (Basel).* 8: 57.

Dillon, A., & Lo, D. D. 2019. M Cells: Intelligent Engineering of Mucosal Immune Surveillance. *Front Immunol.* 10: 1499.

Donato, R. 2001. S100: a multigenic family of calcium-modulated proteins of the EF-hand type with intracellular and extracellular functional roles. *Int J Biochem Cell Biol.* 33: 637-668.

Eleftheriadis, T., Pissas, G., Karioti, A., Antoniadi, G., Golfinopoulos, S., Liakopoulos, V., Mamara, A., Speletas, M., Koukoulis, G., & Stefanidis, I. 2013. Uric acid induces caspase-1 activation, IL-1β secretion and P2X7 receptor dependent proliferation in primary human lymphocytes. *Hippokratia.* 17: 141-145.

Eriksson, A. M., Schön, K. M., & Lycke, N. Y. 2004. The cholera toxin-derived CTA1-DD vaccine adjuvant administered intranasally does not cause inflammation or accumulate in the nervous tissues. *J Immunol.* 173: 3310-3319.

Fagone, P., Shedlock, D. J., Bao, H., Kawalekar, O. U., Yan, J., Gupta, D., Morrow, M. P., Patel, A., Kobinger, G. P., Muthumani, K., & Weiner, D. B. 2011. Molecular adjuvant HMGB1 enhances anti-influenza immunity during DNA vaccination. *Gene Ther.* 18: 1070-1077.

Fan, X. T., Wang, Y. L., Su, Q. D., Qiu, F., Yi, Y., Jia, Z. Y., Wang, D. Y., Qin, K., Zou, Y. N., Bi, S. L., & Shen, L. P. 2019. Intranasal Immunization Using CTA1-DD as a Mucosal Adjuvant for an Inactivated Influenza Vaccine. *Biomed Environ Sci.* 32: 531-540.

Fang, Y., Larsson, L., Mattsson, J., Lycke, N., & Xiang, Z. 2010. Mast cells contribute to the mucosal adjuvant effect of CTA1-DD after IgG-complex formation. *J Immunol.* 185: 2935-2941.

Fang, Y., & Xiang, Z. 2016. Roles and relevance of mast cells in infection and vaccination. *J Biomed Res.* 30: 253-263.

Fang, Y., Zhang, T., Lidell, L., Xu, X., Lycke, N., & Xiang, Z. 2013. The immune complex CTA1-DD/IgG adjuvant specifically targets connective tissue mast cells through FcγRIIIA and augments anti-HPV immunity after nasal immunization. *Mucosal Immunol.* 6: 1168-1178.

Fiebelkorn, A. P., Lawler, J., Curns, A. T., Brandeburg, C., & Wallace, G. S. 2013. Mumps postexposure prophylaxis with a third dose of measles-mumps-rubella vaccine, Orange County, New York, USA. *Emerg Infect Dis.* 19: 1411-1417.

Freedman, D. O., & Chen, L. H. 2019. Vaccines for International Travel. *Mayo Clin Proc.* 94: 2314-2339.

Galli, S. J., Nakae, S., & Tsai, M. 2005. Mast cells in the development of adaptive immune responses. *Nat Immunol.* 6: 135-142.

Galli, S. J., & Tsai, M. 2012. IgE and mast cells in allergic disease. *Nat Med.* 18: 693-704.

Gary, E. N., Kathuria, N., Makurumidze, G., Curatola, A., Ramamurthi, A., Bernui, M. E., Myles, D., Yan, J., Pankhong, P., Muthumani, K., Haddad, E., Humeau, L., Weiner, D. B., & Kutzler, M. A. 2020. CCR10 expression is required for the adjuvant activity of the mucosal chemokine CCL28 when delivered in the context of an HIV-1 Env DNA vaccine. *Vaccine.* 38: 2626-2635.

Gołoś, A., & Lutyńska, A. 2015. Aluminium-adjuvanted vaccines--a review of the current state of knowledge. *Przegl Epidemiol.* 69: 731-734, 871-734.

Gross, C. P., & Sepkowitz, K. A. 1998. The myth of the medical breakthrough: smallpox, vaccination, and Jenner reconsidered. *Int J Infect Dis.* 3: 54-60.

Grover, A., Troudt, J., Foster, C., Basaraba, R., & Izzo, A. 2014. High mobility group box 1 acts as an adjuvant for tuberculosis subunit vaccines. *Immunology.* 142: 111-123.

Guitot, K., Drujon, T., Burlina, F., Sagan, S., Beaupierre, S., Pamlard, O., Dodd, R. H., Guillou, C., Bolbach, G., Sachon, E., & Guianvarc'h, D. 2017. A direct label-free MALDI-TOF mass spectrometry based assay for the characterization of inhibitors of protein lysine methyltransferases. *Anal Bioanal Chem.* 409: 3767-3777.

Gupta, R. K., Relyveld, E. H., Lindblad, E. B., Bizzini, B., Ben-Efraim, S., & Gupta, C. K. 1993. Adjuvants--a balance between toxicity and adjuvanticity. *Vaccine.* 11: 293-306.

Guy, B. 2007. The perfect mix: recent progress in adjuvant research. *Nat Rev Microbiol.* 5: 505-517.

Haberman, A. M., Gonzalez, D. G., Wong, P., Zhang, T. T., & Kerfoot, S. M. 2019. Germinal center B cell initiation, GC maturation, and the coevolution of its stromal cell niches. *Immunol Rev.* 288: 10-27.

Haslam, C., Hellicar, J., Dunn, A., Fuetterer, A., Hardy, N., Marshall, P., Paape, R., Pemberton, M., Resemannand, A., & Leveridge, M. 2016. The Evolution of MALDI-TOF Mass Spectrometry toward Ultra-High-Throughput Screening: 1536-Well Format and Beyond. *J Biomol Screen.* 21: 176-186.

Heib, V., Becker, M., Warger, T., Rechtsteiner, G., Tertilt, C., Klein, M., Bopp, T., Taube, C., Schild, H., Schmitt, E., & Stassen, M. 2007. Mast cells are crucial for early inflammation, migration of Langerhans cells, and CTL responses following topical application of TLR7 ligand in mice. *Blood.* 110: 946-953.

Herbert, W. J. 1968. The mode of action of mineral-oil emulsion adjuvants on antibody production in mice. *Immunology.* 14: 301-318.

Hinc, K., Stasiłojć, M., Piątek, I., Peszyńska-Sularz, G., Isticato, R., Ricca, E., Obuchowski, M., & Iwanicki, A. 2014. Mucosal adjuvant activity of IL-2 presenting spores of bacillus subtilis in a murine model of Helicobacter pylori vaccination. *PLoS One.* 9: e95187.

Hotez, P. J., Bottazzi, M. E., & Strych, U. 2016. New Vaccines for the World's Poorest People. *Annu Rev Med.* 67: 405-417.

Hou, J., Zhang, Q., Liu, Z., Wang, S., Li, D., Liu, C., Liu, Y., & Shao, Y. 2016. Cyclophilin A as a potential genetic adjuvant to improve HIV-1 Gag DNA vaccine immunogenicity by eliciting broad and long-term Gag-specific cellular immunity in mice. *Hum Vaccin Immunother.* 12: 545-553.

Hui, K. P. Y., Cheung, M. C., Perera, R., Ng, K. C., Bui, C. H. T., Ho, J. C. W., Ng, M. M. T., Kuok, D. I. T., Shih, K. C., Tsao, S. W., Poon, L. L. M., Peiris, M., Nicholls, J. M., & Chan, M. C. W. 2020. Tropism, replication competence, and innate immune responses of the coronavirus SARS-CoV-2 in human respiratory tract and conjunctiva: an analysis in ex-vivo and in-vitro cultures. *Lancet Respir Med.* S2213-2600(20)30193-4.

Ibrahim, Z. A., Armour, C. L., Phipps, S., & Sukkar, M. B. 2013. RAGE and TLRs: relatives, friends or neighbours? *Mol Immunol.* 56: 739-744.

Ivanov, K., Garanina, E., Rizvanov, A., & Khaiboullina, S. 2020. Inflammasomes as Targets for Adjuvants. *Pathogens.* 9: 252.

Jang, K. S., & Kim, Y. H. 2018. Rapid and robust MALDI-TOF MS techniques for microbial identification: a brief overview of their diverse applications. *J Microbiol.* 56: 209-216.

Jawdat, D. M., Rowden, G., & Marshall, J. S. 2006. Mast cells have a pivotal role in TNF-independent lymph node hypertrophy and the mobilization of Langerhans cells in response to bacterial peptidoglycan. *J Immunol.* 177: 1755-1762.

Jung, J., Zeng, H., & Horng, T. 2019. Metabolism as a guiding force for immunity. *Nat Cell Biol.* 21: 85-93.

Kang, R., Livesey, K. M., Zeh, H. J., Loze, M. T., & Tang, D. 2010. HMGB1: a novel Beclin 1-binding protein active in autophagy. *Autophagy.* 6: 1209-1211.

Karnezis, T., Farnsworth, R. H., Harris, N. C., Williams, S. P., Caesar, C., Byrne, D. J., Herle, P., Macheda, M. L., Shayan, R., Zhang, Y. F., Yazar, S., Takouridis, S. J., Gerard, C., Fox, S. B., Achen, M. G., & Stacker, S. A. 2019. CCL27/CCL28-CCR10 Chemokine Signaling Mediates Migration of Lymphatic Endothelial Cells. *Cancer Res.* 79: 1558-1572.

Kataoka, H., Kono, H., Patel, Z., Kimura, Y., & Rock, K. L. 2014. Evaluation of the contribution of multiple DAMPs and DAMP receptors in cell death-induced sterile inflammatory responses. *PLoS One.* 9: e104741.

Kayamuro, H., Yoshioka, Y., Abe, Y., Arita, S., Katayama, K., Nomura, T., Yoshikawa, T., Kubota-Koketsu, R., Ikuta, K., Okamoto, S., Mori, Y., Kunisawa, J., Kiyono, H., Itoh, N., Nagano, K., Kamada, H., Tsutsumi, Y., & Tsunoda, S. 2010. Interleukin-1 family cytokines as mucosal vaccine adjuvants for induction of protective immunity against influenza virus. *J Virol.* 84: 12703-12712.

Kool, M., Pétrilli, V., De Smedt, T., Rolaz, A., Hammad, H., van Nimwegen, M., Bergen, I. M., Castillo, R., Lambrecht, B. N., & Tschopp, J. 2008. Cutting edge: alum adjuvant stimulates inflammatory dendritic cells through activation of the NALP3 inflammasome. *J Immunol.* 181: 3755-3759.

Kreutz, M., Tacken, P. J., & Figdor, C. G. 2013. Targeting dendritic cells--why bother? *Blood.* 121: 2836-2844.

Kuka, M., & Iannacone, M. 2018. Viral subversion of B cell responses within secondary lymphoid organs. *Nat Rev Immunol.* 18: 255-265.

Kumar, H., Kawai, T., & Akira, S. 2011. Pathogen recognition by the innate immune system. *Int Rev Immunol.* 30: 16-34.

Kumar, S., Sunagar, R., & Gosselin, E. 2019. Bacterial Protein Toll-Like-Receptor Agonists: A Novel Perspective on Vaccine Adjuvants. *Front Immunol.* 10: 1144.

Kuolee, R., & Chen, W. 2008. M cell-targeted delivery of vaccines and therapeutics. *Expert Opin Drug Deliv.* 5: 693-702.

Lage, S. L., Longo, C., Branco, L. M., da Costa, T. B., Buzzo Cde, L., & Bortoluci, K. R. 2014. Emerging Concepts about NAIP/NLRC4 Inflammasomes. *Front Immunol.* 5: 309.

Landskron, G., De la Fuente, M., Thuwajit, P., Thuwajit, C., & Hermoso, M. A. 2014. Chronic inflammation and cytokines in the tumor microenvironment. *J Immunol Res.* 2014: 149185.

Lee, C., Kim, G. R., Yoon, J., Kim, S. E., Yoo, J. S., & Piao, Y. 2018. In vivo delineation of glioblastoma by targeting tumor-associated macrophages with near-infrared fluorescent silica coated iron oxide nanoparticles in orthotopic xenografts for surgical guidance. *Scientific Reports.* 8: 11122.

Leibinger, M., Müller, A., Gobrecht, P., Diekmann, H., Andreadaki, A., & Fischer, D. 2013. Interleukin-6 contributes to CNS axon regeneration upon inflammatory stimulation. *Cell Death Dis.* 4: e609.

Lewis, D. J., Huo, Z., Barnett, S., Kromann, I., Giemza, R., Galiza, E., Woodrow, M., Thierry-Carstensen, B., Andersen, P., Novicki, D., Del Giudice, G., & Rappuoli, R. 2009. Transient facial nerve paralysis (Bell's palsy) following intranasal delivery of a genetically detoxified mutant of Escherichia coli heat labile toxin. *PLoS One.* 4: e6999.

Li, Z. H., Dulyaninova, N. G., House, R. P., Almo, S. C., & Bresnick, A. R. 2010. S100A4 regulates macrophage chemotaxis. *Mol Biol Cell.* 21: 2598-2610.

Lightman, S. M., Utley, A., & Lee, K. P. 2019. Survival of Long-Lived Plasma Cells (LLPC): Piecing Together the Puzzle. *Front Immunol.* 10: 965.

Liu, F., Endo, Y., Romantseva, T., Wu, W. W., Akue, A., Shen, R. F., Golding, H., & Zaitseva, M. 2019. T cell-derived soluble glycoprotein GPIbα mediates PGE(2) production in human monocytes activated with the vaccine adjuvant MDP. *Sci Signal.* 12: eaat6023.

Liu, R., Mori, S., Wake, H., Zhang, J., Liu, K., Izushi, Y., Takahashi, H. K., Peng, B., & Nishibori, M. 2009. Establishment of in vitro binding assay of high mobility

group box-1 and S100A12 to receptor for advanced glycation endproducts: heparin's effect on binding. *Acta Med Okayama.* 63: 203-211.

Lobaina Mato, Y. 2019. Nasal route for vaccine and drug delivery: Features and current opportunities. *Int J Pharm.* 572: 118813.

Lombard, M., Pastoret, P. P., & Moulin, A. M. 2007. A brief history of vaccines and vaccination. *Rev Sci Tech.* 26: 29-48.

Lotze, M. T., & Tracey, K. J. 2005. High-mobility group box 1 protein (HMGB1): nuclear weapon in the immune arsenal. *Nat Rev Immunol.* 5: 331-342.

Lukanidin, E., & Sleeman, J. P. 2012. Building the niche: the role of the S100 proteins in metastatic growth. *Semin Cancer Biol.* 22: 216-225.

Lycke, N. 2010. Is the choice of vaccine adjuvant critical for long-term memory development? *Expert Rev Vaccines.* 9: 1357-1361.

Lycke, N. 2012. Recent progress in mucosal vaccine development: potential and limitations. *Nat Rev Immunol.* 12: 592-605.

Lycke, N., & Bemark, M. 2010. Mucosal adjuvants and long-term memory development with special focus on CTA1-DD and other ADP-ribosylating toxins. *Mucosal Immunol.* 3: 556-566.

Maeda, K., Mehta, H., Drevets, D. A., & Coggeshall, K. M. 2010. IL-6 increases B-cell IgG production in a feed-forward proinflammatory mechanism to skew hematopoiesis and elevate myeloid production. *Blood.* 115: 4699-4706.

Malik, A., Gupta, M., Gupta, V., Gogoi, H., & Bhatnagar, R. 2018. Novel application of trimethyl chitosan as an adjuvant in vaccine delivery. *Int J Nanomedicine.* 13: 7959-7970.

Mantis, N. J., & Forbes, S. J. 2010. Secretory IgA: arresting microbial pathogens at epithelial borders. *Immunol Invest.* 39: 383-406.

Matzinger, P. 2002. The danger model: a renewed sense of self. *Science.* 296: 301-305.

Matzinger, P. 2012. The evolution of the danger theory. Interview by Lauren Constable, Commissioning Editor. *Expert Rev Clin Immunol.* 8: 311-317.

McLachlan, J. B., Shelburne, C. P., Hart, J. P., Pizzo, S. V., Goyal, R., Brooking-Dixon, R., Staats, H. F., & Abraham, S. N. 2008. Mast cell activators: a new class of highly effective vaccine adjuvants. *Nat Med.* 14: 536-541.

Mehrabi, M., Montazeri, H., Mohamadpour Dounighi, N., Rashti, A., & Vakili-Ghartavol, R. 2018. Chitosan-based Nanoparticles in Mucosal Vaccine Delivery. *Arch Razi Inst.* 73: 165-176.

Mellman, I. 2013. Dendritic cells: master regulators of the immune response. *Cancer Immunol Res.* 1: 145-149.

Miquel-Clopés, A., Bentley, E. G., Stewart, J. P., & Carding, S. R. 2019. Mucosal vaccines and technology. *Clin Exp Immunol.* 196: 205-214.

Mishra, S. K., Siddique, H. R., & Saleem, M. 2012. S100A4 calcium-binding protein is key player in tumor progression and metastasis: preclinical and clinical evidence. *Cancer Metastasis Rev.* 31: 163-172.

Mitsdoerffer, M., Lee, Y., Jäger, A., Kim, H. J., Korn, T., Kolls, J. K., Cantor, H., Bettelli, E., & Kuchroo, V. K. 2010. Proinflammatory T helper type 17 cells are effective B-cell helpers. *Proc Natl Acad Sci U S A.* 107: 14292-14297.

Mohan, T., Deng, L., & Wang, B. Z. 2017. CCL28 chemokine: An anchoring point bridging innate and adaptive immunity. *Int Immunopharmacol.* 51: 165-170.

Mohan, T., Verma, P., & Rao, D. N. 2013. Novel adjuvants & delivery vehicles for vaccines development: a road ahead. *Indian J Med Res.* 138: 779-795.

Mortellaro, A., Conforti-Andreoni, C., Spreafico, R., & Ricciardi-Castagnoli, P. 2012. Uric acid acts as a natural adjuvant by promoting Th17 cell differentiation via an inflammasome-dependent mechanism (176.28). *J Immunol.* 188: 176.128.

Mosmann, T. R., Cherwinski, H., Bond, M. W., Giedlin, M. A., & Coffman, R. L. 2005. Two types of murine helper T cell clone. I. Definition according to profiles of lymphokine activities and secreted proteins. 1986. *J Immunol.* 175: 5-14.

Mshelia, S. E., Blackmore, C., Archer, R., & Booth, A. 2020. Factors affecting the successful implementation of Global Polio Eradication Initiative (GPEI) in low- and middle-income countries. *J Glob Health.* 10: 010322.

Muñoz-Wolf, N., & Lavelle, E. C. 2018. A Guide to IL-1 family cytokines in adjuvanticity. *Febs j.* 285: 2377-2401.

Murakami, Y., Matsumoto, H., Roh, M., Giani, A., Kataoka, K., Morizane, Y., Kayama, M., Thanos, A., Nakatake, S., Notomi, S., Hisatomi, T., Ikeda, Y., Ishibashi, T., Connor, K. M., Miller, J. W., & Vavvas, D. G. 2014. Programmed necrosis, not apoptosis, is a key mediator of cell loss and DAMP-mediated inflammation in dsRNA-induced retinal degeneration. *Cell Death Differ.* 21: 270-277.

Nakamura, Y., Kimura, S., & Hase, K. 2018. M cell-dependent antigen uptake on follicle-associated epithelium for mucosal immune surveillance. *Inflamm Regen.* 38: 15.

Nakayama, T., Hirahara, K., Onodera, A., Endo, Y., Hosokawa, H., Shinoda, K., Tumes, D. J., & Okamoto, Y. 2017. Th2 Cells in Health and Disease. *Annu Rev Immunol.* 35: 53-84.

Newsted, D., Fallahi, F., Golshani, A., & Azizi, A. 2015. Advances and challenges in mucosal adjuvant technology. *Vaccine.* 33: 2399-2405.

Nizard, M., Diniz, M. O., Roussel, H., Tran, T., Ferreira, L. C., Badoual, C., & Tartour, E. 2014. Mucosal vaccines: novel strategies and applications for the control of pathogens and tumors at mucosal sites. *Hum Vaccin Immunother.* 10: 2175-2187.

Oh, S. H., Kim Cho, Y. S., Lee, H. B., Lee, S. M., Kim, W. S., Hong, L., Cho, C. S., Choi, Y. J., & Kang, S. K. 2019. Enhancement of antigen-specific humoral immune responses and protein solubility through conjugation of bacterial flagellin, Vibrio vulnificus FlaB, to the N-terminus of porcine epidemic diarrhea virus surface protein antigen S0. *J Vet Sci.* 20: e70.

Otczyk, D. C., & Cripps, A. W. 2010. Mucosal immunization: a realistic alternative. *Hum Vaccin.* 6: 978-1006.

Ouedraogo, R., Daumas, A., Ghigo, E., Capo, C., Mege, J. L., & Textoris, J. 2012. Whole-cell MALDI-TOF MS: a new tool to assess the multifaceted activation of macrophages. *J Proteomics.* 75: 5523-5532.

Ouedraogo, R., Textoris, J., Daumas, A., Capo, C., & Mege, J. L. 2013. Whole-cell MALDI-TOF mass spectrometry: a tool for immune cell analysis and characterization. *Methods Mol Biol.* 1061: 197-209.

Papa, I., & Vinuesa, C. G. 2018. Synaptic Interactions in Germinal Centers. *Front Immunol.* 9: 1858.

Pasetti, M. F., Simon, J. K., Sztein, M. B., & Levine, M. M. 2011. Immunology of gut mucosal vaccines. *Immunol Rev.* 239: 125-148.

Paul, W. E. 2013. *Fundamental immunology*. Philadelphia: Wolters Kluwer Health/Lippincott Williams & Wilkins.

Perrotta, F., Matera, M. G., Cazzola, M., & Bianco, A. 2020. Severe respiratory SARS-CoV2 infection: Does ACE2 receptor matter? *Respir Med.* 168: 105996.

Petrovsky, N. 2015. Comparative Safety of Vaccine Adjuvants: A Summary of Current Evidence and Future Needs. *Drug Saf.* 38: 1059-1074.

Piot, P., Larson, H. J., O'Brien, K. L., N'Kengasong, J., Ng, E., Sow, S., & Kampmann, B. 2019. Immunization: vital progress, unfinished agenda. *Nature.* 575: 119-129.

Pirahmadi, S., Zakeri, S., Mehrizi, A. A., Djadid, N. D., Raz, A. A., & Sani, J. J. 2019. Combining Monophosphoryl Lipid A (MPL), CpG Oligodeoxynucleotide (ODN), and QS-21 Adjuvants Induces Strong and Persistent Functional Antibodies and T Cell Responses against Cell-Traversal Protein for Ookinetes and Sporozoites (CelTOS) of Plasmodium falciparum in BALB/c Mice. *Infect Immun.* 87: e00911-18.

Pizza, M., Giuliani, M. M., Fontana, M. R., Monaci, E., Douce, G., Dougan, G., Mills, K. H., Rappuoli, R., & Del Giudice, G. 2001. Mucosal vaccines: non toxic derivatives of LT and CT as mucosal adjuvants. *Vaccine.* 19: 2534-2541.

Qi, H. 2016. T follicular helper cells in space-time. *Nat Rev Immunol.* 16: 612-625.

Raker, V. K., Domogalla, M. P., & Steinbrink, K. 2015. Tolerogenic Dendritic Cells for Regulatory T Cell Induction in Man. *Front Immunol.* 6: 569.

Reber, L. L., Sibilano, R., Mukai, K., & Galli, S. J. 2015. Potential effector and immunoregulatory functions of mast cells in mucosal immunity. *Mucosal Immunol.* 8: 444-463.

Rodrigo, M. A., Zitka, O., Krizkova, S., Moulick, A., Adam, V., & Kizek, R. 2014. MALDI-TOF MS as evolving cancer diagnostic tool: a review. *J Pharm Biomed Anal.* 95: 245-255.

Roh, J. S., & Sohn, D. H. 2018. Damage-Associated Molecular Patterns in Inflammatory Diseases. *Immune Netw.* 18: e27.

Romeu, B., Lastre, M., Reyes, L., González, E., Borrero, Y., Lescaille, D., Pérez, R., Nuñez, D., & Pérez, O. 2014. Nasal immunization of mice with AFCo1 or AFPL1 plus capsular polysaccharide Vi from Salmonella typhi induces cellular response and memory B and T cell responses. *Vaccine.* 32: 6971-6978.

Sanchez, J., & Holmgren, J. 2011. Cholera toxin - a foe & a friend. *Indian J Med Res.* 133: 153-163.

Sarkar, I., Garg, R., & van Drunen Littel-van den Hurk, S. 2019. Selection of adjuvants for vaccines targeting specific pathogens. *Expert Rev Vaccines.* 18: 505-521.

Schaefer, L. 2014. Complexity of danger: the diverse nature of damage-associated molecular patterns. *J Biol Chem.* 289: 35237-35245.

Schellack, C., Prinz, K., Egyed, A., Fritz, J. H., Wittmann, B., Ginzler, M., Swatosch, G., Zauner, W., Kast, C., Akira, S., von Gabain, A., Buschle, M., & Lingnau, K. 2006. IC31, a novel adjuvant signaling via TLR9, induces potent cellular and humoral immune responses. *Vaccine.* 24: 5461-5472.

Schiller, J., Suss, R., Fuchs, B., Muller, M., Zschornig, O., & Arnold, K. 2007. MALDI-TOF MS in lipidomics. *Front Biosci.* 12: 2568-2579.

Schulze, K., Ebensen, T., Riese, P., Prochnow, B., Lehr, C. M., & Guzmán, C. A. 2016. New Horizons in the Development of Novel Needle-Free Immunization Strategies to Increase Vaccination Efficacy. *Curr Top Microbiol Immunol.* 398: 207-234.

Schussek, S., Bernasconi, V., Mattsson, J., Wenzel, U. A., Strömberg, A., Gribonika, I., Schön, K., & Lycke, N. Y. 2020. The CTA1-DD adjuvant strongly potentiates follicular dendritic cell function and germinal center formation, which results in improved neonatal immunization. *Mucosal Immunol.* 13: 545-557.

Scott-Taylor, T. H., Axinia, S. C., Amin, S., & Pettengell, R. 2018. Immunoglobulin G; structure and functional implications of different subclass modifications in initiation and resolution of allergy. *Immun Inflamm Dis.* 6: 13-33.

Shakya, A. K., Chowdhury, M. Y. E., Tao, W., & Gill, H. S. 2016. Mucosal vaccine delivery: Current state and a pediatric perspective. *J Control Release.* 240: 394-413.

Sharma, S. K., & Naidu, G. 2016. The role of danger-associated molecular patterns (DAMPs) in trauma and infections. *J Thorac Dis.* 8: 1406-1409.

Shelburne, C. P., Nakano, H., St John, A. L., Chan, C., McLachlan, J. B., Gunn, M. D., Staats, H. F., & Abraham, S. N. 2009. Mast cells augment adaptive immunity by orchestrating dendritic cell trafficking through infected tissues. *Cell Host Microbe.* 6: 331-342.

Shlomchik, M. J., & Weisel, F. 2019. B cell primary immune responses. *Immunol Rev.* 288: 5-9.

Silva-Sanchez, A., & Randall, T. D. 2020. Anatomical Uniqueness of the Mucosal Immune System (GALT, NALT, iBALT) for the Induction and Regulation of Mucosal Immunity and Tolerance. *Mucosal Vaccines*: 21-54.

Sisteré-Oró, M., Pedersen, G. K., Córdoba, L., López-Serrano, S., Christensen, D., & Darji, A. 2020. Influenza NG-34 T cell conserved epitope adjuvanted with CAF01 as a possible influenza vaccine candidate. *Vet Res.* 51: 57.

Smith, M. 2015. Vaccine safety: medical contraindications, myths, and risk communication. *Pediatr Rev.* 36: 227-238.

Soon, M. S., Engel, J. A., Lee, H. J., & Haque, A. 2019. Development of circulating CD4(+) T-cell memory. *Immunol Cell Biol.* 97: 617-624.

Srivastava, A., Gowda, D. V., Madhunapantula, S. V., Shinde, C. G., & Iyer, M. 2015. Mucosal vaccines: a paradigm shift in the development of mucosal adjuvants and delivery vehicles. *Apmis.* 123: 275-288.

Su, F., Patel, G. B., Hu, S., & Chen, W. 2016. Induction of mucosal immunity through systemic immunization: Phantom or reality? *Hum Vaccin Immunother.* 12: 1070-1079.

Suan, D., Sundling, C., & Brink, R. 2017. Plasma cell and memory B cell differentiation from the germinal center. *Curr Opin Immunol.* 45: 97-102.

Sun, B., & Xia, T. 2016. Nanomaterial-Based Vaccine Adjuvants. *J Mater Chem B.* 4: 5496-5509.

Sun, J. B., Holmgren, J., Larena, M., Terrinoni, M., Fang, Y., Bresnick, A. R., & Xiang, Z. 2017. Deficiency in Calcium-Binding Protein S100A4 Impairs the Adjuvant Action of Cholera Toxin. *Front Immunol.* 8: 1119.

Suto, H., Nakae, S., Kakurai, M., Sedgwick, J. D., Tsai, M., & Galli, S. J. 2006. Mast cell-associated TNF promotes dendritic cell migration. *J Immunol.* 176: 4102-4112.

Takatsuka, S., Yamada, H., Haniuda, K., Saruwatari, H., Ichihashi, M., Renauld, J. C., & Kitamura, D. 2018. IL-9 receptor signaling in memory B cells regulates humoral recall responses. *Nat Immunol.* 19: 1025-1034.

Tangye, S. G., & Ma, C. S. 2020. Regulation of the germinal center and humoral immunity by interleukin-21. *J Exp Med.* 217: e20191638.

Tesfaye, D. Y., Gudjonsson, A., Bogen, B., & Fossum, E. 2019. Targeting Conventional Dendritic Cells to Fine-Tune Antibody Responses. *Front Immunol.* 10: 1529.

Thompson, A. L., & Staats, H. F. 2011. Cytokines: the future of intranasal vaccine adjuvants. *Clin Dev Immunol.* 2011: 289597.

Turula, H., & Wobus, C. E. 2018. The Role of the Polymeric Immunoglobulin Receptor and Secretory Immunoglobulins during Mucosal Infection and Immunity. *Viruses.* 10: 237.

van Beijnum, J. R., Buurman, W. A., & Griffioen, A. W. 2008. Convergence and amplification of toll-like receptor (TLR) and receptor for advanced glycation end products (RAGE) signaling pathways via high mobility group B1 (HMGB1). *Angiogenesis.* 11: 91-99.

Vela Ramirez, J. E., Sharpe, L. A., & Peppas, N. A. 2019. Corrigendum to 'Current state and challenges in developing oral vaccines' [Adv. Drug Deliv. Rev. 114 (2017) 116-131]. *Adv Drug Deliv Rev.* 139: 158.

Veldhoen, M., Hocking, R. J., Atkins, C. J., Locksley, R. M., & Stockinger, B. 2006. TGFbeta in the context of an inflammatory cytokine milieu supports de novo differentiation of IL-17-producing T cells. *Immunity.* 24: 179-189.

Vénéreau, E., Ceriotti, C., & Bianchi, M. E. 2015. DAMPs from Cell Death to New Life. *Front Immunol.* 6: 422.

Vliagoftis, H., & Befus, A. D. 2005. Rapidly changing perspectives about mast cells at mucosal surfaces. *Immunol Rev.* 206: 190-203.

Wang, L., Chitano, P., & Murphy, T. M. 2005. Length oscillation induces force potentiation in infant guinea pig airway smooth muscle. *Am J Physiol Lung Cell Mol Physiol.* 289: L909-915.

Wang, Y., Shi, J., Yan, J., Xiao, Z., Hou, X., Lu, P., Hou, S., Mao, T., Liu, W., Ma, Y., Zhang, L., Yang, X., & Qi, H. 2017. Germinal-center development of memory B cells driven by IL-9 from follicular helper T cells. *Nat Immunol.* 18: 921-930.

Waters, L. R., Ahsan, F. M., Wolf, D. M., Shirihai, O., & Teitell, M. A. 2018. Initial B Cell Activation Induces Metabolic Reprogramming and Mitochondrial Remodeling. *iScience.* 5: 99-109.

Weisel, F. J., Mullett, S. J., Elsner, R. A., Menk, A. V., Trivedi, N., Luo, W., Wikenheiser, D., Hawse, W. F., Chikina, M., Smita, S., Conter, L. J., Joachim, S. M., Wendell, S. G., Jurczak, M. J., Winkler, T. H., Delgoffe, G. M., & Shlomchik, M. J. 2020. Germinal center B cells selectively oxidize fatty acids for energy while conducting minimal glycolysis. *Nat Immunol.* 21: 331-342.

Wong, C. K. H., Liao, Q., Guo, V. Y. W., Xin, Y., & Lam, C. L. K. 2017. Cost-effectiveness analysis of vaccinations and decision makings on vaccination programmes in Hong Kong: A systematic review. *Vaccine.* 35: 3153-3161.

Wright, A. K., Briles, D. E., Metzger, D. W., & Gordon, S. B. 2008. Prospects for use of interleukin-12 as a mucosal adjuvant for vaccination of humans to protect against respiratory pneumococcal infection. *Vaccine.* 26: 4893-4903.

Yusuf, H., & Kett, V. 2017. Current prospects and future challenges for nasal vaccine delivery. *Hum Vaccin Immunother.* 13: 34-45.

Zhang, Q., Raoof, M., Chen, Y., Sumi, Y., Sursal, T., Junger, W., Brohi, K., Itagaki, K., & Hauser, C. J. 2010. Circulating mitochondrial DAMPs cause inflammatory responses to injury. *Nature.* 464: 104-107.

Zhu, J., & Paul, W. E. 2010. CD4+ T cell plasticity-Th2 cells join the crowd. *Immunity.* 32: 11-13.